Nanofer Zero-Valent Iron Nanoparticles: Surface Morphology, Structure and Reactivity with Contaminants

Mahmoud M. Eglal

Thesis
In
Environmental Engineering
Department of Building, Civil and Environmental Engineering

Submitted in partial fulfillment of the requirements
for the Degree of Doctor of Philosophy at
Concordia University
Montreal, Quebec, Canada

2014

CONCORDIA UNIVERSITY

School of Graduate Studies

This is to certify that the thesis prepared

By: Mahmoud Eglal

Entitled: Nanofer Zero-Valent Iron nanoparticles: Surface Morphology, Structure and Reactivity with Contaminants,

and submitted in partial fulfillment of the requirements for the degree of

Doctorate of Philosophy (Environmental Engineering)

complies with the regulations of the University and meets the accepted standards with respect to originality and quality

Signed by the final Examining committee:

----------Chair
Chair's name

----------Examiner
Examiner's name

----------Examiner
Examiner's name

----------Examiner
Examiner's name

----------Supervisor
Supervisor's name

Approved by----------
Chair of Department of Graduate Program Director

----------2014 ----------

Dean of Faculty

ABSTRACT

Nanofer Zero-Valent Iron Nanoparticles: Surface Morphology, Structure and Reactivity with Contaminants

Mahmoud M. Eglal

Nanoscale zero valent iron is emerging as a new option to treat contaminated groundwater. Despite its high potential for environmental application, there is only a limited knowledge about the fundamental properties of nZVI, particularly, its structure, surface composition and the change in these characteristics in an aqueous media, as nanoparticles interact with aqueous contaminants. Nanofer zero valent iron (nanofer ZVI) is a new and innovative nanomaterial capable of removing organic as well as inorganic contaminants in water. It displays a decrease in agglomeration, when it is coated with Tetraethyl orthosilicate (TEOS). TEOS imparts an increase in reactivity and stability to nanofer ZVI. The present study investigates the structure and surface chemistry of nanofer ZVI to understand the mechanism of reactivity towards organic and inorganic contaminants in water. The characteristics of nanofer ZVI were determined using scanning electron microscope/electron dispersive spectroscope (SEM/EDS), transmission electron microscope (TEM) and X-ray diffraction (XRD). The nanoparticle size varied from 20 to100 nm and its surface area was in the range of 25-30 $m^2 g^{-1}$. The thickness of the oxidizing layer had a range of 2 to 4 nm.

The adsorption and the oxidation behavior of nanofer ZVI used for the removal of Cu (II), Pb (II), Cd (II) ions and TCE from aqueous solutions was investigated. The optimal pHs for Pb (II), Cu (II), Cd (II) and TCE removal were found to be 4.5, 4.8, 5.0 and 6.5 respectively. Test data were used to form the Langmuir and the Freundlich model isotherms. The maximum loading capacity was estimated as 270, 170, 110, 130 mg per gram of nanofer ZVI for Cu (II), Pb (II), Cd (II) and TCE respectively. The adsorption of metal ions were compared with their hydrated ionic radii and their electronegativity. TCE oxidation followed the dechlorination pathway resulting in nonhazardous byproducts. Kinetic experiments indicated that the adsorption of heavy metals [Pb (II), Cd (II), and Cu (II)] and TCE was very rapid during the initial step of 50 minutes, which was followed by a much slower second step that was related to the solid state diffusion rate and the available surface area. Removal rates of 99.7% for Pb (II), 99.2% for Cd (II), 99.9% for Cu (II), and 99.9 % for TCE were achieved in less than 180 minutes.

The Lagergren model (LM) and the single diffusion model (SDM) were used to understand the removal mechanism associated with nanofer ZVI. The time interval for particles to agglomerate and settle was between 4-6 hrs. SEM/EDS images showed that the particle size increased from 50 nm to 2 μm due to the particle agglomeration.

The competitive adsorption and displacement of mixed metals are complicated processes that are influenced by several factors. The occurrence of more than one possible adsorption mechanism, on nanofer ZVI contributes to the multi-faceted nature of these interactions. The binding of metal ions is thought to depend on the hydrated ionic radii and the electronegativity of metals. The mechanisms for binary and multi adsorption involved are influenced by time, pH and initial adsorbent concentration as well as the presence and properties of competing metal ions in the solution. In the isotherm and kinetic studies performed for binary and multi metal adsorption experiments, compared to Pb II and Cd II, Cu II achieved the higher adsorption capacity during the initial 5 min. However, after 120 min, all metals achieved removal efficiency in the range of 95 to 99%. Comparing the results of single and competitive adsorption kinetic tests for all the three metals during the initial 5 min, the presence of other metals slightly reduced the removal efficiency.

A part of the studies was devoted to the removal of mixed organic and inorganic contaminants. To this end, the removal of TCE by nanofer ZVI in the presences of Cu II at different environmental conditions was investigated. The kinetics of TCE degradation by nanofer ZVI was observed. At a dosage of 25 mg of nanofer ZVI, only 45% TCE was removed. However, when 0.01M Cu II and 0.15 TCE were present, 80 % degradation of TCE was achieved due to the presence of Cu II. SEM/EDS images indicated that Cu II is reduced to form Cu^0 and Cu_2O. These formations are considered to be responsible for enhancing TCE degradation. Direct TCE degradation in presence of Cu II involves hydrogenolysis and β-elimination, while indirect reduction involves atomic hydrogen and no direct electron transfer from the metal to reactants. Most of the iron present in nanofer ZVI could get dissolved causing the generation of localized positive charge regions and form metal chlorides to maintain electro neutrality in the system. Local accumulation of hydrochloric acid inside the pits regenerates new reactive surfaces to serve as sources of continuous electron generation. However, no significant effect of TCE was noticed for either increasing or decreasing Cu II sequestering on the surface of nanofer ZVI.

Dedication

To my family & friends

Acknowledgement

I would like to thank my supervisor, Dr. A.S Ramamurthy for his help and support throughout my PhD program. My sincere appreciation goes to both Dr Maria Elektorowicz and Dr. Catharine Mulligan for letting me to use some of their facilities. Much appreciation is extended to the TMG group in Mechanical engineering Laboratory, especially Mr. M. Samara for his help in using the SEM/EDS and XRD devices. My warm thanks goes to Nanoiron. Ltd for providing the nanofer ZVI particles that were used my studies.

My special thanks extend to the staff and personnel on both The Canadian Bureau of International Education (CBIE) and the Libyan Ministry of Education for their financial support. Also I would thank Madm. Diane Cry (academic manger in CBIE) for the help and the follow up all the way through my Ph. D program.

Lastly, I would like to thank my friends and family in both Libya and Canada for being a constant source of patience, understanding, love, and encouragement. I am most grateful to my brother Mustafa for giving me endless support and being my close companion during these years.

Selected main contributions

- A new nanomaterial nanofer ZVI was coated with TEOS to render it environmentally friendly and inexpensive. The engineered nanoparticles (ENP) overcomes the drawback of the conventional nanofer ZVI 25 which agglomerates quickly in the aqueous media. The coated nanofer ZVI is highly reactive and was found to be a very highly effective removing both organic and inorganic contaminants from polluted water.
- The new ENP was effective in removing contaminants such as heavy metals [(Cu (II), Pb (II) and Cd (II)] as well as organic contaminants [TCE] from polluted water. Almost all (99%) of the heavy metals such as ((Cu (II), Pb (II) and Cd (II)) were removed. In the case of TCE, nanofer ZVI got oxidized and releases electrons which reduce the reaction with water.
- Both the film diffusion model and the intraparticle diffusion confirmed that compared to Pb (II) and Cd (II), the diffusion of Cu (II) was much faster. The models implied that metals transfer involved the rapid step controlled by liquid diffusion as well as a slower step controlled by intraparticle diffusion.
- The test data indicated that TCE degradation results in less hazardous substances such as ethanol and vinyl chloride.
- Due to its relatively large surface area, small amounts (10 mg) of nanofer ZVI can effectively remove metals as well as TCE.
- In competitive adsorption kinetic tests for all three metals, during the initial 5 min, the presence of other metals slightly reduced the removal efficiency.
- Test data related to degradation of TCE in the presence of Cu II indicated that although Cu gets adsorbed faster to nanoferZVI, it works as an intermediate catalysis to enhance TCE degradation.

Publications

- **Published**

  Eglal, M. M., and Ramamurthy, S.A, (2014) "**Nanofer ZVI: morphology, particle characteristics, kinetics and applications**" Journal of Nanomaterial, dx.doi.org/10.1155/2014/152824

- **Revised version submitted**

  Eglal, M. M., and Ramamurthy, S.A, (2014) "**Removal of Pb (II), Cd (II), Cu (II) and TCE from Water by Nanofer ZVI: Modeling and Isotherm Studies,**" Clean Air, Soil and Water (revised version resubmitted).

- **Submitted**

  Eglal, M. M., and Ramamurthy, S.A, (2014) "**Competitive adsorption and oxidation behavior of Heavy metals on new coated zero valent iron nanoparticle with tetraethyl orthosilicate**" Colloids and Surfaces A: Physicochemical and Engineering Aspects (under review).

  Ramamurthy, S.A., and Eglal, M. M., (2014) "**Degradation of TCE by TEOS coated nZVI in the presence of Cu II for groundwater remediation,**" Journal of Nanomaterial, (under review).

Table of Contents

Abstract i

Chapter One

Introductions

1.1 Background and motivation 1
1.2 Research objectives 2
1.2.1 Statement of the problem 2
1.2.2 Objectives 3
1.3 Methodology 4
1.4 Thesis overview 4
1.5 References 5

Chapter Two

Literature review

2.1 Overview of groundwater technology development 5
2.1.1 Groundwater contaminants 5
2.2 Selected organic and organic contaminants 7
2.2.1 Lead 8
2.2.2 Cadmium 9
2.2.3 Copper 10
2.2.4 Trichloroethylene 12
2.3 Remediation of water 14
2.3.1 Treatment of single contaminant 15
2.3.2 Treatment of mixed metal contaminants 18
2.3.3 Treatment of mixed organic and inorganic contaminants 20
2.4 Zero valent iron 21
2.4.1 Degradation of organics by ZVI 22
1.4.2 Removal of heavy metals by ZVI 23
2.5 Zero valent iron nanoparticules 24
2.5.1 Nanoparticle characteristics 26
2.5.2 Modified nanoparticle 28
2.5.3 Reaction of nZVI with contaminants 29
2.5.4 Application of nZVI in groundwater 30
2.4.5 Impact of nZVI particle size on the adsorption 36
2.6 References 37

Chapter Three

Experimental and analytical methods

3.1 Experimental and analytical methods 45
3.1.1 Nanofer zero valent iron 45
3.1.2 Chemical solutions 45
3.2 Experimental procedures 47
3.2.1 Batch equilibrium experiments 47
3.2.2 Batch kinetic experiments 47
3.3 Aqueous analysis 48
3.3.1 Atomic absorption spectrometer (AA) 47
3.3.2 Gas chromatograph 47

3.3.3 Temperature, pH and ORP measurements 47
3.4 Solid phase analysis 49
3.4.1 Scanning electron microscopy 49
3.4.2 Transmission electron microscopy 49
3.4.3 BET surface area 49
3.5 Analytical techniques 50
3.6 References 51

Chapter Four

Nanofer ZVI: morphology, particle characteristics, kinetics and applications

4.1 Introduction 52
4.2 Material and methods 55
4.3 Surface morphology and particle characteristic 55
4.3.1 Transmission electron microscope images 55
4.3.2 Scanning electron microspcope/ electron dispersive microscope 56
4.3.3 X-ray diffractometer 56
4.3.4 BET method 56
4.3.5 ζ potential and iso-electric point 56
4.4 Batch Kinetic adsorption experiments 57
4.5 Kinetic Experimental and modeling 57
4.6 Results and discussions 58
4.6.1 Morphology and surface chemistry 58
4.7 Kinetics of Pb (II), Cu (II), Cd (II) and TCE adsorption 63
4.8 Sorption Kinetics 64
4.8.1 First order kinetic model 66
4.8.2 Adsorption diffusion model 66
4.9 Conclusions 69
4.10 References 70

Chapter Five

Removal of Pb (II), Cd (II), Cu (II) and TCE from water by nanofer ZVI: modeling and isotherms studies

5.1 Introduction 75
5.2 Material and methods 76
5.2.1 Batch kinetic adsorption experiments 76
5.3 Results and discussions 77
5.3.1 Effect of pH 77
5.3.2 Effect of nanofer ZVI dose 80
5.3.3 Effect of metal ion concentration 82
5.4 Sorption isotherms models 82
5.5 Effect of particle Aging and agglomeration 85
5.6 Conclusions 87
5.7 References 88

Chapter Six

Competitive adsorption and oxidation behavior of heavy metals on new coated zero valent iron nanoparticle with tetraethyl orthosilicate

6.1 Introduction 91
6.2 Material and methods 94
6.3 Experimental procedures 94
6.3.1 Batch equilibrium experiments 94
6.3.2 Batch kinetic experiments 95
6.4 Results and discussions 96
6.4.1 Isotherm studies 96
6.4.2 Kinetic studies 100
6.4.3 Kinetic adsorption models 102
6.5 Conclusions 104
6.6 References 104

Chapter Seven

Degradation of TCE by TEOS coated nZVI in the presence of Cu II for groundwater remediation

7.1 Introduction 106
7.2 Material and methods 108
7.3 Experimental procedures 108
7.3.1 Batch equilibrium experiments 108
7.3.2 Batch kinetic experiments 109
7.4 Results and discussions 110
7.4.1 Oxidative degradation of TCE by nanofer ZVI suspension in the presence of Cu (II) 110
7.4.2 Effect of Cu II on the degradation isotherm of TCE by nanofer ZVI 110
7.4.3 Effect of Cu II on degradation kinetic of TCE by nanofer ZVI 113
7.4.4 Sequestration of Cu II by nanofer ZVI in the presence of TCE 115
7.5 Conclusions 116
7.6 References 117

Chapter Eight

Conclusions and future studies

8.1 Summery of contributions
8.1.1 Morphology and characterization of the nanofer ZVI 121
8.1.2 Reactivity of nanofer ZVI with single contaminant 121
8.1.3 Competitive adsorption and displacement of metal on nanofer ZVI 122
8.1.4 Competitive adsorption of Cu II and TCE degradation 123
8.2 Future studies 123

List of Figures

Fig 1.1 Adsorption using 1 g/l goethite, 4- hr equilibrium adsorption a: Cu, b: Pb, c: Cd, d: mixed, Cu, Pb, Cd. Taken after (Christophi and Axe 2000)

Fig 2.2 Effect of phosphate on total arsenic uptake (%) from spiked groundwater at pH 6.5 (Total arsenic Conc: 1.13 mg/L) taken after (Chowdhury and Yanful, 2010)

Fig 2.3 The core-shell model of zero-valent iron nanoparticles (taken after Zhang et al. 2007)

Fig 2.4 TEM image of nZVI produced by borohydride (taken after Zhang et al. 2006)

Fig 2.5 Comparison of the media treated, particle types used, and target compounds of nZVI- applications in Europe and USA. (Muller et al 2012, EPA, 2010 and Karn et al 2011)

Fig 3.1 Calibration curves for Pb (II), Cu (II), Cd (II) &TCE

Fig 4.1 SEM images of nanofer ZVI (a): particle size in the range of 40 nm

Fig 4.2 TEM images of nanofer ZVI with the oxide shell. Tip of arrow indicates zoom location

Fig 4.3 XRD nanofer ZVI of α-Fe the particle size: 50-100 nm and high content of iron range of 70-90 wt. %, (λ=1.5418 Å, U=40 Kv, I 30= 30 mA).

Fig 4.4 Fig. 3.4 SEM images: (a) non-coated nanofer 25 taken after (Lenka et al 2012). (b) Coated with Silicon nanofer ZVI produce in TMG Lab Concordia University

Fig 4.5 ζ potential as function of pH for nanofer ZVI

Fig. 4.6 Kinetic adsorption of organic and inorganic contaminants by nanofer star ZVI dose,10 mg, Conc. 0.01 M, T: 20-22 ºC a: Cd (II), B: Cu (II), C: Pb (II) ,& D: TCE

Fig 3.5 SEM images: (a) non-coated nanofer 25 taken after (Lenka et al 2012). (b) Coated with Silicon nanofer ZVI produce in TMG Lab Concordia University.

Fig 5.1 Effect of pH on the removal of metal ions & TCE using nanofer ZVI star, Dose: 10 mg, Conc: 0.01 mM, T: 20-22 0C, a: Cu II, b: Pb II, c: Cd II and d: TCE

Fig 5.2 Effect of adsorbent on the removal of metal ions & TCE using nanofer ZVI star, Dose: 10 mg, Conc: 0.01 mM, T: 20-22 0C, a: Cu II, B: Pb II, C: Cd II and D: TCE

Fig 5.3 Effect of ion and TCE concentration on the removal efficiency of nanofer ZVI star, Dose: 10 mg, a: Cu II pH- 4.5, b: Pb II pH-4.8, c: Cd II, pH-4.9 and D: TCE, pH-6.5, T: 20-22 ^{0}C

Fig. 5.4 Settling of nanofer ZVI in de-ionized water;
a: Sample after adding the nanofer ZVI and placed in 250 rmp shaker,(at 0.02 hrs)
b: Sample after adding the nanofer ZVI and placed in 250 rmp shaker, (at 24 hrs)

Fig. 5.5 SEM/EDS images for nanofer ZVI before and after the hydroxyl experiment; a: image before the experiments, b: image after 24 hr of settling

Fig. 6.1 Isotherm studies of metal competition, Cu II - Cd II, insert: Single isotherm studies of metals pH: 4.5 , T: 22 ^{O}C

Fig.6.2 Isotherm studies of metal competition, Pb II - Cd II, insert: Single isotherm studies of metals, pH: 4.5, T: 22 ^{O}C

Fig. 6.3 Isotherm studies of metal competition, Cu II - Pb II, insert: Single isotherm studies of metals, pH: 4.5, T: 22 ^{O}C

Fig. 6.4 Isotherm studies of metal competition, Cu II - Pb II- Cd II, insert: Single isotherm studies of metals pH: 4.5, T: 22 ^{O}C.

Fig. 6.5 Kinetic studies of metal competition, a. Cu II vs. Cd II, b. Pb II vs. Cd II. C. Cu II vs. Pb II and d. Cu II, Cd II , Pb II. Error bar: ± 0.1, pH: 5.5, T: 20 ^{O}C, insert: Single adsorption experiment for each metal.

Fig. 7.1 Effect of concentration on the TCE removal by nanofer ZVI in presence of Cu II. nanoferZVI dose =10mg, initial pH=6, T: 21^{0} C, standard error 1%, TCE standard solution in de-ionized water. a: Cu II (0.1 M), control = TCE (40 mL) in de-ionized water. b: TCE (40 mL),

Fig. 7.2 Effect of dosage response on the adsorption of TCE by nanofer ZVI in presence of Cu II), initial pH=6, T: 21^{0} C, standard error 1%. a: Conc. Cu II (0.05, 0.1 and 0.15 M), TCE constant (40 mL), b: TCE (20,30 and 40 mL), Cu II (0.1 M)

Fig. 7.3 Effect of time on the adsorption of Cu II by nanofer ZVI in presence of TCE (40 Ml), Conc. 0.1mM, 0.05 mM and 0.15 mM, initial pH=6, T: 21^{0} C, standard error 1%.

Fig. 7.4 EDS analysis of nanofer ZVI after the experimental test, pH =6 T= 21^{0} C, a: TCE concentration (1 mM) and Cu II concentration (1 mM), b: nanofer ZVI in de-ionized water

Fig 7.5 Schematic diagram illustrating the effect of cations on degradation of TCE by nanofer ZVI

Fig. 7.6 XRD image of nanofer ZVI before and after the experiments; (λ = 1.5418 ˚ A, = 60 Kv, and *I*30 = 30 mA); Green line represent the TCE experiment; TCE Conc.40 ml; Blue line represent Cu II Conc. 0.1 M and TCE Conc. 40 ml; Red line represent the nZVI before the experiment. Time: 2 hrs. T; 22 ^{0} C.

List of Tables

Table 1.1 Compression of metal removals using different techniques

Table 2.2 Some of pilot tests with nZVI (based on Muller et al. 2012 and EPA, 2010)

Table 3.1 Presents the selected organic and inorganic chemicals used in the study

Table 3.2 Metal ion characteristics, (taken after David, 1998)

Table 4.1 SEM/EDS analysis of kinetic experiments for single metal adsorption (Step 1; rapid rate)

Table 4.2 Calculated parameters of both liquid film diffusion model and intraparticle diffusion model from kinetic data (C_0 =40 mg/l, T=21-25 ^{0}C)

Table 5.1 Sorption isotherm models parameters.

Table 5.2 SEM/EDS analysis of before and after the particle settling experiments with di-ionized water

Table 6.1 Langmuir parameters for adsorption of metal at binary and multi system at pH 4.5

Table 6.2 SEM/EDS analysis of kinetic experiments for mixed metal adsorption

Table 6.3 Pseudo-first and pseudo-second model parameters and correlation coefficients calculated using the multi metal adsorption experimental data.

Symbols and abbreviations

AAS	Atomic absorption spectroscope
BET	Brunauer-Emmett-Teller
BNP	Bimetallic nanoscale particles
BTEX	Benzene, toluene, ethylbenzene, and xylenes
CMC	Carboxymethyl cellulose
CT	Carbon tetrachloride
DCE	1,2- Dichloroethene
DOE	US-department of energy
E^0	Standard redox potential
EDTA	Ethylene-diaminetetraacetic
EPA	US-Environmental protection agency
FE-SEM	Field-emission scanning electron microscope
GC	Gas chromatography
HCl	Hydro chloric acid
IEP	Iso-electic point
LFDM	Liquid film diffusion model
LM	Lagergren model
MTBA	Methyl tert-butyl alcohol
MTBE	Methyl tert-butyl ether
nanofer ZVI	Nanofer zero valent iron
NAPL	Nanaqueous phase liquid
NDA-1000	Phenol by a polymeric adsorption
NMR	Manganese nodule residue
NRTEE	National round table on the environment and the economy
nZVI	Nano zero valent iron
ORP	Oxidation-reduction potential

OSWER	Office of solid waste and engineering response
PCB	Polychlorinated biphenyls
PCE	Perchloroethylene
Pd-ZVI	Palladium-zero valent iron
PRB	Preamble reactive barrier
PVP	Polyvinylpyrrolidone
RNIP	Regulatory nuclear interface protocol
SE	Secondary electron
SEM-EDS	Scan electron microscopy- energy- dispersive X-ray spectroscope
TCA	1,1,1Trichloroethane
TCE	Trichloroethylene
TCM	Trichloromethane
TEM	Transmission electron microscopy
TEOS	Tetraethyl orthosilicate
TMG	Thermo mechanical group
VC	Vinyl Chloride
VC	Vinyl chloride
WHO	World health organization
XPS	X-ray photoelectron spectroscopy
XRD	X-ray diffraction
ZVI	Zero valent iron
δ-MnO_2	Hydrous manganese oxide

CHAPTER ONE

Introduction

1.1 Background and motivation

Nanoscience and nanotechnology have entered all fields of science. Currently, environmental application of nanotechnologies provide new opportunities for one to detect, control and remediate environmental pollution. However, as with any new nanomaterial or technology, there is a potential harm and this should be taken into consideration while developing the technology. For these reasons, research related to environmental nanotechnology mainly focus on two major directions: (a) synthesizing new nanomaterial or developing new techniques and (b) defining the problems and processes that might occur in the environment by evaluating the economic and environmental benefits as well as risks of the new materials.

Larsen, (2005) stated that it is difficult to tract when nanomaterials were first used for environmental applications. The nanoparticle (NP) based catalytic converter placed in the exhaust manifold of automobiles since the early 70s can be considered as the earliest application of nano-catalyst. Some studies of using NP for environmental remediation occurred in the early 90s. However, since 2000, zero valent iron nanoparticles (nZVI) have been used for remediation of groundwater contamination specially TCE to replace the zero valent iron powder (ZVI) and overcome its limitations. The application of nZVI evolved in several different directions for research and application. One aim was to develop a different zero valent iron. The second was the application potential for environmental remediation. The third approach was to modify the surface properties by coating nZVI with different chemical function groups to overcome all problems related to the application of uncoated nZVI. The surface coated or modified nZVI may have much higher stability or can be used to target contaminants or to improve the traveling distance of nZVI. The bimetallic nZVI can prevent the formation of a passive layer at the iron surface and thus maintain the reactivity of iron. The coating of nZVI with Cu for instance can dechlorinate halogenated contaminants that can be degraded by either conventional nZVI or other bimetallic systems. Research efforts are more focused on the second and the third approaches, because these approaches are often linked with each other where the studies improve the stability of nZVI or metal coated nZVI. Finally, the remediation of the process related to

nZVI has been evolved into the oxidative process driven by zero-valent iron in the presence of oxygen. Although the mechanisms are still under investigation, it is highly possible that nZVI are capable of producing highly reactive and unselective hydroxyl radicals in the presences of oxygen. In addition, the process appear to continue to be an effective oxidant generator over longer time periods and over wide range of pH (Joo and Cheng 2006). Therefore, these processes can be extensively used to treat organics and inorganics contaminants as well as to purify contaminated water for different purposes.

While nanotechnology may bestow endless benefits, the application of nanotechnology may have some potential risk to human and ecosystems. In general, conventional nZVI or the nZVI coated with metals can bring immediate concern because of their mobility and their increased reactivity (DEFRA, 2006). Accumulated evidence indicates that the adsorption of metal coated nZVI in organs (lung, skin and gut) can occur. However, no clear understanding of their distribution in the body (toxic kinetics) is available (Brooker and Boysen, 2005). Considerable current research is focused on developing nZVI coated with environmentally friendly materials which are less toxic to humans (Mavarro, 2008).

Important research questions to be answered are related to the application of the new environmentally friendly nZVI for remediation of groundwater contamination. These are related to the following: i. dose response relationship (e.g. are they affected by particle size, number or shape), ii interaction between nZVI coated with any new material, iii fate and transport of the nZVI materials (e.g. more persistent, bioaccumulation, agglomeration and other fate behavior), iv development of structure/ activity relationships to predict fate and transport of coated nZVI to the environment.

1.2 Research objectives

1.2.1 Statement of the problem

Focus on removing inorganic contaminants in groundwater has been relatively recent, since organic are increasingly used in industry and are seen to have posed a more challenging removal problem when they appear with inorganic contaminants. Many inorganic contaminants, specially, Pb (II), Cd (II), and Cu (II) are toxic and poses great health and environmental

concerns even at very low concentration. Most of the earlier studies have focused on a single form of contaminant either organic or/ and inorganic and the efficiency of their removal.

Several research studies have focused on investigating the properties of new adsorbents. However, less attention is given to the removal of mixed contaminants formed by both organics and inorganics. EPA. (USA) and Environment Canada have stated that 90% or more of these sites are contaminated by binary or mixed contaminants. The removal of mixed contaminants has received greater attention recently. The detailed research objectives are presented below:

1.2.2 Objectives

The goal of the present study is to investigate the ability of the nanoparticle adsorbent media (nanofer ZVI) to effectively remove Pb (II), Cd (II), Cu (II) and TCE which formed the mixed contaminant. The study will also examine the ability of adsorbent to promote a more rapid mass transport of individual and mixed contaminants into the media, and possibly possess a greater selectivity than the adsorbent media commercially available. The following are the specific objectives:

- Evaluate the structure and morphology of the new nanofer ZVI using a variety of microscopic methods such as SEM/EDS, TEM and XRD.
- Measure the effects of pH and zeta potential profiles on nanofer ZVI through laboratory batch experiments. The latter will provide the efficiency of nZVI in sequestering water contaminants. Candidate contaminants studied here are of vital environmental concern. The contaminants considered are copper, cadmium, lead and TCE.
- Examine the product of reactions between nanofer ZVI and the selected contaminants with series of batch isotherm and kinetic experiments for a wide range of physical and chemical parameters (contact time, concentration, pH and dosage).
- Investigate the impact of the presence of binary and multiple metal ions [Pb (II), Cd (II) and Cu (II)].
- Study the impact of Cu II on the degradation of TCE.
- Integrate results from the above experiments and know the appropriateness of using models to interpret adsorption capacity data of both isotherm and kinetic experiments.

- Study the physical and chemical factors such as iron passivation (non-target reactions), particle agglomeration, and particle diffusion.

1.3 Methodology

Chapter 3 describes in detail the materials and methods used in this study to examine the efficiency of nZVI in removing organic and inorganic contaminants selected. The nZVI used in this study was supplied by Nanoiron Inc Rajhrad, (Czech Republic). All chemicals were of reagent grade and were used as purchased without further purification. Instrument analyses, unless otherwise noted, were performed mainly in the Department of building, Civil and Environmental Engineering and partly in Department of mechanical engineering at Concordia University. A series of batch isotherm and kinetic experiments were performed. During the experiment, the effect of varying the physical and chemical characteristics (pH, dosage, contaminants concentration) on the results were examined for both single and mixed contaminants). Also, batch test techniques were selected to investigate both the particle agglomeration and iron passivation. Several models were selected to describe the adsorption capacity and particle diffusion.

1.4 Thesis overview

This section provides an overview of the thesis layout and highlights the focus of the interconnections of later chapters. The sequence of the layout is as follows:

- Chapter 2 gives a comprehensive literature review about the groundwater treatment, ZVI technology for water remediation, and some groundwater contaminants. Also, the current state-of-knowledge regarding the underlying mechanisms, and engineering experiences from *in situ* field applications.
- Chapter 3 discusses the experimental procedure and the methodology adopted in this study with detailed descriptions of instrument analysis.
- Chapter 4 deals with the structural and chemical properties of nanofer ZVI using advanced spectroscopic and microscopic techniques and discusses the role of kinetic reactions between the nanoparticles and the selected contaminants [Cu II, Pb II, Cd II and TCE].

- Chapters 5 investigates the reactivity of nZVI towards a group of well-chosen inorganic contaminants with varying coordinative, electrochemical and redox properties. These contaminants are selected as molecular probes to evaluate the multi-faceted functionality of nZVI imparted by its core-shell composite structure. Specifically, it focuses on the role of adsorption, reduction, surface precipitation and mineralization processes in the sequestration of Cu (II), Pb (II), Cd II and TCE.
- Chapter 6 examines the adsorption competition between well-chosen inorganic contaminants by investigating the effect of both ionic radii and the electronegativity on the adsorption, redox reaction and metal sequestrating. Four different environmental factors (pH, Dosage response, time and Concentration) were chosen to complement the studies.
- Chapter 7 describes mainly the role of the co-existence of organic and inorganic contaminants. The metal chosen was Cu II due to its frequent presence in groundwater. TCE is the most commonly organic contaminant removed by nZVI. The study also investigates the chemical reaction of TCE on the surface of nanofer ZVI as well as Cu II reduction.
- Chapter 8 summaries the major results of this study, identifies new questions or research areas.

1.5 References

1. Brooker, R., and Boysen, E., 2005 " Nanotechnology for dummies" Wiley Publishing, Inc. Hoboken, NJ
2. DEFRA, (Department for environment, food, and rural affairs), 2006, " Charactering the potential risks posed by engineered nanoparticles" UK Government research- a progress report, DEFRA, London, 2006.
3. Joo, S. H., and Cheng, I.F., 2006 " Nanotechnology for environmental remediation" springer, Inc, New York, pp 1-165
4. Larsen, S.C., 2005 "Nanoctalysts for environmental technology," in Nanotechnology and the Enomrment- application and implication by Karn B, Masciangioli T, Zhang W-X, Colvin V, and Alivisatos, P. (ed), Chapter 36, ACS symposium series 890, ACS, Wahington, DC.
5. Navarro, E. Baun, A Behra, R Haartmann, B Filser J, Miao A-J, Quigg A, Santschi H, and Sigg L, 2008 "Envonmental behavior and ecotoxicity of engeeringed nanoparticles to algae, plants and fungi" *Ecotoxicology*, vol.17, pp. 372-386

CHAPTER TWO

Literature Review

2.1 Overview of groundwater technology development

Today water pollution is main concern due to lack of fresh water. Many water resources are polluted by so organics, inorganic, and pathogenic contaminants. The source of these contaminants include residential, agricultural and industrial. The public concern over the environmental impact of water pollution as increased. Report publish by EPA in 2008 estimated that more than 1.1 billion shorten in water supply. It estimated that by 2025 half of countries water supply will face challenge in removing persistent contaminants.

Nanotechnologies solutions are essential because the abiotic and biotic impurities most difficult to separate in water are in the nanoscale range. The promise is that nanotechnology brings breakthrough technologies for improving water quality and often consumes less material and generates less waste. The investment in nanotechnology applications for clean water processing in the world was estimated at about $1.5 billion in 2007. However, the face of nanotechnology is evolving and so the interest and available expertise for using nanotechnology for clean water is moving up on the list of priorities.

2.1.1 Groundwater contaminants

Groundwater is considered to be one of the most important sources of potable water in the world. However, as the population growth increases rapidly, the availability of this resource is becoming increasingly scarce. For decades, contaminants were often injected to the subsurface where the latter acted as a natural filter. The contaminants potentially migrated through the subsurface and contaminated groundwater sources. The contaminants have significant detrimental impacts on the environment and human health. Also, both economic and social costs are associated with contaminated groundwater. Canada is home to an estimated thirty thousand brownfiled sites, many of which exhibit contamination of soil and groundwater by hazardous industrial chemicals (NRTEE. 2003). The restorations of these brownfield provide significant economic, environmental, and social benefits. This has been identified as critical to the health and overall sustainability of the nation, (NRTEE. 2003). It represents approximately 0.6 percent of Canada's

gross domestic product. However, the US national research council report (1997) suggested that there are between three hundred thousand and four hundred thousand contaminated sites in the United States requiring cleanup. A large of these sites is contaminated by nonaqueous phase liquids (NAPL). However, the rest of the sites is polluted either by metals or/by mixed contaminants containing both NAPLs and metals (NRTEE. 2003).

The groundwater contaminants were often generated in various industrial processes prior to their disposal to the subsurface. For example chemical solvents were commonly used to clean cutting tools, entraining small heavy metal fragments from the cutting process and generating significant quantities of waste liquids. A survey of U.S. Department of Energy (DOE, 1991) wastes sites found that 20 percent of their sites were contaminated with the complex waste mixtures. Other industrial and commercial sources of common groundwater contaminants include polychlorinated biphenyls (PCB) in electrical transformers, heavy metals as paint additives or in metal plating and smelting operations, pesticides for agriculture, and chlorinated solvents from dry cleaning installations (National research council., 1997). All these operations have caused subsurface contamination due to their mismanaged disposal of the chemical wastes. Common disposal practices include accidental releases due to leaky underground storage tanks or compromised landfill liners and intentional releases from underground storage systems designed to slowly leach liquids into the subsurface, subsurface injection wells, or land application of contaminants (National research council., 1997). U.S. EPA (2008) has stated that these contaminants can cause serious health problems and even death. The PCBs, the chlorinated solvent and DNAPL such as trichloroethylene (TCE), are carcinogens. Furthermore, these practices can lead to the impairment of organ development in fetuses. Unfortunately, groundwater contamination of drinking water sources is widespread in the developing and developed world due to poor disposal practices, causing significant health problems. Consequently there is a need for research and development of economical innovative remediation technologies to meet the standards and regulations.

2.2 Selected organic and inorganic contaminants

Heavy metal can be defined as positive ions in solution and have density five times greater than that in water. Many metallic elements play an essential role in the function of living organisms. Others considered toxic or nonessential such as cadmium, nickel, sliver, and lead can cause death.

EPA, health Canada and WHO listed, Cu (II), Cd (II), Pb (II) and TCE as class schedule list A. Whenever they are present in environmental media, action should be taken. The following section provides a brief description including short comments on the chemistry of inorganic (lead, cadmium, and copper) and organic (trichloroethylene) contaminants chosen for the study:

2.2.1 Lead

Pb is a naturally occurring element found in small amounts in the earth's crust. It is naturally occurs in bedrock, soils, tills, sediments, surface waters, groundwater and sea water (Reimann and de Caritat, 1998). It has been used extensively in a variety of applications primarily owing to its low melting point and excellent corrosion resistance in the environment. In the past Pb was used in plumbing and pipes (Cotton, 1972). Solid and liquid sludge wastes account for more than 81% of the Pb discharged into the Canadian environment, usually into landfills, but much less has been dispersed more widely in the environment through car exhausts (Jaques, 1985). In natural environments, it does not find in its elemental form, but is complexes with other elements in mineral form, and it also co-exists with other metals in ore deposits (Reimann and de Caritat 1998). It is also known that specific physical and chemical properties of water such as pH, alkalinity, hardness and dissolved organic carbon content may considerably alter the toxicity of Pb to freshwater fish and daphnids. It tends to be more bioavailable when pH, water hardness and organic matter content are low (U.S. EPA 2011).

The EPA sets the standard for allowable Pb concentration for drinking water as 29 μg/d for children and 64 μg/d for adults. Inorganics lead is a general metabolic poison and enzyme inhibitor, like most of heavy metals. Organic lead is even more poisonous than inorganic lead. The effect of Pb to human can seem to be psychical such as excitement, depression, and irritability). The young children are more effect and can suffer mental retardation and brain damage (Shih et al. 2006). Worldwide the concentration of 0.2 ppm seems to be an accepted. The disturbing fact is that the natural levels in human blood are already very close to what is considered a reasonable toxicological, not leaving one with any margin for exposure to Pb (U.S. EPA 2011).

Lead chemistry

Pb has three oxidation states that should be considered when looking at aqueous reactions, IV, II and 0. Pb (IV) is so insoluble that the species it forms do not need to be considered in the aqueous phase. Pb(II) dissolves in the aqueous phase to form six compounds including Pb (II), Pb(OH), $Pb(OH)_2$, $PbCO_3$, $Pb_3(CO_3)_2(OH)_2$ and $Pb(OH)_3$-. Finally, Pb (0) as with Pb (IV) has a negligibly small dissolved concentration (Brady and Holum, 1996).

2.2.2 Cadmium

Cd is a rare element which is a shiny white metal. It is soft, ductile and has a relatively high vapor pressure. It is nearly always divalent. It is close to zinc, and occurs in almost all zinc ore by isomorphous replacement (Cotton & Wilkinson 1972). It is found in nature and used for electroplating, paints pigments, plastic, silver-cadmium batteries, coating operations, and photography. Discharge of Cd into natural waters is partly from the electroplating industry which accounts for about 50% of the annual Cd consumption in United States (EPA, 1985). Environment of Canada However, in 1976 report stated that the Cd is used on the manufacture of stearate stabilizers for plastics, polyvinyl chloride, and pigments. Applications consuming lesser amounts of Cd include the following: fungicides for golf courses, control rods and shields for nuclear reactors, television picture tube phosphors, nickel-cadmium batteries, motor oils, and curing agents for rubber. It was noted that the use of Cd products has expanded in recent years at a rate of 5 to 10 percent annually, and the potential for further growth is very high (Env. of Canada, 1976). It can cause diarrhea, stomach pains and severe vomiting at higher concentration. Bone fracture Reproductive failure and possibly even infertility for long run (Piscator, M. Copper, 1979). Due to its acute toxicity, Cd has joined Pb and mercury in the most toxic category of heavy metals with the greatest potential hazard to humans and the environment. It is one of the metals most strongly absorbed by living cells accumulated by vegetation. It leaches through soils to ground water. However, when Cd compounds do bind to the sediments of rivers, they can be more easily bioaccumulated or re-dissolved (Piscator, M. Copper, 1979). The maximum contaminant level set by both Heath Canada and US EPA for drinking water is 5 ppb. Food is the main source of Cd intake for individuals who are not exposed. The (WHO, 1985) has estimated the weekly intake for an adult is in between 0.4-0.5 mg. since it is difficult to reduce the Cd intake in food, intake from

other source such as water should reduce to the minimum or 0 mg/l. However, most of the conventional treatment cannot reach the desired standard and search for new method of removal is needed (Government of Canada (1994).

The solubility of Cd in water is influenced to a large degree by the acidity of the medium. Dissolution of suspended or sediment-bound Cd may result when there is an increase in acidity. The need to determine Cd levels in suspended matter and sediments in order to assess the degree of contamination of a water body is necessary (Fleischer et al. 1974). The amount of Cd in waters can be too small to detect even when large concentrations are present in solids, especially under alkaline or neutral conditions (Fleischer et al. 1974).

Cadmium chemistry

It is not usually present in the environment as a pure metal, but is most often present as complex oxides, sulphides, and carbonates in zinc, lead, and copper ores. Cd does not have any recognizable taste or odour. Cadmium sulphate and cadmium chloride are quite soluble in water, and other polar solvents. In water, its high solubility is due in part to the formation of complex ions. Because of this behavior, $CdCl_2$ is a mild component:

$$CdCl_2 + 2\ Cl^- \rightarrow [CdCl_4]^{-2} \qquad (2\text{-}1)$$

Solubility in water at 100 ^oC is 135 g /100 ml. However, cadmium oxide and cadmium sulphide are almost insoluble in water or aqueous solutions.

2.2.3 Copper

Copper is a heavy metal found in natural deposits as ores containing other elements. It is widely used in household plumbing materials. It may occur in drinking water either by contamination of the source water used by the water system, or by corrosion of copper plumbing. Corrosion of plumbing is by far the greatest cause for concern. Based on NAQUADAT data on copper. It is commonly found in source water. Also other sources are mining and smelting operations and municipal incineration. Concentrations in Canadian surface and lake waters from 1980 to 1983, extractable copper levels ranged from 0.001 to 0.080 ppm (Canadian quality guideline, 1987)

All water is corrosive toward copper to some degree, even water termed noncorrosive or water treated to make it less corrosive (Cotton, Wilkinson 1972). Corrosivity toward copper is greatest in very acidic water. Many of the other factors that affect the corrosivity of water toward lead can also be expected to affect the corrosion of copper (Cotton, Wilkinson 1972).

Copper may occur as the metal and in oxidation states as Cu (I) and Cu (II). An unstable Cu (III) is also known. In aqueous solution, copper is present mainly as the Cu (II) ion, depending on pH, temperature, the presence of bicarbonate and sulphide, and the potential to form ligands with organic species, such as humic, fulvic, and amino acids, certain polypeptides, and detergents (Cotton, Wilkinson 1972). The free Cu (I) ion can exist in aqueous solution only in exceedingly low concentrations, and the only Cu (I) compounds that are stable in water are the highly insoluble ones, such as chloride or cyanide (Cotton, Wilkinson 1972) . Some Cu (II) salts, including the chloride, nitrate, and sulphate, are soluble at low pH under oxidizing conditions (Cotton & Wilkinson, 1972). The carbonate, hydroxide, oxide, and sulphide are less soluble, particularly at pH 7 or higher. In alkaline waters with high carbon dioxide content, copper may precipitate as copper carbonate.

The Long term exposure to Cu can cause irritation of the nose, mouth and eyes. It can cause vomiting and diarrhea. Furthermore, the higher concentration may cause liver and kidney damage and even death. However, no research has determined its carcinogenicity (Piscator & Copper. 1979, WHO, 1984. The Health Canadian standard for Cu present in water is $\leq$ 1.0 ppm. This level is below the taste threshold for Cu in water, is protective of health, and contributes to minimum nutritional requirements.

Copper chemistry

Cu has a single *s* electron in its fourth shell. One may be inclined to think, based on its electronic configuration, that it has similar properties to the alkali metals. Cu (II) is the more stable than Cu (I). Copper chloride dissociates in aqueous solution to give the blue color of $[Cu\ (H_2O)_6]^{+2}$ and yellow or red color of the halide complexes of the formula $[CuCl_2^{+x}]^{x-}$. The solubility in water is 0.0075 mg/100ml at 25 ^{o}C. Simple Cu (I) compounds that can exist in the presence of water are

those with low-charge anions whose compounds are insoluble in water, $CuCl_2$, CuBr, CuI, and CuCn, In aqueous solution, Cu (I) is readily oxidized to Cu (II) in the presence of oxygen:

$$4Cu+ + O_2 + 4H^+ \rightarrow 4Cu^{2+} + 2H_2O \qquad (2\text{-}2)$$

Moreover, Cu (I) undergoes spontaneous autoredox:

$$2\ Cu^+ \rightarrow Cu + Cu^{2+} \qquad (2\text{-}3)$$

2.2.4 Trichloroethylene

Trichloroethylene (TCE) is an unsaturated, chlorinated, aliphatic compound (chemical formula C_2HCl_3) with a low molecular weight (131.4 g/mol). At room temperature, it is volatile, and has a high density (1.46 g/mL). Under conditions of normal use TCE is considered nonflammable, soluble in water (1.1 to 1.4 g/L). Generally TCE is produced by chlorinating ethylene or ethylene dichloride.

The fate of trichloroethylene released to the environment is influenced by transport processes, including volatilization, diffusion and advection, and by transformation processes, including photooxidation and biodegradation. TCE detected in all environmental media in Canadian environments. Critical data on concentration in surface water, groundwater and atmosphere is available in reports (Gov. of Canada, 1993). Schwille, (1988) stated that most of the TCE released onto soil surfaces will volatilize to the atmosphere. TCE presents in subsurface soil may be transported by diffusion, advection or dispersion of the pure liquid, as a solute in water, or by gaseous diffusion throughout the spaces within porous soils. However, the highest concentration of TCE will always be in groundwater. The Highest concentration detected on Canada is ranged between 102 mg/l to 12,950 mg/l in Ville Mercier landfill Quebec.

Both Canada health and EPA listed TCE in class schedule A as a toxic substance. For humans, it can cause variety of disorders, such as headaches, fatigue, memory loss, irritability, depression and reduced ability to think. It can cause kidney cancer, liver cancer, and cancer of the lymphatic system (Canada, 1993). For the environment, the Governments of Canada 1993 reports include all information for the toxicity of the TCE in both animals and wildlife. The maximum allowable

concentration for drinking water is in between 0 to 5 ppb. However, if concentration passes the allowable limit, immediate action should be taken to remove the contaminant (EPA, 2011).

Trichloroethylene chemistry

The chemical compound Trichloroethylene ($ClCH=CCl_2$) is colorless, non-inflammable with a sweet smell and is commonly used as a solvent. Degradation of chlorinated hydrocarbons can occur by four reductive mechanisms; three of which can be classified as dehalogenation reactions (Arnold et. al, 1999). These are hydrogenolysis reaction (Eq.1-4). Its elimination can be through β-elimination (Eq.1-5) or α-elimination (Eq.1-6), dehydrohalogenation (Eq.1-7) and hydrogenation (Eq.1-8).

$$Cl_2C=CCl_2 + H^+ + 2e^- \longrightarrow Cl_2C=CClH + Cl^- \quad (2\text{-}4)$$

$$Cl_2C=CCl_2 + 2e^- \longrightarrow ClC\equiv CCl + 2Cl^- \quad (2\text{-}5)$$

$$CCl_3H \longrightarrow CCl_2 + HCl \longrightarrow \text{variety of products} \quad (2\text{-}6)$$

$$RCl_2C\text{-}CClHR \longrightarrow RClC=CClR + H^+ + Cl^- \quad (2\text{-}7)$$

$$RClC=CClR + H_2 \longrightarrow RHClC\text{-}CClHR \quad (2\text{-}8)$$

The reactions (Eqs. 2-4 & 2-5) are the dominant pathways, with the major pathway determined by reaction conditions. Arnold et al. (1999) stated that, the proton availability may influence the rate of reaction in Eq.2-4. Also, they observed that the rate of hydrogenolysis of carbon tetrachloride by ZVI increases linearly with decreasing pH. However, the relationship between bulk pH and availability of protons at the metal surface is unknown. Chen et al. (2001) suggests that there is a trade-off between the increased degradation rate constant of TCE at a lower pH and the consumption of ZVI by corrosion thus effectively decreasing the surface area. They found that there was a maximum in the degradation rate at a pH of 4.9.

2.3 Remediation of polluted water

U.S. National Research Council (2005) grouped remediation technologies of groundwater containing organic and inorganic contaminants. The treatment classified to extraction and transformation of many of these remediation alternatives could be used for a variety of different pollutants. The extraction refers to the removal of the contaminant from the subsurface for subsequent aboveground treatment and disposal. Earlier extraction technologies included excavation besides pumps and treat methods. Transformation refers to the conversion of hazardous contaminants to less harmful forms. The transformation technologies include chemical oxidation, chemical reduction, thermal and surfactant treatments, cosolvent flushing and enhanced bioremediation. These technologies are successful in removing specific contaminants such as volatile organics in homogeneous sands. However, very few are considered effective to address DNAPL contamination especially in fractured bedrock. Also removing mixed contaminants especially organic and inorganic has not been investigated sufficiently (U.S. National Research Council, 2005). Sites contaminated with chlorinated hydrocarbons are difficult to address because they are hydrophobic and very persistent. They migrate in the subsurface and slowly dissolve in groundwater. Based on this report and other similar studies, existing technologies for the remediation of more persistent contaminants (i.e., chlorinated solvents and heavy metals) are rarely removed from polluted sites to meet drinking water standard. Rao et al., (2003) stated that the difficulty relates to the inability of existing remedial technologies to remove enough contaminant mass in the subsurface to significantly reduce dissolved aqueous phase concentrations. Until 1992, the predominant treatment technology to address groundwater contamination was the pump and treat method (Karn et al., in press; U.S.EPA, 2005). This treatment was very expensive and slow. The average pump and treat system operates for about 18 years (U.S. EPA, 2001). Public sites in the U.S. remediated by pump and treat have decreased to less than 20% in 2005 (Karn et al., 2009).

2.3.1 Treatment of the single contaminant

There are various physical and chemical methods used to treat waters contaminated by Pb (II), Cu (II), Cd (II) and TCE. Those methods can be broadly divided into the following categories: chemical methods, membrane, ion exchange, and solvent extraction and adsorption techniques.

Of all the treatment techniques, heavy metal hydroxide precipitation is the most commonly employed because of its low cost and simplicity. This process is quite simple as the pH of the effluent is increased by using lime (CaO) or caustic soda (NaOH) to precipitate and hence immobilize the heavy metals as their respective hydroxides. Lin et al., 2005 found out that lime and magnesium can precipitate Cd and achieve 99% removal efficiency.

Ku *et al.* (2002) reported that Cd could be removed from solutions by cementation with zinc powder. The optimum pH found was 4-5. The reaction rate was approximately first order with respect to both the amount of zinc and the concentration of Cd ion. Among the surfactants used in this study, only the presence of sodium dodecyl sulfonate, an anionic surfactant, noticeably enhanced the cementation rate of Cd by zinc powder. The presence of ethylene-diaminetetraacetic acid (EDTA) in aqueous solutions inhibited the removal of Cd by zinc due to the possible formation of Cd-EDTA chelates, which possess higher redox potential than that of free Cd ions.

Solvent extraction is another technique, which is used mainly for recovering separated metal ions from aqueous solutions having higher concentrations to obtain highly pure solutions (Takeshita *et al.,* 2004). The principle of solvent extraction is that when a metal ion solution is contacted with a solvent, the metal ion is distributed between the two phases. Liquid–liquid extraction from aqueous media by using specific extractants is also applied for separation of Cd (Takeshita et al*.,* 2004).

Table 1 presents some data and techniques used to remove and recover Cd and other metals. However, it can be seen that both precipitation and solvent extraction give high removal efficiency. However, the precipitation reaction rates are fast, and this makes it difficult to measure reaction rate (Lin et al., 2005). In case of solvent extraction, the contact time for organic and aqueous phase is only a few minutes and this separation technique is governed more through the distribution co-efficient (Reddy et al. 2006). The high cost of solvents coupled with solvent losses during continuous operations remains to be a costly affair, especially for water treatment (Reddy et al

2006). In case of separation by membrane the efficiency depends on the nature of membrane (Mortaheb et al. 2009). Some of the ion exchange resins like Amberlite IRC-718, Amberlite IR-120 are extremely efficient for cadmium - zinc separation when compared to Dowex 50W or S-950. But it remains a fact that this technique is more relevant for separation of Cd from multi cation containing solutions rather than for remediation of Cd (II) for treatment of water (Kumar et al., 2009, Touati et al., 2009, Reddy et al 2006).

The use of the electro-dialysis technique for the treatment of a wastewater containing metals was studied using different electro-dialysis cell (Marder *et al.,* 2003). Electrolysis allows the removal of metal ions from the solution in a solid metallic form for recycling. The advantage of this method is that there is no need for additional chemicals, and hence, there is no sludge generation. However, it is inefficient at low metal concentration and treating contaminants in groundwater in deep aquifers (Elektorowicz, 2009).

The adsorption process has many advantages such as low cost of adsorbent, easy availability, utilization of industrial, biological and domestic waste as adsorbents, low operational cost, ease of operation compared to other processes, reuse of adsorbent after regeneration, capacity of removing heavy metal ions over wide range of pH and to a much lower level, the ability to remove complex form of metals that are generally not possibly by other methods, environmentally friendly, cost effective and technically feasible alternative due to utilization of biomaterials (Rao et al. 2010). The activated carbon, synthetic metal oxides especially iron oxides/hydroxides, aluminum oxides/hydroxides, mixed Fe-Al oxides and doped oxides are generally the most common adsorbent (Sen and Sarzali. 2008). In order to develop low-cost adsorbents, a number of low grade ores and industrial wastes have been used to investigate the removal of action/anion uptake from water and wastewater treatment (Barton et al 1997). A number of low-cost adsorbents have been projected as potential candidates for removal of heavy metal from aqueous solutions. There is a lack of data on regeneration/reuse and safe disposal of loaded adsorbent. More attention needs to be paid to evaluate their commercial utilization.

Table 2.1: Compression of metal removals using different techniques

Techniques	Kinetic %	Initial Conc.	Final Conc.	Reference
Precipitation				
Aerophine 3481	99.7%	18 mg/l	0.05 mg/l	Rickelton ., 1998
Na_2S	99.9%	7500 mg/l	10 mg/l	Islamoglu et al., 2006
Lime/Mg/$(HO)_2$	100%	1 mM	Nil	Lin et al., 2005
Electro coagulation	≥ 99%	50-250 mg/l		Bazrafshan et al., 2006
Cementation				
Zinc powder	1st order	≤ 500 mg/l		Ku et al., 2002
Zinc powder	1st order			Younesi et al., 2006
Zinc powder +SDS	95.5%	6.5 µg/l	0.28 µg/l	Taha and Ghani, 2004
Membrane separation				
TOPS 99	99%	0.89 Mm		Swain et al., 2006
D2EHPA+TRPO	98.6%	0.18 mM	2.5 µg/M	He et al., 2007
Cyannex 923	85.8%	0.89 mM	0.13 mM	Alquacil and Navarro, 2001
Ion exchange				
Amberlite IRC-718	99.5%	20 mg/l	0.1 mg/l	Fernandez., 2005
Resin A	91%	1060 mg/l	96.46 mg/l	Wang and Fthenakis, 2005
Na-AmberliteIR120	93.4%	20 mg/l	1.32 mg/l	Kocaoba and Akcin, 2005
S-950	83.9%	1mM	0.16mM	Koivula et al., 2000
Dowex 50 W	97%	5 mM	0.15 mM	Pehlivan and Altun, 2006
Amberlite IR 120	97.4	20 mg/L	0.52 mg/L	Kocaoba, 2007
Solvent extraction				

0.15M D2EHPA	100%	4.45 Mm	Nil	Kumar et al., 2009
D2EHDTPA	99.1%	1 g/l	1µg/l	Touati et al., 2009
Cyanex 301		2.4 g/l	2.4 mg/l	Reddy et al 2006
Adsorption				
Activated carbon	99%	2 mg/l	0.1mg/l	Barton et al. 1997
Synthetic iron oxides	99.5%	10 ppm	0.1ppm	Sen *et al.*, 2002
Synthetic aluminum oxides	99.9%	1 mg/l 2 mg/l	0.5 mg/l	Sen and Sarzali 2008
Synthetic manganese oxides	99%		0.01 mg/l	Tripathy *et al.* 2006
Biosorbents	100%			Volesky, 1995

2.3.2 Treatment of mixed metal contaminant

Competition of metals or displacement on solid surface is complicated and influence by multitude of factors. However, there have been relatively few studies discuss the fundamental aspect of competition between two or more metals which both strongly get adsorbed.

Benjamin and Leckie, (1980a, b) studied the competitive removal of Cd, Cu, Zn and Pb on amorphous iron oxyhydroxide. The conditions were such that if the metals competed for the same group of surface sites, the weaker binding metal should be reduced whenever the second metal was added to the solution. Nevertheless, competitive interactions were minimal, which indicated that many of binding strong sites are not available for other metals. Christophi and Axe (2000) studied the competition of Cd, Cu, and Pb adsorption of goethite. They state that the adsorption of these mixed metals depends on nature of the metal ion, oxide surface and metal electronegativity. Fig. 2.1 shows that the adsorption of the metals follows the order of Cu > Pb > Cd. The degree of affinity is a function of site capacity and the equilibrium constant, which often coincide with the electronegativity of the ions. They concluded that electronegativity plays a major role in the

adsorption of metals on goethite more than the ionic radii or hydrated radii (Table 2-1). Their observations were in agreement with results of other studies. The metal speciation can be defined at pH 6 where metal become uncomplexed divalent. However, both hydrated radii and electronegativity play a role in the competition between Cr (II) and Cd (II) adsorption. Cr (II) which has a smaller hydrated radius and a greater electronegativity has a higher affinity for sites than Cd (II). However, in the case of Cd (II) and Pb (II), 97% of Cd (II) was replaced by Pb (II) due to its extremely high site adsorption characteristics. In case of Cr (II), Pb (II), Cr (II) displaced Pb (II) due to the fact that both metals were competing for the same site. Speciation in this case is not a contributing factor as the only difference is related to 0.1% increase in Cr (II) ion concentration (Christophi and Axe, 2000). . However, studies of Schwets and Taylor (1989) found that Co has a greater affinity than Ni, although Ni has a greater electronegativity than Co. The difference in metal adsorption of Cr (II), Pb (II) and Cd (II) range from 10 to 90 % at different pH. Gao and Mucci, (2001) have shown that high concentrations of phosphate (PO_4^{3-}) in synthetic water decrease sorption capacity of iron oxide.

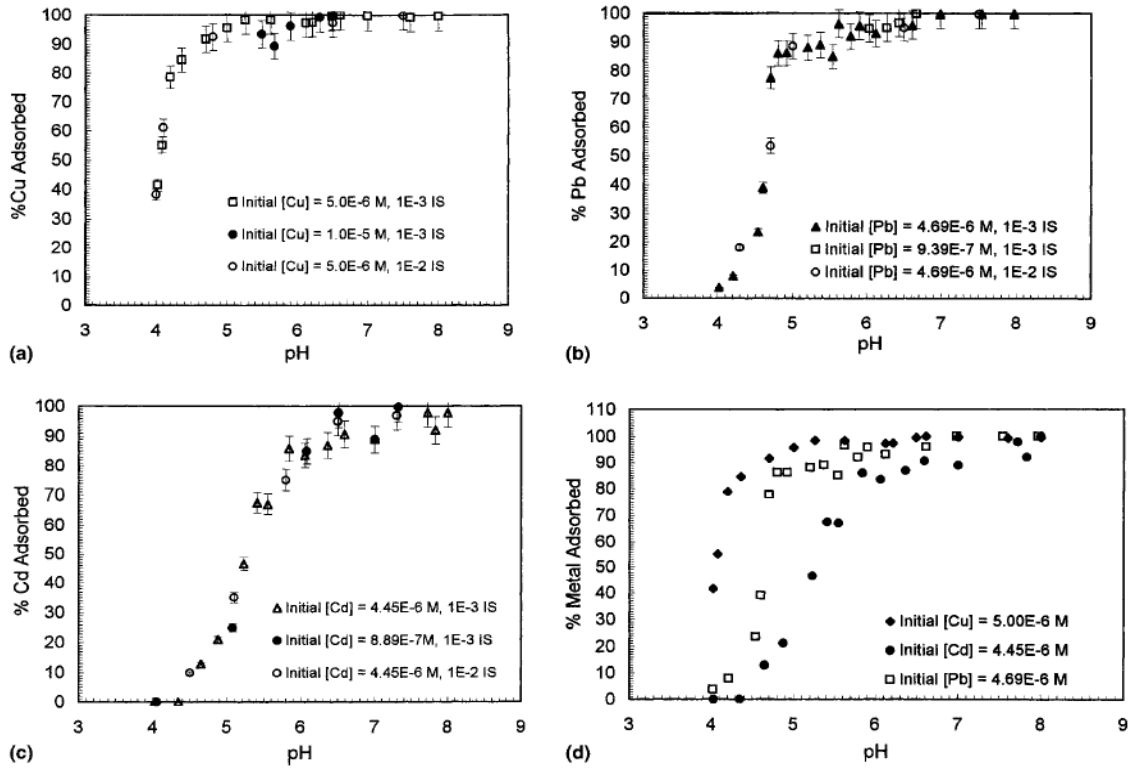

Fig 2.1: Adsorption using 1 g/l goethite, 4- hr equilibrium. Adesorption a: Cu, b: Pb, C: Cd: D: mixed , Cu, Pd, Cd. Taken after (Christophi and Axe 2000)

More recently, Chowdhury and Yanful (2010) used magnetite maghemite nanoparticles to determine the effect of phosphate on the removal efficiency of As and Cr. Their results conclusively demonstrated that more than 50% reduction of As and Cr removal occurs whenever phosphate was present. Fig. 2.2 presents that the concentration of phosphate increase as the As uptake decreases.

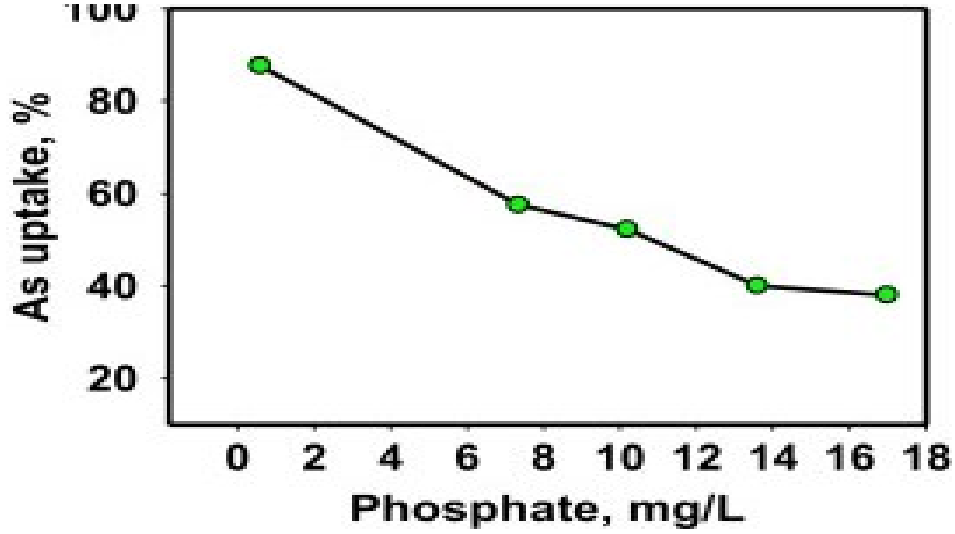

Fig. 2.2: Effect of phosphate on total arsenic uptake (%) from spiked groundwater at pH 6.5. (Total arsenic Conc: 1.13 mg/L) taken after (Chowdhury and Yanful, 2010)

2.3.3 Treatment of mixed organic and inorganic contaminants

The treatment of mixed contaminants poses a challenge to environmental remediation technologies because of the vast difference in the physicochemical properties of the contaminants to be treated. This is particularly true when we are dealing with aliphatic chemicals, such as polychlorinated biphenyls (PCBs), hydrocarbons, and polar contaminants, such as heavy metals and radionuclides. Consequently, mixed pollutants can be removed only in small quantities. This may not meet the regulations.

Reddy and Cameselle (2009) studied the electrokientic removal of multiple heavy metals from porous media. They concluded that it is essential to understand the main parameter affecting the transport and electrokientic phenomena. The ionic mobility is related to the ionic valance and the molecular diffusion coefficient of species, the retardation effect caused by the affinity of heavy

metal in matrix, and the chemical form of metal presented in the media. Generally, the electrokientic remediation of mixed contaminants shows lower removal efficiency than that for individual metal contaminants. Despite of advancement of the remediation technology, there are still some limitations on the removal of mixed metals such as Cr, Cd and Pb (Reddy and Cameselle. 2009). The need for further studies related to simultaneously removal of mixed metals was emphasized by Kang et al. (2008).

Elektorowicz, (2009) stated that mixture of organic and inorganic contaminants especially from petroleum source can pose a difficult challenge for remediation technology. Whenever, the organic and inorganic contaminants are present, their behavior and properties can get altered. This could make it difficult to achieve the removal of the target contaminants. Also it was concluded that the mobility of inorganic contaminants to the solid surface in the present of organics could be difficult. Using either integration treatment such as applying an electric field can enhance ionic migration and metal removal. However, it was also noted that it can be difficult if several contaminants are simultaneously present. As such, it was observed that further studies are needed in the area of mixed contaminant removal.

2.4 Zero valent iron (ZVI)

The use of zero-valent iron (Fe^0) is promising a reactive medium for water treatment, because of it's of low-cost, availability, effectiveness and its ability to degrade contaminants (Lee et al 2003). To date, granular ZVI has been used for many years at numerous sites (Nowack, 2008) in the form of preamble reactive barrier (PRB) and they are still the state-of-the-art technique. Their major drawback is that they can only address contaminants that flow through the barrier.

The mechanism of degradation of contaminants in the presence of iron is not fully understood. There are many studies related to degradation mechanism comprising heterogeneous reactions (Nowack, 2008). The reactions occur when the reactant molecules reach the iron solid surface. They then associate with the surface at sites that may be either reactive or nonreactive. Competition can also occur between the reactant solute of interest and other solutes for the available sites (Nowack, 2008). The reactive sites refer to those where the breaking of bonds in the reactant solute

molecule take place (i.e. chemical reaction) whilst non-reactive sites are those where only sorption interactions occur and the solute molecule remains intact.

2.4.1 Degradation of organics by ZVI

ZVI has been used to rapidly dehalogenate a wide range of halogenated organic compounds (Gillham et al 1994, Janda et al 2004). The degradation hypothesis for halogenated compounds by iron is better accepted as there is a reductive dehalogenation of the contaminant coupled with corrosion of the iron. With a standard reduction potential ($E_h\pm$) of -0.44 V, ZVI primarily acts as a reducing agent. Iron is oxidized (Eq.2-9) while alkylhalides (RX) are reduced (Eq.2-10). Because the estimated standard reduction potentials of the dehalogenation (half-reaction) of various alkyl halides range from + 0.5 to + 1.25 V at pH 7 (Ghauch, et al 2001), the net reaction is thermodynamically very favorable under most conditions Eq. 2-11.

$$Fe^0 \longrightarrow Fe^{2+} + 2e^- \qquad (2\text{-}9)$$

$$RX + 2e^- + H^+ \longrightarrow RH + X^- \qquad (2\text{-}10)$$

$$Fe^0 + RX + H^+ \longrightarrow Fe2^+ + RH + X^- \qquad (2\text{-}11)$$

For example, groundwater contaminated with chlorinated solvents such as trichloromethane (TCM), trichloroethylene (TCE) and perchloroethylene (PCE) are treated using iron barriers. The preferred electron acceptor is typically dissolved oxygen under aerobic conditions (E_h +1.23 V). This acceptor can compete with chlorinated hydrocarbons that have similar oxidizing potentials to oxygen. Aerobic groundwater enters the iron fillings wall and causes the oxidation of metallic iron (Fe^0) to ferrous iron (Fe^{2+}), with the subsequent release of two electrons (Eq. 2-9). Chlorinated solvents also react as electron acceptors, resulting in dechlorination and release of a chloride ion (Eq. 2-10). The reaction takes place in several steps resulting in reducing halogenated organic compounds through intermediates to non-toxic compounds such as ethylene, ethane, and acetylene (Farrell et al 2000). Intermediate compounds like vinyl chloride, which has a higher toxicity than the original compounds, are not formed in high concentrations (Janda et al. 2004).

Zero-valent iron also reacts with water producing hydrogen gas and hydroxide ions resulting in an increase in the pH of water (Eq. 2-12). The resulting hydrogen gas can also react with alkyl halides (Eq.2-13).

$$Fe^0 + 2H_2O \longrightarrow Fe^{2+} + 2OH^- + H_2 \qquad (2\text{-}12)$$

$$RCl + H_2 \longrightarrow RH + HCl \qquad (2\text{-}13)$$

According to Deng, et al (1999) the bulk dehalogenation reaction is usually described by first-order kinetics. They found that the lower the degree of chlorination, the slower the rate of dechlorination. Batch and column tests have also indicated highly variable degradation rates due to operating conditions and experimental factors such as pH, metal surface area, concentration of pollutants, and mixing rate. Wang, et al. (1997) suggested that since the reaction is heterogeneous, the rate of reaction is proportional to a specific surface area of the iron used. Therefore the adsorption, desorption or diffusion of reactants and chemical reaction itself can limit the processes. Several limitations of this technique, including the accumulation of chlorinated by-products and the decrease in the activity of iron over time have been reported (Doong et al. 2003). Wang, et al. (1997) improved methods that involve physical and chemical processes which increase the surface area of iron by reducing its particle size to enhance reactivity.

2.4.2 Removal of heavy metals by ZVI

ZVI has been widely studied for removal of heavy metals such as chromium, arsenic (Nikolaidis et al. 2003, and Lee et al. 2004). The removal mechanisms are based on transformation from toxic to non-toxic forms or adsorption on the iron surface depending on the type of heavy metals. The removal of chromium by ZVI is based on transformation from toxic to non-toxic forms. Hexavalent chromium, which is a strong oxidant, a potential carcinogen and more mobile in soils and aquifers, is transformed to trivalent chromium [Cr(III)], which is less hazardous and less water soluble and associated with solids (Lee et al 2003). The reduction rate (Eq. 2-14) of Cr (VI) by ZVI produces ferric ion Fe (III) and chromium ion (Cr III). Nikolaidis et al (2003) state that Cr (III) may be removed through the precipitation or co-precipitation of mixed Fe(III) and Cr(III) hydroxide as shown in (Eq. 2-15) or (eq. 2-16).

$$Cr^{6}+ + Fe^{0} \longrightarrow Cr^{3+} + Fe^{3+} \quad (2\text{-}14)$$

$$(1\text{-}x)Fe^{3+} + (x)Cr_3+ + 3H_2O \longrightarrow (Cr_xFe_{(1-x)})(OH)_3\ (s) + 3H^{+} \quad (2\text{-}15)$$

$$(1\text{-}x)Fe^{3+} + (x)Cr_3+ + 3H_2O \longrightarrow Fe_{(1-x)}Cr_xOOH\ (s) + 3H^{+} \quad (2\text{-}16)$$

Buerge et al (1999) found that the reduction rate of Cr (VI) by Fe^0 is accelerated when mineral surfaces such as goethite (FeOOH) and aluminum oxide (...-Al_2O_3) are present and the pH of the solution is low. They stated that the reaction rate is quite fast compared with the result presented in literature. Therefore, it was concluded that, the oxidation of the Fe^0 and Fe (II) is not only dependent on the type of contaminants but also the operating conditions. However, in case of arsenic, Daus, et al. (2004) stated that, its removal by zero-valent iron does not involve reduction to metallic form, it only involves surface complexation.

2.5 Zero valent iron nanoparticles (nZVI)

The nanoparticles (<100 nm) discussed in this contribution are zero-valent iron (ZVI) particles and exhibit a typical core shell structure as shown in Fig. 2.3. The core consists primarily of zero-valent or metallic iron while the mixed valent (i.e., Fe (II) and Fe (III)) oxide shell is formed as a result of oxidation of the metallic iron. Iron typically exists in the environment as iron (II) and iron (III) oxides, and as such, ZVI is a manufactured material. Thus far, applications of ZVI have focused primarily on the electron-donating properties of ZVI. Under ambient conditions, ZVI is fairly reactive in water and can serve as an excellent electron donor, which makes it a versatile remediation material.

The nZVI technology can be an extension of using ZVI-PRB technology of reactive barrier. Because of their small size, nanoparticle slurries in water can be injected under pressure and/or even by gravity flow to the contaminated area and under certain conditions to remain in suspension and flow with water for extended periods of time (Zhang et al 2006).

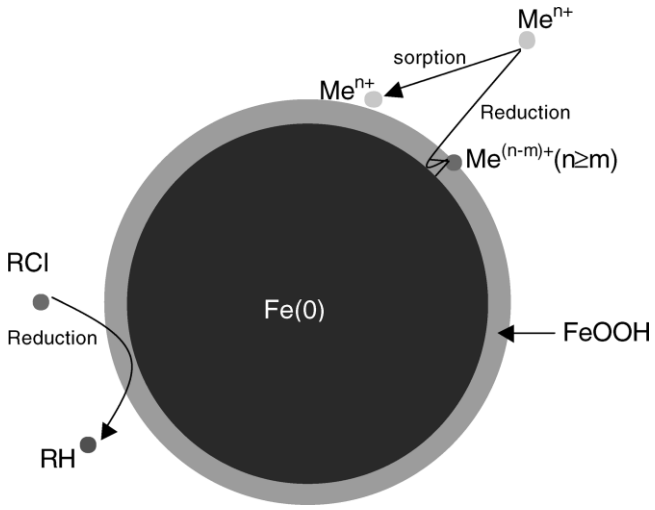

Fig. 2.3: The core-shell model of zero-valent iron nanoparticles (taken after (Li et al. 2009)

Over the past decade, extensive studies have demonstrated that ZVI nanoparticles are effective for the treatment of many pollutants commonly identified in groundwater, including perchloroethene (PCE) and trichloroethene (TCE), carbon tetrachloride (CT), nitrate, energetic munitions such as TNT and RDX, legacy organohalogen pesticides such as lindane and DDT, as well as heavy metals like chromium and Pb . Dozens of pilot and large-scale in-situ applications have also been conducted and demonstrated that rapid in-situ remediation with nZVI can be achieved Muller and Nowack. 2010)

Robust methods for large-scale and cost-effective production of nanomaterials are essential to the growth of nanotechnology. Soils/water treatments often require usage of considerable quantities of treatment reagents and/or amendments for the remediation of huge volumes of contaminants. Unlike many industrial applications, environmental technologies often exhibit relatively low market values. Therefore, the application of these technologies can be particularly sensitive to the costs of nanomaterials. This may have been the main factor for the relatively slow advancement of nanotechnologies in water and soils contaminants.

Zhang (2003) present two general strategies in synthesizing the nZVI of nanoparticle. The first one is top-down and bottom-up, which start with large size (i.e., granular or microscale) materials with the generation of nanoparticles by mechanical and/or chemical steps including milling,

etching, and/or machining. The second one is involve the growth of nanostructures atom-by-atom or molecule-by-molecule via chemical synthesis, self-assembling, and positional assembling. Both strategies have been successfully applied in the preparation of nZVI nanoparticles. For example, ZVI nanoparticles have been fabricated by vacuum sputtering, synthesized from the reduction of goethite and hematite particles with hydrogen gas at elevated temperatures (e.g., 200–600◦C) by decomposition of iron pentacarbonyl ($Fe(CO)_5$) in organic solvents or in argon, and by electrodeposition of ferrous salts. Eq. 2-17 represents the generation of nZVI by the "bottom-up" reduction of ferric (Fe (III)) or ferrous (Fe (II)) salts with sodium borohydride:

$$4Fe^{+3} + 3BH_4^- + 9H_2O \rightarrow 4Fe^0 \downarrow +3H_2BO^{-3} + 12H^+ +6H_2 \uparrow \quad (2\text{-}17)$$

A major advantage of this reaction is its relative simplicity with the need of two common reagents and no need for any special equipment/instrument. It is achieved by adding 1:1 volume ratio of 0.25 M sodium borohydride into 0.045 M ferricchloride solution. Each ZVI nanoparticles produced by the different methods differ in their structural configurations, size distribution, surface area, different reactivity and aggregation properties. Comprehensive studies are needed to order to investigate the physical and chemical properties of the new born reagent.

2.5.1 Nano-particle characteristics

Although information on nZVI nanoparticle is extremely important, few studies have been published on the investigation of the nZVI surface properties. The reaction mechanism, kinetics, intermediate/product profile as well as, transport, distribution and fate of nanoparticles on the media depend on the surface properties (Muller and Nowack 2010).

Fig. 2.4 represents the (TEM) images of nanoparticle produced by borohydride. The particles are almost spherical in shape and they have diameters ranging between 60 to 100 nm. The average particle surface area is between 30 - 35 m^2/g. More detail can be found on (Muller and Nowack 2010).

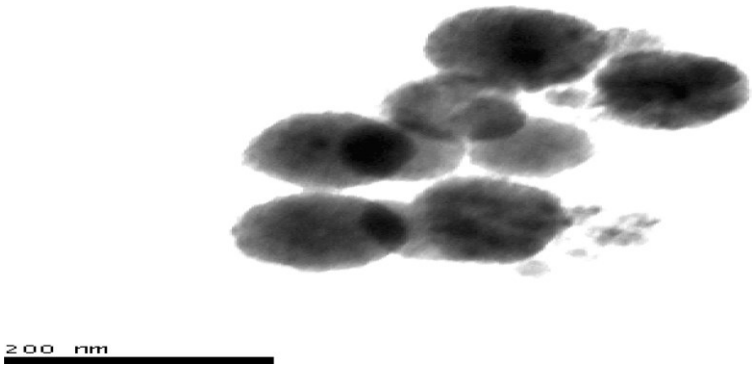

Fig. 2.4: TEM image of nZVI produced by borohydride (taken after Li et al. 2009)

nZVI can exhibit metal-like or ligand-like coordination properties depending on the solution chemistry. Solution has pH 8, the nZVI characterize as positively charged and attracted more anionic ligands such as sulfate and phosphate However, if pH is above 8 the nZVI will carry negative charge and can form surface complexes with metal ions. ZVI (Fe^{+2}/Fe) has a standard reduction potential (E_o) of -0.44 V, which is lower than most of metal ions and chlorinated hydrocarbon. This makes it an excellent agent to reduce and react with different contaminants (Li et al 2006).

nZVI is not particularly stable. In dry form, the powder ignites immediately when in contact with air. Storage in dry form is only possible in an inert atmosphere. For safety reasons, nZVI is thus in most cases provided as a slurry. However, in suspension, it also oxidizes fairly rapidly to iron oxides. Possible oxidants – besides the target contaminants - are oxygen, sulphate, nitrate or water. This fact has implications not only for the application in the soil, but also for its transport and storage. nZVI suspensions may have to be transported in air-conditioned containers to minimize oxidation reactions and thus H_2 production. For these reasons, the transport and storage time should be kept minimal (Lowry et al. 2005).

The particle inherent mobility depends mainly on two factors: size (degree of aggregation) and pretreatment (dispersion, surfactants). It is not yet clear if a primary particle and an aggregate of the same size behave differently. Zhang (2003) studied the mobility of nZVI in soil. He found that the particles tend to agglomerate and adhere to soil surfaces resulting in a limited dispersion below ground and thus in a less effective treatment of the contaminated ground water. However, Lowry

et al. (2005) found the transport of unmodified Nanoiron in porous media is limited to a few meters. Experiments have also shown that the mobility of untreated pure nZVI was even limited to a few centimeters. Particles treated with magnetite and coated with a surfactant moved around 10 cm. proceeding of EPA nanotechnology workshop (2005) indicated that dispersion of nZVI in soil or pores medium from 3-30 m considered be a realistic. Zhang (2003) studied the mobility of nZVI of different sizes. They found that particles with 100-150 nm have the highest mobility. They estimate that, depending on the permeability of the soil, particles between 0.1-5 μm have the highest mobility.

Phenrat et al. (2007) studied the aggregation of nZVI particles at different concentrations by dynamic light scattering. They found that at very low nZVI concentrations (about 2 mg/L) the particle size increased from 20 nm to a final size of about 125-1200 nm after 10min. At high concentrations about 60 mg/L, most of the particles reached their final size between 20-70 μm after 30 minutes. They concluded that the individual particles should be designed to have a range of 20 to 50 nm. Since the nanoparticles interact with soils which limit its mobility and dispersion, it was necessary to increase mobility to reach the desire area. One possibility is by coating the particles surface with polyelectrolyte, surfactants, and cellulose/polysaccharides (U.S.EPA, 2005). (Lowry et al. 2005) states that it is possible to select the distance one would like the particles to move based on the surface coating. However, it is important to note that the design of particles is always a tradeoff between high reactivity and stability/mobility. Other possibilities to increase the stability, reactivity and/or the mobility of nZVI-particles are to combine them with other metals bimetallic nZVI, carbonaceous material nZVI on carbon support or embed the particles in organic membranes emulsified nZVI.

2.5.2 Modified nanoparticle

The iron nanoparticles are colloidal in nature and exhibit a strong tendency to aggregate as well as adhere to the surfaces of natural materials such as soil and sediment. Increasing efforts have been directed on the dispersion of iron nanoparticle. Bimetallic iron nanoparticles, in which a second and often less reactive metal such as Pd, Ni, Pt, or Ag can be prepared simply by soaking the freshly prepared nZVI in a solution of the second metal salt (Karn et al., 2009, Nowack, 2008, U.S.EPA,2005). Houben and Kringel, (2007) prepared new nZVI by soaking new freshly

nanoparticle with other bimetallic particles such as Fe/Ag and Fe/Ni to form BZVI. The resulting BZVI has a higher reaction rate but consequently a shorter lifetime and toxicity. Several other modified nZVI studies are reported by Muller and Nowack (2010).

2.5.3 Reactions of nZVI with contaminants

The range of possible applications is wide, as nZVI can not only effectively degrade or immobilize organic contaminants (TCE, BCE, PCB and other organochlorine pesticides), it can also remove/recover inorganic anions such as Cd, Ni, Zn, As, Cr, Ag, and Pb (Zhang et al., (2003); Parbs and Birke., 2005; Muller et al., 2006; Rickerby and Morriso., 2007; Nowack., 2008). According to David Sedlak (EPA, 2005) nZVI acting as an oxidizing agent might also be used to treat low concentrations of recalcitrant, miscible, volatile organics such as MTBE, MTBA, and 1,4-dioxane.

nZVI will react with dissolved oxygen, water and if present with other oxidants such as nitrate and possible contaminants (Zhang et al. 2003). The application of nZVI results in an increase of pH and a decrease of the oxidation-reduction potential, due to the redox reactions taking place (Zhang et al. 2003, Nowack, 2008). The consumption of oxygen further leads to an anaerobic environment while the reduction of water yields hydrogen. If chlorinated hydrocarbons are present, the following reaction takes place.

$$R\text{-}Cl + Fe^0 + H_2O \longrightarrow R\text{-}H + Fe^{2+} + Cl^- + OH^- \quad (2\text{-}18)$$

Karn et al (2009) found that there are two pathways for the degradation of chlorinated hydrocarbon by nZVI. The first is hydrogenolysis (Eq. 2-4) through sequential dehalogenetion (PCE to TVE to DCE to VC to ethane). The second pathway is through beta elimination (TCE to acetylene).

Several studies have investigated the reduction and complexities of metals ion on nZVI. As it is stated earlier, ZVI can rapidly remove or reduce metal ions and has higher capacity than conventional sorptive media. For instance, Zhang, (2007) studied the reaction between ZVI and Cr (IV). They found that the reaction is a pseudo first order in which the rate constant is normalized to the total surface area of iron. Cr (VI) is reduced to Cr (III), which is then incorporated into the iron oxide layer as $(Cr_xFe_{1-x})(OH)_3$ or $Cr_xFe_{1-x}(OOH)$. Also, Chowdhury et. al., (2010) studied

the removal of arsenic and chromium by mixed magnetite maghemite nanoparticle. Using different batch techniques, the nanoparticle solution was used to uptake the desired metal from different water simples. The results achieved 96-99% removal efficiency under controlled pH conditions. The maximum adsorption capacity achieve at pH 2 for both As and Cr. However, in the presences of an anion such as phosphate, sulfate, the removal efficiency decreases, as an anion concentration increases (Aguila et al. 2001).

2.5.4 Application of nanoparticles for groundwater contaminants

Several studies have been completed in the area of removing and degrading organic and inorganic contaminants in groundwater using nanoparticles. Elliott and Zhang (2001) reviewed the application of iron nanoparticle for groundwater remediation. Significant research innovations have been made in terms of synthesizing nanoparticles modification to enhance field delivery and reactions by modifying particle surface properties. Nanoparticles could be applied along with common remediation technologies (Karn et al. 2009). Muller et al (2012) and Karn et al. (2009) have compiled a comprehensive overview of some of the sites treated with nZVI (Table2.2 and Fig 2.5). Most of these sites are located in the USA and Europe and details can be found at the website of the Project on Emerging Nanotechnologies. Comprehensive descriptions of case studies in the USA are found in the proceedings of an EPA workshop (EPA 2005). Nonetheless, there are still considerable knowledge gaps on many fundamental scientific issues such as fate, transport, and effect of mixed organics and inorganics, as well as the impact on the environmental and economic hurdle, which down grade the acceptance of the technology within both the researcher and the private sector (Muller et al. 2012).

The nZVI undergoes random motions which make it difficult to control their physical movement or transport in groundwater. The absences of the electrostatic forces between particles disperse the particles and make it easier to suspend them water (Zhang. 2003). However, coating the nZVI to improve mobility and reaction rates is essential. In most of the field studies, the particles flowing with the groundwater remain in suspension for a longer period of time, whereas other nanoparticles bind to soil particles during injection make an in situ treatment zone (Muller et al. 2012).

The first field application using nZVI to remove TCE from groundwater was reported in 2000 (Zhang 2003). It was noticed that the particles remained reactive in both soil and groundwater for more than 8 weeks and could flow with the groundwater for almost 20 m from the injection wells. 99% reduction of TCE was achieved within the period of the remediation. Muller et al. (2012) has reported that in Europe, several pilot remedial actions are going on in which 70% dealt with chlorinated ethenes (PCE, TCE, DCE) or other chlorinated hydrocarbons (PCB), 20% of other carbonaceous materials (BTEX, HC, VC), and 10% involved the immobilization of metals (Cr, Ni). Applications in the USA (EPA 2010), using nZVI was in most cases used to treat a source zone of TCE, and Cr (VI). Golder Associates suggests nZVI for the individual treatment of chlorinated solvents, Cr (VI), and perchlorate, while Aquatest Company applied nZVI for both source and diffuse zones (Mueller et al 2012). At the site contaminated by TCE in Czech Republic for instance, the contaminated area was around 2,000 m^2. One ton of TCE was treated at a depth of 20–35 m below the surface. In total, 2000 kg of nZVI were injected. The results showed a significant decrease in TCE concentration from 40–80%. The remediation began at the end of 2009 and followed one year later by the second injection. Three months later, the concentration of TCE dropped to 20% of the initial concentration (Table 1.2). Project details are listed by Muller et al. (2012). In Permon, CZ (2006) which is a mining development company treated site contaminated with Cr (VI) using RNIP nanoparticle. The area contaminated was almost 1000 m^2 and the depth of groundwater was 30-35 m. Two months later, the concentration of Cr (IV) decrease up to 70% of the initial concentration. Nine months later, with the second injection, almost 20-30% concentration dropped from the initial concentration leaving some area free of Cr (IV). However, the concentration drop was not uniform in all the areas which may due either the nanoparticle suspended during the injection or utilize by the present of microorganism in the bedrock (Nanoiron, 2010). No significant pilot studies either in Europe or US have been listed on the remediation of groundwater with other metals or metal alloy contaminants such as Cd, Cu, Ni, and Pb and As or mixed wastes containing both organics and inorganics.

An important aspect for the use of nZVI in groundwater remediation is the adequate site characterization including information about site location, geologic conditions, and the concentration and types of contaminants (Rickerby and Morrison 2007). Soil matrix, porosity, hydraulic conductivity, groundwater gradient and flow velocity, depth to water table, and

geochemical properties (pH, ionic strength, dissolved oxygen, ORP, and concentrations of nitrate, nitrite, and sulfate) are variables that are to be considered. All these variables are to be evaluated before nanoparticles are injected to determine whether the particles can penetrate the remediation source zone, and whether the conditions are favorable for reductive transformation of contaminants. The sorption or attachment of nanoparticles to soil and aquifer materials depends on the surface chemistry (i.e., electrical charge) of the soil and nanoparticles, groundwater chemistry (e.g., ionic strength, pH, and presence of natural organic matter), and hydrodynamic conditions (pore size, porosity, flow velocity). The reactions between the contaminants and nZVI depend on contact between the pollutant and nanoparticles (EPA, 2005).

Table 2.2: Pilot tests with nZVI (based on Muller et al. 2012 and EPA, 2010)

Site	year	Contaminant	nZVI kg	nZVI conc. g/l	Particle type	Injection technique	Media
Uzin, CZ	2009	Cl-ethenes	150	1-5	Nanofer 25	Infiltration drain	Low permeable aquifer
Rozmital Cz	2007-2009	PCB	150	1-5	RNIP Nanofer	Infiltration well	Fractured bedrock
Spolchemie, CZ	2004-2009	Cl-ethenes	20	1-10	Fe(B), Nanofer	Infiltration well	Porous aquifer
Uhersky bord, CZ	2008	Cl-ethenes	50	1-5	Nanofer 25	Infiltration well	Porous aquifer
Hluk, CZ	2007-2008	Cl-ethenes	150	1-5	RNIP Nanofer 25	Infiltration well	PRB filter
Hannover, D	2007	CHC, BTEX , HC	1	n.a	na	Infiltration well	Unspecified
Asperg, D	2006	Cl-ethenes	44	30	RNIP	Sleeve pipe	Fractured bedrock
Gaggenau, D	2006	PCE	47	20	RNIP	Sleeve pipe	Porous aquifer
Permon CZ	2006	Cr (VI)	7	1-5	RNIP	Infiltration wells	Fractured bedrock
Kunivody, CZ	2005-2006	Cl-ethenes	50	1-10	Fe (B), RNIP	Infiltration wells	Fractured bedrock
Biella, I	2005	TCE, DCE	10	1-10	nZVI	*Gravity infiltration*	Porous aquifer

Table 2.2 Continued							
Piestany, CZ	2005	Cl-ethenes	20	1-5	Fe (B)	infiltration	High permeable aquifer
Schonebeck, D	2005	CAH, Ni, Cr(VI), nitrate	120	10	nZVI	Injection wells	Porous aquifer
Brownfield, Sk	n.a	TCE, DCE	na	na	n.a	n.a	Unconsolidated sédiments
Lakehurst, NJ	2005-2006	TCE , PCE 0.9, 1.2 mg/l	137	2	BNP	Injection wells	sand and gravel
Former UST site CERCLA & RCRA	2004-2007	PCE, TCE ,TCA 0.26 , 26 8.5 mg/l,	173	10	BNP	Injection wells	Medium grained sand and sandy fill.
Patrick AFB, OT-30 CERCLA & RCRA	2005-2010	TCE 150 mg/l	na	na	EZVI	High pressure pneumatic injection	fine to medium grained sands with occasional silt/clay
Phoenix Goodyear Airport – North CERCLA & RCRA	2010	TCE, PCE Perchlorale 3.5-11 mg/l	na	2.1	nZVI	Injection wells	middle fine-grained unit, and lower conglomerate unit
Santa Maria, CA CERCLA	2008-2009	TCE, DCE 2.5 mg/L	na	na	Nanoscale porous metallic iron	Injection wells	sands, silts, and clays
Passaic, NJ	2005	TCE 1.4 mg/l	na	na	nZVI	Injection wells	Soils are composed of high permeability sands from
Rochester, NY	2004	Methylene chloride, 1,2-DCP, 1,2DCA 500 mg/l	100	10-20	nZVI	Injection wells	Fractured sedimentary bedrock.

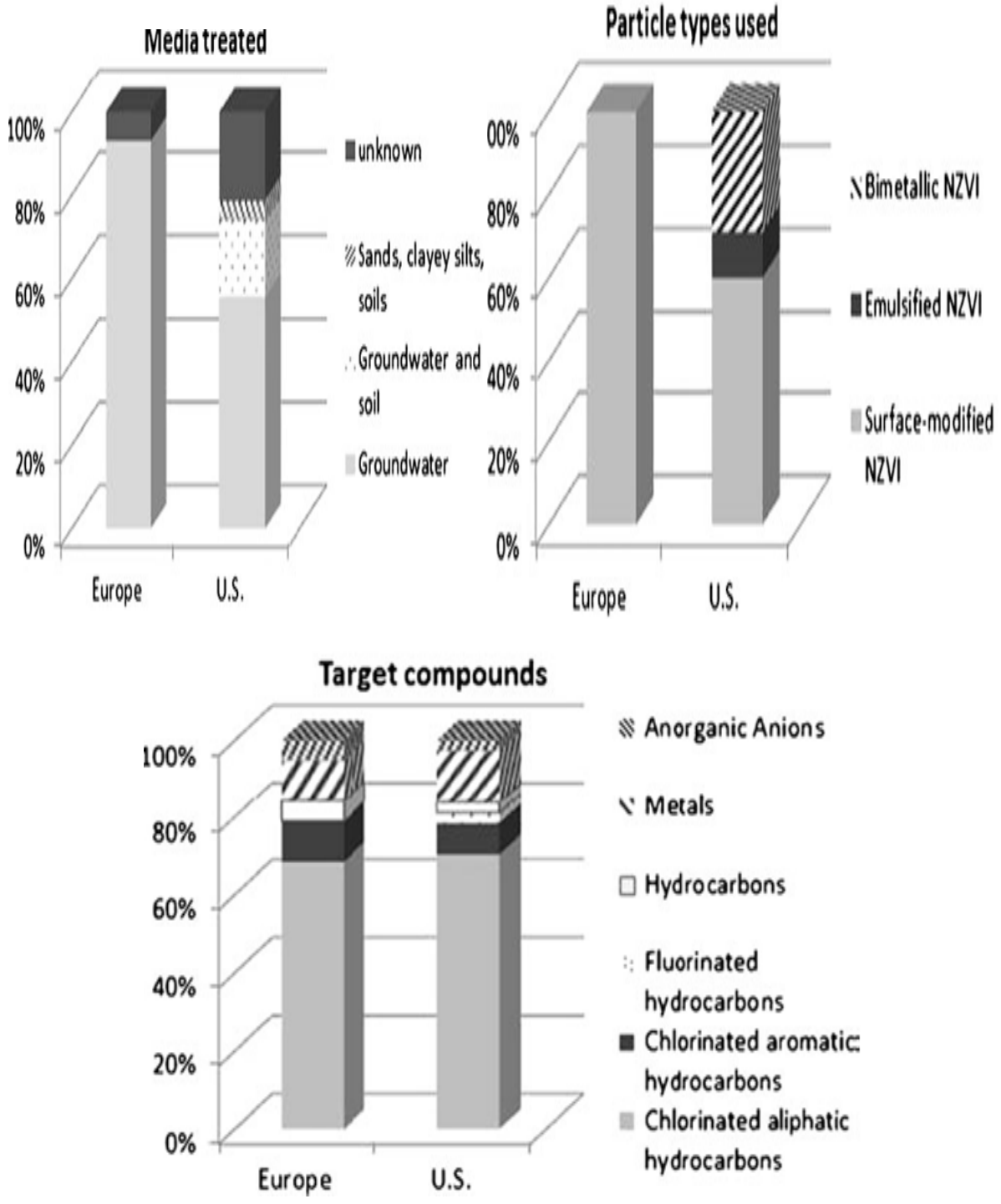

Fig 2.5: Comparison of the media treated, particle types used, and target compounds of nZVI-applications in Europe and USA. (Muller et al 2012, EPA, 2010 and Karn et al 2011)

2.5.5 Impact of nZVI particle size on adsorption equilibria and rate of reaction

The biggest feature of nanoparticle is its unique size which provides a huge surface area, a high adsorption capacity, an ability to remain in suspension, and possess high mobility in environmental media. However, evidence suggests that iron nanoparticles have a strong tendency to form much larger aggregates and particles precipitate. These characteristics lower the rate of reaction, and decrease the surface area (Li et al. 2006). Li et al. (2006) studied the impact of nano/micro ZVI particle size distribution on the adsorption equilibria and the rate of reaction. They found that the nano-ZVI promises to be significantly more effective than micro-ZVI. The reaction rates for the nano-ZVI are 25-30 times faster and the sorption capacity is much higher compared with micro-ZVI. It is suggested that, this is due to the large reactive surface area with 2-5 nm particles giving approximately142 m^2/g. nano-ZVI has surface areas up to 30 times greater than micro-ZVI which results in 10 -1000 times more reactivity (EPA, 2005). Li et al. (2006) studied the impact of ZVI developed on nanotechnology lab center, Lehigh University on the removal of Cr (VI). It was found that one gram of nano-ZVI can reduce and immobilize 65–110 mg Cr (VI). In comparison, the capacity for Cr (VI) removal by mico-ZVI is only 1–3 mg Cr (VI) per gram of micro- ZVI. Furthermore, the reaction rate with the ZVI nanoparticles is at least 25–30 times faster. Also, the reduction of nitrate by nano-ZVI was faster than micro-ZVI even at high pH (e.g., 8-10). Another study done on Nanotechnology Lab at Lehigh University is the removal of Perchlorate using nano/ micro ZVI. The perchlorate is persistent in the environments due to its intrinsic chemical stability. The ZVI in both sizes were observed to be capable of reducing it to chloride. However, compared to nano-ZVI the reduction by micro-ZVI is negligibly slow. This can be traced to the low activation energy of micro-ZVI (79 kJ/ mole) indicating that the reduction is limited by its slow kinetics. Phenrat et al. (2007) suggested that, because of the fast aggregation of nZVI in solution, it is impossible to achieve such results. The particle aggregation reduces the surface area and consequently decease the rate of reaction and lowers the adsorption capacity. 100% removal efficiency can be achieved using nZVI where the sample can be kept in suspension for a longer period of time. Otherwise, the particles start to aggregate as soon as they are introduced to the aqueous solution. Hence, more studies are needed to define the impact of ZVI particle size distribution on adsorption equilibria and the rate of reaction.

2.6 References

1. Aguila, A., O'Shea, E., Tobien, T., and Asmus, D., 2001 "'Reactions of hydroxyl radical with dimethyl methylphosphonate and diethyl methylphosphonate. A Fundamental Mechanistic Study," *Journal of Physical Chemistry A*, vol. 105, pp. 7834-7839.
2. Alguacil F.J., Navarro P., 2001 "Permeation of Cd through a supported liquid membrane impregnated with CYANEX 923," *Hydrometallurgy*, vol.61, pp.137–142.
3. Arnold, W.A., Ball, W.P., Roberts, A.L., 1999 "Polychlorinated Ethane reaction with zero-valent zinc: pathways and rate control," *Journal of Contaminant Hydrology*, vol.40, pp. 183 - 200.
4. Barton S.S., Evans M.J.B., Halliop E., MacDonald J.A.F., 1997 "Acidic and basic sites on the surface of the porus carbon," *Carbon*, vol. 35, pp. 1361-1366.
5. Bazrafshan E., Mostafapoor F.K., Zazouli M.A., Eskandari Z., Jahed Gh.R., 2006 " Study on the removal of Cd (II) from plating baths wastewater by electrochemical precipitation method," *Pakistan Journal of Biochemical Science*, Vol.9, pp. 2107-2111.
6. Benjamin M.M., and Leckie J.O., 1981a "Multiple-site adsorption of Cd, Cu, Zn and Pb on amorphous iron oxide," *Journal of Colloid Interface Science,* vol.79, pp.209–221.
7. Benjamin, M.M., and Leckie, J.O., 1981b "Competitive adsorption of Cd, Cu, Zn, and Pb on amorphous iron oxyhydroxide," *Journal Colloid Interface Science*, vol 83, pp.410– 419.
8. Brady, J.E., Holum, J. R., 1996 "Descriptive chemistry of the elements" John Wiley and Sons.
9. Buerge, I.J., Hug, S.J., 1999 "Influence of mineral surfaces on chromium (VI) reduction by iron (II)," *Environmental Science and Technology*, vol. 33, pp. 4285-4291.
10. Canadian Council of Resource and Environment Ministers. Canadian water quality guidelines. Inland Waters Directorate, Environment Canada, Ottawa (1987).
11. Chen, J.L., Al-Abed, S.R., Ryan, J.A., and Li, Z., , 2001 "Effects of pH on dechlorination of trichloroethylene by zero-valent iron," *Journal of Hazardous Materials*, vol. 83, pp. 243-254.
12. Chowdhury, R., Yanful, K., 2010 "Arsenic and chromium removal by mixed magnetite emaghemite nanoparticle sand the effect of phosphate on removal," *Enviromental Mangement Journal*, vol. 91, pp. 2238-2247.
13. Christophi, C.A., Axe, L., 2000 "Competition of Cd, Cu, and Pb adsorption on goethite," *Journal of Environmental Engineering, ACSE*, vol. 126, pp. 66–74.

14. Cotton, F.A., Wilkinson, G., 1972 “Advanced inorganic chemistry,” 3rd edition. Wiley-Interscience, Toronto.
15. Deng, B., Burris, D.R., Campbell, T.J., 1999 “Reduction of vinyl chloride in metallic iron-water system,” *Environmental Science and Technology*, vol. 33, pp 2651-2656.
16. DOE (US Department of Energy), 1991. http://science.energy.gov/budget/fy1991/
17. Doong, R.A., Chen, K.T., Tasi, H.C., 2003 “Reductive dechlorination of carbon tetrachloride and tetrachloroethylene by zero-valent silicon-iron reductants,” *Environmental Science and Technology*, vol. 37, pp. 2575-2581.
18. Elektorowicz, M., 2009 Ch 15 “Electrokientic remediation of mixed metals and organic contaminants,” in (Electorchemical rmediation technologies for polluted soils, sediments and groundwater)., Wiley & Son, Inc.
19. Elliott D. and Zhang W. (2001) Field assessment of nanoscale biometallic particles for groundwater treatment,” *Environmental Science & Technology*, vol. 35, pp24-35.
20. Environment Canada. National inventory of sources and emissionsof cadmium (1972). Report APCD 76-2, Air Pollution Control Directorate, Ottawa, June (1976).
21. Environment Canada. National Water Quality Data Bank (NAQUADAT) dictionary. Data Systems Section, Water Quality Branch, Ottawa (1985).
22. Farrell, J., Kason, M., Melitas, N., Li, T., 2000 “Investigation of the long-term performance of zero-valent iron for reductive dechlorination of trichloroethylene,” *Environmental Science and Technology*, vol. 34, pp 514-521.
23. Fernandez Y., Maranon E., Castrillon L., I. Vazquez I., 2005 “Removal of Cd and Zn from inorganic industrial waste leachate by ion exchange,” Journal of Hazardous Material, vol. B126, pp. 169–175.
24. Fleischer, M., 1974 “Environmental impact of cadmium: a review by the panel on hazardous trace substances,” *Environmental Health Perspective*, vol 7, pp 253-260.
25. Gao Y., Mucci A., 2001 “Acid base reaction, phosphate and arsenate complexation, and their competitive adsorption at the surface of goethite in 0.7 M NaCl,” *Geochimical Cosmochimical Acta,* vol. 65, pp. 2361-2378
26. Ghauch, A., Gallet, C., Charef, A., Rima, J., Martin-Bouyer, M., 2001 “Reductive degradation of carbaryl in water by zero-valent Iron,” *Chemosphere,* vol. 42, pp. 419-424.

27. Gillham, R.W. and O' Hannesin, S.F., 1994 "Enhanced degradation of halogenated aliphatics by zero-valent Iron," *Ground Water*, vol.32, pp. 958-967
28. Government of Canada 1993 "Trichloroethylene. Priority Substances List Assessment Report. Government of Canada, Environment Canada and Health Canada" ISBN 0-662-21065-4.
29. Government of Canada 1994 "Cadmium and its compounds. Priority Substances List Assessment Report. Government of Canada, Environment Canada and Health Canada" ISBN 0-662-22046-3.
30. He D., Gu, S., Ming Ma M., 2007 "Simultaneous removal and recovery of cadmium (II) and CN− from simulated electroplating rinse wastewater by a strip dispersion hybrid liquid membrane (SDHLM) containing double carrier," *Journal of Membrane Science*, vol. 305, pp. 36–47.
31. Houben G., Kringel R., (2007 of Conference) "Remediation of contaminated groundwater with nanoparticles," *DECHEMA - In situ Sanierung*, Frankfurt am Main, Germany.
32. Islamoglu S., Yilmaz L., Ozbelge H.O., 2006 "Development of a precipitation based separation scheme for selective removal and recovery of heavy metals from cadmium rich electroplating industry effluents," *Seperation Science Technololgy*, vol. 41, pp. 3367–3385.
33. Janda, V., Vasek, P., Bizova, J., Belohlav, Z., 2004 "Kinetic models for volatile chlorinated hydrocarbons removal by zero-valent Iron," *Chemosphere,* vol. 54, pp. 917-925.
34. Jaques, A.P. 1982 "National inventory of sources and releases of lead" Report No. EPS 5/HA/3, Environmental Protection Service, Environment Canada, Ottawa, September (1985).
35. Kang K.C., Kim S.S., Choi J.W., Kwon. S.H., 2008 "Sorption of Cu2+ and Cd2+ onto acid and base pretreated granular activated carbon and activated carbon fiber samples," Journal of Industrial and Engineering Chemistry, vol. 14, pp. 131–135.
36. Karn, B., Todd K., Otto M., 2009 "Nanotechnology and in situ remediation: A review of the benefits and potential risks," *Environmental Health Perspective*, vol. 117, pp. 1813-1831.
37. Kocaoba S., 2007 "Comparison of amberlite IR 120 and dolamite's performance for the removal of heavy metals," *Journal of Hazardous Material*. vol. 147, pp. 488-496.
38. Kocaoba S., Akcin G., 2005 "Removal of chromium (III) and cadmium (II) from aqueous solutions," *Desalination*, vol.180, pp. 151-156.

39. Koivula R., Lehto J., Pajo L., Gale T., Leinonen H., 2000 "Purification of metal plating rinse waters with chelating ion exchangers," *Hydrometallurgy,* vol. 56, pp. 93-108.
40. Ku Y., Wu M-H., Shen Y-S., 2002 "A study on the cadmium removal from aqueous solutions by zinc cementation," *Seperation Science Technology.*, vol. 37, pp. 571-590.
41. Kumar V., Kumar M., Jha M.K, Jeong J., Jae-chun Lee J.C., 2009 "Solvent extraction of cadmium from sulfate solution with di- (2-ethylhexyl)phosphoric acid diluted in kerosene," *Hydrometallurgy,* vol. 96, pp.230-234.
42. Lee T., Lim H., Lee Y. and Park J-W., 2003 "Use of waste iron metal for removal of Cr(VI) from water," *Chemosphere*, vol. 53, pp. 479-485.
43. Li X.-q., Elliott D. W., and Zhang W.-x. 2006 "Zero-valent iron nanoparticles for abatementof environmental pollutants," *Materials and Engineering Aspects. Critical Reviews in Solid State and Materials Sciences*, vol. 31, pp. 111–122.
44. Li, S. L., Yan, W. L., Zhang, W. X., 2009 "Solvent-free production of nanoscale zerovalent iron (nZVI) with precision milling," *Green Chemistry*, vol. 11, pp. 1618-1626.
45. Lin X., Burns R.C., Lawrance G.A., 2005 "Heavy metals in wastewater: the effect of electrolyte composition on the precipitation of cadmium(II) using lime and magnesia," *Water, Air, & Soil Pollution,* vol. 165, pp. 131-152.
46. Lowry, G., Liu, Y., Saleh, N., Phenrat, T., Dufour, B., Tilton, R., Matayjhaszewski, K., 2005 "Nanoiron in the subsurface: How far will it go and how does it change," US EPA Nanotechnology and the Environment: Applications and Implications Progress Review Workshop III, Washington D.C., October 26-28, 2005.
47. Lowry, G. V**., 2005** "Delivering polymer-modified Fe0 nanoparticles to subsurface chlorinated Organic Solvent DNAPL," US EPA Nanotechnology and the Environment: Applications and Implications Progress Review Workshop III, Washington D.C., October 26-28, 2005
48. Marder L., Sulzbach G.O., Bernardes A.M., Ferreira J.Z., 2003. Removal of cadmium and cyanide from aqueous solutions through electrodialysis," *Journal of Brazilian Chemical Society*, vol. 14, pp. 610-615.
49. Mortaheb R.H., Kosuge H., Mokhtarani B., Amini M.H., Banihashemi H.R., 2009, "Study on removal of cadmium from wastewater by emulsion liquid membrane," *Journal of Hazardous Material,* vol. 165, pp. 630–636.

50. Mueller, N., Nowack B., 2010 “Nanoparticles for remediation solving big problems with little particles,” *Elements Elements*, vol. 6, pp. 395-400.
51. Mueller. N., Braun. J., Bruns. J., Černík. M., Rissing. P., Rickerby. D., Nowack. B., 2012 “Application of nanoscale zero valent iron (NZVI) for groundwater remediation in Europe,” *Environmental Sciences and Pollution Reseach*, vol. 19, pp. 550–558.
52. National Research Council, Assessing the human health risks of trichloroethylene: Key scientific issues, Washington, D.C., National Academies Press, 2006.
53. National Research Council, Contaminants in the Subsurface: Source Zone Assessment and Remediation , Committee On Source Removal of Contaminants in the Subsurface, ed., Washington, D.C., National Academies Press, 2005.
54. National Research Council, Innovations in Ground Water and Soil Cleanup: From Concept to Commercialization, Washington, D.C., National Academy Press, 1997.
55. Nikolaidis N.P., Dobbs G.M. and Lackovic J.A., 2003 “Arsenic removal by zero-valent iron: Field, laboratory and modeling Studies,” *Water Research*, vol. 37, pp. 1417-1425.
56. Nowack B., 2008 “Pollution prevention and treatment using nanotechnology.” In Nanotechnology,” vol. 2 (ed. H. Krug). WILEY-VCS Verlag GmbH&Co.
57. NRTEE, Cleaning up the Past, Building the Future , Govt. of Canada, 2003.
58. Parbs A., and Birke V., 2005 “State-of-the-art report and inventory on already demonstrated innovative remediation technologies,” EuroDemo Report D6-2. Available at http://www.eurodemo.info/project-information-2/
59. Pehlivan E., Altun T., 2006 “The study of various parameters affecting the ion exchange of Cu2+, Zn 2+, Ni2+, Cd2+, and Pb2+ from aqueous solution on Dowex 50 W synthetic resin,” *Journal of Hazardous Material*, vol. B134, pp. 149-156.
60. Phenrat T., Saleh N., Sirk K., Tilton R., and Lowry G., 2007 “ Aggregation and sedimentation of aqueous nanoscale zerovalent iron dispersions.” *Environmental Science andTechnology,* vol. 41, pp. 214-221
61. Piscator, M., Copper. I ., 1979 “Handbook on the toxicology of metals” L. Friberg, G.F. Nordberg and V.B. Vouk (eds.). Elsevier/North-Holland Biomedical Press, Amsterdam. p. 411.

62. Rao, S.C., Jawitz, J.W., 2003 "Comment on 'Steady state mass transfer from single component dense nonaqueous phase liquids in uniform flow fields' by T.C. Sale and D.B. McWhorter," *Water Resource Research*, vol. 39, pp.217-223
63. Reddy B.R., Priya D.N., Park K.H., 2006. Separation and recovery of cadmium(II), cobalt(II) and nickel(II) from sulphate leach liquors of spent Ni-Cd batteries using phosphorus based extractants," *Seperation and Purification Technology*, vol.50, No.2, pp.161-166.
64. Reddy, R., Cameselle. C., 2009 "Electrochemical remediation technologies for polluted soils, sediments and groundwater." Wiley, New York, USA. 760 pages. ISBN: 978-0-470-38343-8
65. Reimann, C., de Caritat, P., 1998 "Chemical Elements in the Environment: Factsheets for the Geochemist and Environmental Scientist" New York (NY): Springer-Verlag.
66. Rickelton W.A., 1998 "The removal of cadmium impurities from cobalt–nickel solutions by precipitation with sodium diisobutyldithiophosphinate," *Hydrometallurgy*, vol. 50, pp. 339-344.
67. Rickerby D., Morrison M., 2007 "Report from the workshop on nanotechnologies for environmental remediation, JRC Ispra"
68. Schwille, F., 1988 "Dense chlorinated solvents in porous and fractured media: model experiments". Lewis Publishers, Inc., Chelsea, MI
69. Sen K., Sarzali V., 2008 " Removal of cadmium metal ion (Cd2+) from its aqueous solution by aluminium oxide (Al2O3): A kinetic and equilibrium study" *Chemical Engineering Journal*, vol. 142, pp.256–262.
70. Sen T.K., Mahajan S.P., Khilar K.C., 2002 "Sorption of Cu2+ and Ni2+ on iron oxide and kaolin and its importance on Ni2+ transport in porous media." *Colloids Surfaces A: Physicochemistry and Engineering Aspects*, vol. 211, pp.91–102.
71. Shih, R.A., Glass, T.A., Bandeen-Roche, K., Carlson, M.C., Bolla, K.I., Todd, A.C., Schwartz, B.S., 2006 "Environmental lead exposure and cognitive function in community-dwelling older adults" *Neurology*, vol. 67, pp. 1556-1562.
72. Taha A.A., Ghani, S.A., 2004 "Effect of surfactants on the cementation of cadmium," *Journal of Colloid and Interface Sciences*, vol. 280, pp. 9–17.
73. Takeshita K., Watanabe K., Nakano Y., Watanabe M., 2004 "Extraction separation of Cd(II) and Zn(II) with Cyanex 301 and aqueous nitrogen-donor ligand TPEN," *Solvent Extrasion and Ion Exchange*, vol. 22, pp. 203–218.

74. Touati M., Zayani M.B., Ariguib N.K., Ayadi M.T., Buch A., Grossiord J.L., Pareau D., Stambouli M., 2009 "Solvent extraction of cadmium from sulfate solution with di-(2-ethylhexyl)phosphoric acid diluted in kerosene," *Hydrometallurgy*, vol. 95, pp.135- 140
75. Tripathy S. S., Bersillon J.L., Gopal K., 2006 "Adsorption of Cd2+ on hydrous manganese dioxide from aqueous solutions." *Desalination*, vol. 194, pp. 11-21.
76. U.S EPA OSWER., 2010 "Selected sites using or testing nanoparticles for remediation" http://www.epa.gov/tio/download/remed/nano-site-list.pdf
77. U.S. Environmental Protection Agency. Updated mutagenicity and carcinogenicity assessment of cadmium: addendum to the health assessment document for cadmium. Report No. EPA/600/8-83/025F, Office of Health and Environmental Assessment, Office of Research and Development, Washington, DC (1985).
78. U.S. EPA, cited January 4, 2008, available:http://www.epa.gov/pcb/pubs/eff ects.htm.
79. U.S.EPA., 2005 "U.S. EPA Workshop on Nanotechnology for Site Remediation" http://epa.gov/ncer/publications/workshop/pdf/10_20_05_nanosummary.pdf
80. US EPA. 2011 "Region 5 Superfund, Ecological Toxicity Information" U.S. Washington (DC): Environmental Protection Agency. [cited January 2011]. Available from: http://www.epa.gov/region5superfund/ecology/toxprofiles.htm
81. Volesky B., Holan Z.R., 1995 "Biosorption of heavy metals," *Biotechnology Progress*, vol. 11, pp. 235-250.
82. Wang W., Fthenakis W., 2005 "Kinetics study of cadmium from tellurium in acidic solution media using ion-exchange resins," *Journal Hazardous Material*, vol. B125, pp. 80-88.
83. Wang, C.B. and Zhang, W.X., 1997 "Synthesizing nanoscale iron particles for rapid and complete dechlorination of TEC and PCBs," *Environmental Science and Technology*, vol. 31, pp. 2154-2156.
84. Wei-xian Zhang ., 2003 "Nanoscale iron particles for environmental remediation: An overview," *Journal of Nanoparticle Research,* vol. 5, pp. 323–332.
85. World Health Organization., 1973 "Trace elements in human nutrition; a report of a WHO Expert Committee," WHO Technical Report Series 532, Geneva. p. 70.
86. World Health Organization., 1984 "Guidelines for drinking-water quality," vol. 2. Geneva.

87. Xiao-qin Li, Daniel Elliott and Wei-xian Zhang 2006 " Zero-valent iron nanoparticles for abatement of environmental pollutants: material and engineering aspects," *Critical Reviews in Solid State and Materials Sciences*, vol. 31, pp.111–122,
88. Younesi R., Alimadadi H., Alamdari K., Marashi H., 2006 "Kinetic mechanisms of cementation of cadmium ions by zinc powder from sulphate solutions," *Hydrometallurgy*, vol. 84, pp. 155–164.
89. Zhang W., 2003 "Nanoscale iron particles for environmental remediation: An overview," *Journal of Nanoparticle Research*, vol. 5, pp. 323-332.

CHAPTER THREE

Experimental and Analytical Methods

This chapter describes in details the materials and methods use in this study. The iron nanoparticle used in this study is Nanofer ZVI. All chemicals were of reagent grade and were used as purchased without further purification. Instrument analyses, unless otherwise noted, were performed in department of building civil and environmental engineering, Mechanical engineering and chemistry at Concordia University.

3.1 Nanofer ZVI

The iron suspension characterized and modified in this study was supplied by the Czech company, NANOIRON ltd. The material was developed to overcome the uncoated nanofer 25 which was produced via a dry reduction of iron oxide. However, the coated nanofer ZVI is a new innovative material produced by impregnating the iron oxide with polyvinylpyrrolidone (PVP) and socked and coated with Tetraethyl orthosilicate (TEOS). Lenka et al. (2012) provide more information about these two products. De-ionized water was used in all experiments. The product is surface stabilized, transportable, air-stable and reactive, which means, it is much easier and safer to store, transport and process comparing to other non-stabilized nZVI.

3.2 Chemical solutions

The details related to different chemical solutions used in the study are presented in the following tables.

Table 3 .1: Presents the selected organic and inorganic chemicals used in the study.

Reagent	Formula	Source
Inorganic		
Cu(II)	$CuCl_2$	Fisher
Cd(II)	$CdCl_2$	Fisher
Pb (II)	Pb (II)Cl_2	Fisher
Organic		
TCE	C_2HCl_3	Fisher
PVP	$(C_6H_9NO)n$	Sigma Aldrich
TEOS	$SiC_8H_{20}O_4$	Sigma Aldrich

Table 3.2: Metal ion characteristics, (taken after Christophi and Axe, 2000)

	metals		
Characteristics	Cu (II)	Pb (II)	Cd (II)
Hydrated radius (A°)	4.19	4.01	4.26
Ionic radius (A)	0.72	1.2	0.97
Electronegetivity	1.8	1.6	1.5
Electron configuration	4s 3d 1B	6s 4f 5d 6p 4A	5s 4d 2B
Group			
Present speciation in present of another metal	97.0 Cu^{+2} 1.8 Cu(OH)	96.4 Pb^{+2} 1.7 $PbOH^{+}$ 1.2 $PbNO_3^{-}$	99.7 Cd^{+2}
presence of	Cd 97.1 Cu^{+2} 1.8 Cu(OH)	Cd 97.1 Pb^{+2} 1.7 $PbOH^{+}$ 1.2 $PbNO^{-}_3$	Pb 99.8 Cd^{+2}
Presence of	Pb 97.1 Cu^{+2} 1.8 Cu(OH)	Cu 96.4Pb^{+2} 1.7 $PbOH^{+}$ 1.2 $PbNO^{-}_3$	Cu 99.7 Cd^{+2}
Presence of	Cd and Pb 82.6 Cu^{+2} 2.3 $CuOH^{+}$ 97.1 Cu^{+2} 15.0 Cu(OH)	Cd and Cu 93.6 Pb^{+2} 5.2 $PbOH^{+}$ 1.2 $PbNO^{-}_3$	Pb and Cu 99.8 Cd^{+2}

3.3 Experimental procedures

3.3.1 Batch equilibrium experiments

Stock solutions were prepared using the indicated chemicals (Table 3.1). Equilibrium tests were performed in closed, 1000-ml glass serum bottles in which the solution volume was 1000 ml. An appropriate volume of the stock solution was diluted with de-ionized water to 1000 ml. The solutions were mixed using a magnetic mixer and left over night. After the mixing, the amount of nZVI and stock solution were added to a 40 ml bottle. Following this, the bottles closed and the cap was sealed with a Teflon liner to prevent air leakage. The bottles were agitated on a mechanical shaker at 250 rpm at 21^0 C. After a suitable time interval (typically 24 hours for reactions with metal species), the reaction was stopped by separating the solution and the particles with a vacuum filtration using 0.2 μm filter supplied by (grad 42 Whatman). The particles were dried and stored in a N_2-filled glove box ahead off solid phase analysis, and the solution was acidified with HNO_3 to pH less than two and stored at 4^0 C before solution analysis. For each set of experiments, a control was performed under identical conditions in parallel except for the case where no iron nanoparticles were added. For experiments involving volatile compounds (e.g.TCE), 250-ml serum bottles containing 40 ml aqueous solutions were used. After charging a small amount of nZVI, the bottles were capped with Teflon Mininert valves and placed on a mechanical shaker at 250 rpm at 25 ^{o}C. Both pH and temperature were measuring before and after adding the nZVI to each bottle. All bottles were cleaned using 0.1 mole HCl and washed to insure that no residual contaminants could occur.

3.3.2 Batch kinetic experiments

Kinetic experiments of reactions with selected organic and inorganic species were performed. The amount of chemical added was diluted with de-ionized water to 1000 ml, sealed and were left in the mixer overnight. After mixing, nZVI and stock solution were added to 40 ml bottle. Following this, the bottles were closed and the caps with a Teflon liner sealed the bottles to prevent leakage. The head room in the bottle was kept to the minimum. The bottles were agitated on a mechanical shaker at 250 rpm at 21^0 C. Time was recorded for each bottle at the moment of adding the nZVI. Each bottle was given suitable time and code. After a suitable time interval, the bottles the nZVI were separated using with vacuum filtration with 0.2 μm filter supplied by (grad 42 Whatman).

The pH and temperature were measured before and after adding the nZVI. The filtered solutions was immediately, acidified, and stored at 4^0 C prior to analysis.

3.4 Aqueous analysis

3.4.1 Atomic Absorption spectrometer

Total aqueous concentrations of Cu, Pb, and Cd were measured with a Perkin Elmer atomic absorption (AA) spectrometer (A Analyst 100). For analysis of each species, a five-point calibration curve was obtained with solutions prepared from the respective AA standards (1000 mg/L standards purchased from Fisher). Three replicate readings were taken for each sample. Sample concentrations exceeding linear concentration range of the respective wavelength were diluted accordingly. The set up and selected wavelength for each metal were taken from the AA spectrometer manual. The stock solution for the calibration curve was used to insure consistency after each 5 reading. After completing the reading samples were storage in 4 ^{0}C.

3.4.2 Gas chromatography

The concentrations of TCE were measured by a Varian GC analyzer (3800) equipped with a flame ionization detector (FID) and a SUPELCO SPB 624 capillary column. The injection port temperature was set at 180^o C. The oven temperature was set to 50 ^{0}C and ramped to 200 ^{0}C at 10 ^{0}C/min. The detector temperature was 300 ^{0}C. The Helium gas was used as carrier gas. A five-point calibration curve was obtained with solutions prepared from the respective standards (1000 mg/l standards purchased from Fisher). The method used for the analysis selected followed the GC Varian 3800 manual for liquid. After completing the analysis, all samples were capped and storage in 4 ^{0}C.

3.4.3 pH, ORP and T measurements

Solution pH and Temperature were measured with bench pH-mV meter Hanna pH 209. Three-point calibration was performed daily using pH 4.0, 7.0, and 10.0 standard pH buffers (Fisher). Oxidation-reduction potential (ORP) was measured using the same analyzer equipped with an ORP electrode (Pt band with Ag/AgCl/Saturated KCl reference cell). One-point ORP calibration was performed using a Zobel standard solution (Sigma), which gives a reading of ~ +230 mV at

22 ^{0}C. ORP reading can be converted to the standard hydrogen electrode potential (Eh) by adding +197 mV at 25 ^{0}C. Temperature was recorded daily before and after the analysis.

3.5 Solid phase analysis

The nature of solid phase analysis requires extensive characterizations of the morphology, internal structure, composition, and surface chemistry of the nZVI reacting with contaminants. This section presents an overview of the techniques used to conduct the solid-phases analyses. However, the analysis of solid phase characterization is based on tests conducted at the Nanoiron laboratory in (Rajhrad, Czech Republic) and the mechanical engineering TMG lab facility of Concordia University.

3.5.1 Scanning electron microscope

The morphology characterization of nZVI nanofer star was carried out using a field-emission scanning electron microscope (FE-SEM) (Hitachi 4300). The popularity of SEM for characterizing nanomaterials stems from its capability of obtaining 3-dimensional-like topographical images in secondary electron (SE) imaging mode, Z-contrast imaging (Fig 2-1) using back-scattered electrons (Goldstein, et al., 2003).

3.5.2 Transmission electron microscope

Various transmission electron microscopy (TEM) techniques were used to characterize the nanofer star iron. Bright field TEM imaging was conducted using JOEL 2000FX at 200 kV for microstructure characterization and selected area electron diffraction pattern. Phase contrast TEM imaging (Fig 2-2) was obtained with a JOEL 2200FS at 220 kV. High angle annular dark field imaging (HAADF) and chemical mapping were carried out at laboratory in Nanoiron (Rajhrad, Czech Republic). The STEM-XEDS imaging was conducted at 200 kV.

3.5.3 BET surface area

Specific surface area of the nanofer ZVI particles was measured using a Micrometrics Flowsorb 2305 in chemistry lab facility (Concordia University) following the classic Brunauer-Emmett-Teller (BET) method (Bruauer et al., 1938). Dried samples were first degassed at 170°C for 40

minutes. Adsorption of pure nitrogen by iron sample was done in a sample tube at liquid nitrogen temperature followed by desorption of nitrogen as temperature ramps up to room conditions. The amounts of nitrogen adsorbed and desorbed by the iron particles were measured by a potentiometer and were used to calculate the total surface area.

3.6 Analytical techniques

The concentration of Pb (II), Cu (II), Cd (II) and TCE, were measured by both atomic adsorption and gas chromatography techniques. Fig 3.1 presents the calibration curve following the instruction in the manuals. A linear relationship between concentration and absorbance in the range of 0.1 to 0.9 was indicated.

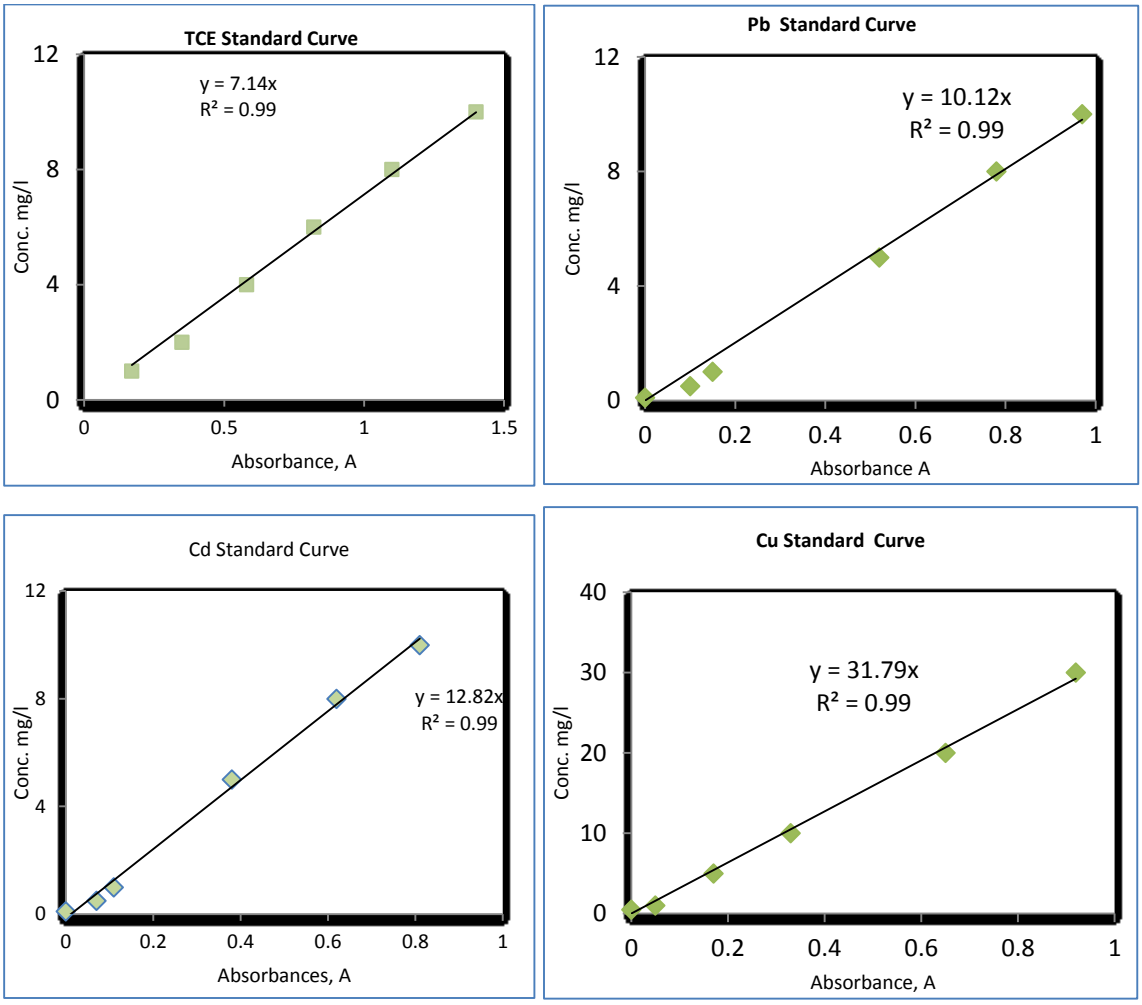

Fig 3.1: Calibration curves for Pb (II), Cu (II), Cd (II) &TCE

3.6 References

1. Brunauer, S. Emmett P. H.. Teller E., 1938 “Adsorption of Gases in Multimolecular Layers,” *Journal of American Chemical Society*, vol. 60, pp. 309-313.
2. Christophi C.A., Axe L., 2000 “Competition of Cd, Cu, and Pb adsorption on goethite,” *Journal of Environmental Engineering ACSE*, Vol. 126, pp. 66–74.
3. Goldstein, J. I., Lyman, C. E., Newbury, D. E., Lifshin, E., Echlin, P., Sawyer, L., Joy, D. C., Michael, J. R., 2003 “Scanning electron microscopy and X-ray microanalysis, Springer”.
4. Lenka. H., Petra. J., and Zdenek. S., 2012 “ Nanoscale zero valent iron coating for subsurface application,” *Brno Czech Republic, EU.* vol. 10, pp.23-25.

CHAPTER FOUR

Nanofer ZVI: Morphology, Particle Characteristics, Kinetics and Applications

Abstract

Nanofer zerovalent iron (nanofer ZVI) is a new and innovative nanomaterial capable of removing organic as well as inorganic contaminants in water. It displays a decrease in agglomeration, when it is coated with tetraethyl orthosilicate (TEOS). TEOS imparts an increase in reactivity and stability to nanofer ZVI. Characteristics of nanofer ZVI were determined using scanning electron microscope/electron dispersive spectroscope (SEM/EDS), transmission electron microscope (TEM), and X-ray diffraction (XRD). Nanoparticle size varied from 20 to 100 nm and its surface area was in the range of 25–30m2g−1.The present study examined its structure before and after kinetic experiments. Kinetic experiments indicated that adsorption of heavy metals [Pb (II), Cd (II), and Cu (II)] and TCE is very rapid during the initial step which is followed by a much slower second step. Removal rates of 99.7% for Pb (II), 99.2% for Cd (II), 99.9% for Cu (II), and 99.9% for TCE were achieved in less than 180 minutes. Lagergren models (LM), liquid film diffusion model (LFDM), and interparticle diffusion model (IDM) were used to understand the removal mechanism associated with nanofer ZVI. In this study, interactions of nanofer ZVI with individual metals as well as TCE are examined.

4.1 Introduction

It is almost a decade since the zero valent iron nanoparticle application was engineered. The application of conventional nanoparticles to remove organic and inorganic contaminants from water has received considerable attention. The new nanofer ZVI is the third generation of iron nanoparticles (nZVI) produced in 2012. It is highly applicable in the oxidation-reduction technologies of water remediation (Mace et al.2006, Mueller et al 2012). The oxidation of organic contaminants produces hydroxyls, superoxides and hydrogen gas. They play a significant role in the degradation of organic contaminants (Keenan and Sedlak, 2008, Cwierthny et al. 2007, Liu et al. 2005 and Lowry and Johnson, 2004). Iron particle disassociation and metal adsorption by nanoparticles are the mechanisms by which nZVI removes inorganics. The study of nanofer ZVI to remove organic and inorganic contaminants in water is crucial.

The life time and agglomeration of particles are the main hurdles for the use of the conventional nZVI for the remediation of contaminated water. The particle life time varies from 2 hours to a few days. Further, in some cases, the particle agglomeration can be even shorter than 2 hrs. In the last decade, extensive research was focused on enhancing the mobility and dispersion of particles by adding transitional metals or coating the nZVI particles with silicon based materials. The NANOIRON Company produced nanofer ZVI (Lenka et al. 2012) by coating the conventional nZVI particles with Tetraethyl orthosilicate (TEOS). Other types of coatings such as carboxymethyl cellulose (CMC) and polyacrylic acid-stabilized are also reported to be effective in increasing the stability of nZVI while passing through soil, when nanoparticles are injected into the soil to reduce groundwater contamination (Raychoudhury et al.2010 and Cirtiu et al. 2011).

Due to the presence of the coating, the nanofer ZVI is stable transportable, reactive and air-stable. Hence, it is much easier and safer to store, handle, transport and process compared to other non-stabilized conventional nZVI. It maintains its extreme reactivity in the presence of reducible pollutants in the water environment (Lenka et al. 2012). As such, the (new) nanofer ZVI is suitable for direct application to remove contaminants from polluted water as well as for the preparation of slurries injected for in-situ groundwater remediation. Its advantages include the stabilization of particles by the thin layer which inhibits particles against rapid oxidation when they are in contact with air. Also, it maintains its high reactivity in water, in spite of surface stabilization with silica coating. Further, this coating enables it to be free of pyrophoric properties and permits easy handling. Hence, it results in much lower packaging and transportation costs compared to other conventional nZVI (Wiele, 2011). Only few feasible procedures have been suggested in literature to dispose the spent nanoparticle used remediation processes. For instance, Karn et al. (2009) have suggested that the spent nanoparticle are susceptible to taken up by microorganism. U.S EPA (2007) has also suggested possibility of biomagnification of nanoparticles as intermediate for eventual disposal. After completing the treatment at the point source, Nowack, (2008) has suggested that, the residual water left should be pumped out to the surface and separate the nZVI containing the contaminants using filters.

The adsorption or reaction kinetics of nanoparticle system in the presence of contaminated water must be studied to determine the appropriate design that results in the extended lifetime and reactivity of particles (Stone et al. 2010 and Mueller and Nowack, 2010). Recently, several studies

have investigated the use of nZVI that were coated by other metals such as Pd and Ni which impart higher stability and reactivity to nZVI particles. For instance, Greenlee et al. (2012) studied the kinetic adsorption as well as the oxidation of TCE by bimetallic nanoparticles (Ni-Fe nZVI) using the results based on SEM/ EDS data analysis. They found that bimetallic nanoparticles have increased reactivity well above the conventional nZVI. Also it was noticed that nZVI got primarily oxidized to iron oxide-hydroxide (lepidocrocite) in the presence of oxygenated water. Li et al. (2006) have examined the injection of bimetallic nanoparticles (Pd-Fe nZVI) to a sand aquifer that was contaminated by TCE. They found that the nanoparticles injected to the aquifer did not reach the target area due to their reactivity with the soil. Both Environmental protection agency (EPA, 2012) and the office of solid waste and emergency response (OSWER, 2012) investigated the scope of remedying several sites contaminated with organic and inorganic contaminants using different nZVI. They treated almost 90 percent of sites by bimetallic nanoscale particles (BNP) produced by Lehigh University (USA) and the conventional nZVI. 95% of target contaminants were organics such as Trichloroethylene (TCE), polychlorinated biphenyls (PCB), 1,1,1Trichloroethane (TCA), Vinyl Chloride (VC) and others. In most cases, a second injection of nZVI was needed to reach the desired contaminant concentration level.

Little is known about the reaction kinetics and products formed during metal adsorption or oxidation- reduction by nZVI, especially the coated form. Even fewer studies have investigated TCE dechlorination by coated nZVI with metal or different polymer (Greenlee et al. 2012, Li et al. 2006 and Liu et al. 2005). However, only few details of the nanoparticle distribution and reaction kinetics have been provided. The pathways of TCE dechlorination and metal removal by coated nZVI have not been explored.

Several methods such as precipitation, electrochemical reduction, adsorption, ion exchange, solvent extraction and nano-filteration are used to remove heavy metals (Cu, Pb and Cd) from groundwater. These operations are expensive, often generate excessive sludge and lead to operational problems (Li and Zhang, 2007). Heavy metals in groundwater can be removed more efficiently using nanomaterials. Considerable attention is currently paid to study the use of nZVI to remove heavy metals from groundwater (Li and Zhang, 2007). The mechanisms of heavy metal removal using nZVI depend on the standard redox potential (E^0) of the metal contaminant. Metals that have an E^0 which is more negative than or similar to that of Fe^0 (e.g. Cd) are removed by

adsorption to the iron hydroxide shell. On the other hand, metals with E^0 which is much more positive than Fe^0 (e.g. Cu) are preferentially removed by reduction and precipitation. Metals for which E^0 is only slightly more positive than that for Fe^0 (e.g. Pb) can be removed by reduction and adsorption (Li and Zhang, 2007). O'Carroll et al. (2013) rightly stated that oxidation and co-precipitation involved in heavy metal removal depend upon the prevailing chemical conditions (pH, initial concentration and speciation of contaminant metals). In most cases, addition of nZVI to the aqueous solution increases pH due to the generation of OH^- resulting in the immobilization of metal by precipitation as the hydroxide (O'Carroll et al. 2013). This also suggests that other metal contaminants with more negative redox potential than Fe^0 may be removed by adsorption and precipitation on the nZVI surface.

Recently, Rangsivek and Jekel, (2005) studied the removal of Cu II by macroscale ZVI and showed that a substantial portion of Cu II is reduced and transformed to insoluble form of Cu and Cu_2O. More recently, Ayob et al. (2012) studied the adsorption of Cu II by nZVI coated by carboxylmethyl cellulose (CMC-nZVI) and found that the removal efficiency is highly pH dependent. The removal of Pb II by bimetallic nanoparticles (Ni/Fe) has also been reported by Saberi, (2012). O'Carroll et al. (2013) have indicated that only a few studies have investigated the adsorption kinetic of metal removal by nZVI. They also suggested that more research is needed to investigate the adsorption mechanism and kinetics associated with other metal that can be removed by nZVI.

In the presence study, surface morphology and surface chemistry of the new nanofer ZVI was determined using spectroscopic image data (SEM/EDS, TEM, and XRD). The surface area of nanofer ZVI was obtained using the BET procedure. The kinetics of adsorption of heavy metals ((Pb (II) II, Cu (II), Cd (II)) and dechlorination of TCE present in polluted water by the new nanofer ZVI was investigated. To achieve this goal, the experimental data were collected and the results were used to validate the Lagergren model as well as the liquid diffusion model. The study also scrutinizes the reaction pathways of the removal of metals and TCE by the new nanofer ZVI from contaminated water.

4.2 Materials and Methods

The chemical solutions used in the study are presented in the previous chapter [Tables (3.1) and (3.2)]. Nanofer zero valent iron particles were prepared as previously discussed earlier (Chapter 3).

4.3. Surface morphology and particle characteristics

4.3.1 Transmission electron microscope images.

Images of the nanofer ZVI particles were recorded with the JOEL 2000 FX Transmission microscope (JOEL ltd, Japan). The samples deposited on the top of the sample holder by adding two to three droplets of nanofer ZVI onto the carbon film. The sample holder was cleaned by air to removal unglued particles. Using the TEM, the particle structure was examined by passing beam of electrons through the specimen. The transmission of the electron beam depends on the properties such as density and composition of materials. The image appeared as a shadow of the specimen on the screen. The best image showing the particle characteristics was selected from the data collected. More detail are given in (chapter 3)

4.3.2 Scanning electron microscope/ Electron dispersive microscope.

The SEM was operated using the Hitachi S3400N equipped with the EDS system. The samples were placed on top of the sample holder using carbon duck liquid. The operating voltage was 15 kV. The energy- dispersive X-ray spectroscope (EDS) was conditioned at 55 kV, dead time 35 % and a stage working distance between 9.8 and 10. More detail are presented in (chapter 3)

4.3.3 X-ray diffractometer.

The Philips X pert Pro multipurpose X-ray diffractometer was used with parafocusing Bragg-vrentano geometry and CuKa radiation column (λ=1.5418 Å, V=40 kV, i = 30 mA). The particles were placed in a glass holder and scanned from 20^0 to 75^0. This scan range covered all major species of iron and iron oxides. The scan rate was set at 2.0^o per min. More detail are presented in (chapter 3)

4.3.4 BET method.

Specific surface area of the nanofer ZVI was determined with the classic Brunauer-Emmer-Teller isotherm (BET) method. The BET isotherm was the basis for determining the extent of nitrogen adsorption on the particle surface. The nitrogen physio-sorption with Coulter SA 3100 analyzer (Barrett-Joyner-Hanleda) was used in this study. The sample was placed on a glass tube was exposed to nitrogen gas at precisely controlled pressures. As the pressure increased, the number of nitrogen molecules increased. The pressure at which adsorption equilibrium occurred was measured and the universal gas law was applied to determine the quantity of gas molecules adsorbed. The process continued until the point of bulk condensation of nitrogen. Following this, the reverse sequence of desorption occurred. The systematic sorption and desorption of nitrogen provided the important information related to surface area characteristic. More and simlair detail are presented in (Chapter 3).

4.3.5 ζ potential and iso-electric point.

The surface charge of nanofer ZVI is often characterized by the zeta potential (***ζ)***. Surface charge or zeta potential is the major factor determining the mobility of particles in an electrical field. The pH versus ***ζ*** potential diagram was employed to determine the Iso-electric point (IEP) for the nanofer ZVI. pH of the solution was adjusted with 2.0 N NaOH. An electromagnetic mixer was used to achieve rapid mixing. The titration began after the iron nanoparticles were suspended with de-ionized water for 30 min to allow the solution to reach equilibrium. The diagram of pH vs. ***ζ*** yielded the IEP data. More detail can be found in (Chapter 3)

4.4 Batch Kinetic adsorption experiments

Batch experiments were conducted to determine the kinetics of adsorption of heavy metals and dechlorination of TCE by nanofer ZVI. 0. 01 M of metals chloride was prepared, sealed and was left in the shaker for 24 hrs (250 rpm). Nanofer ZVI and stock solution of metal chloride were added to 40 ml bottles. Following this, the (sample solution) bottles were closed and the caps with a Teflon liner sealed the bottles to prevent leakage. The head room in the bottle was kept to the minimum. The sample solution bottles were agitated on a mechanical shaker (250 rpm) at 21^0 C.

Time was recorded for each bottle at the moment of adding the nZVI. Each bottle was assigned a time and a code. After regular time intervals, the nZVI particles were separated using vacuum filtration with 0.2 μm filter (grade 42 Whatman). The pH and temperature were measured before and after adding the nZVI. The filtered solutions were immediately acidified and stored at 4^0 C prior to metal analyses. The Atomic absorption spectroscope (AAS, Perkin Elmer) was used for analysis of metals. Similar procedure was used to prepare the TCE solution samples. However, TCE concentration after reduction-oxidation was obtained by gas chromatography (GC Varian 3800). More detail are presented in (Chapter 3)

4.5 Kinetic experiments and modeling

Batch kinetic experiment techniques were used to study the adsorption of metals and the degradation of TCE from contaminated water by nanofer ZVI. Both the liquid film diffusion model (LFDM) and the intreparticles diffusion model were selected to describe the behavior of contaminants through the liquid phase (aqueous) to the solid phase surface of nanoparticle (nanofer ZVI). The main reason to select these two models is linked to the fact that adsorption between metal and nZVI is diffusion controlled. Besides the diffusion models, the Lagergren model was also used to describe the kinetics of both metals and TCE removal by nanofer ZVI. Qiu et al. (2009) have provided a comprehensive discussion of several other related models.

4.6 Results and discussions

4.6.1 Morphology and surface chemistry.

Nanofer ZVI was characterized using images recorded by (XRD), (SEM), and (TEM). The specific surface area of the nanofer ZVI was determined by BET analysis. The division shown in the SEM images indicates 1/10 of the range shown (i.e., 40 nm subdivision Figs. 4.1(a)). Figs. 4.1(a) and 1(b) show that the average particle size was 50 nm (20-100 nm). The surface area ranged from 25-30 m^2g^{-1}. The XRD analysis (Fig. 4.3) indicated two distinct peaks at scanning angles corresponding to 45^0 and 65^0. The XRD index software (JCPDS) indicated that these peaks denote ferrite (αFe, 97.9%) and magnetite (Fe_3O_4, 2.1%). The increase of pure iron (ferrite) is caused by the coating of nanofer ZVI with TEOS. However, Lenka et al. (2012) found that the percentage of

α-Fe for uncoated ZVI 25 is 60% and 70% for coated ZVI 25. Further, Nurmi et al. (2005) investigated the hydrogen reduction of iron oxides while Sun et al. (2006) reduce Fe^{3+} by borohydride to form zero valent nanoparticles. It was found that nZVI contains two phases. The α-Fe was ranged from 30 to 70 % and Fe_3O_4 was the surrounding oxide layer that ranged from 30 to 70 %. Broad peaks were observed by Sun et al. (2006) in the TEM images for α-Fe and FeO. This contrasts with the slim peak for ferrite (98%) in the image for the new nanofer ZVI (Fig. 4.3). For fresh iron particles to be used for remediation of organic and inorganic from aqueous solutions, the fraction of the α-Fe is expected to be higher than 80% to remain effective (Cornell and Schwerthmann, 2003). The higher percentage (98%) of α-Fe in nanofer ZVI clearly indicates that it is very highly reactive adsorbent.

The surface area of the nanofer ZVI was determined to be 27.5±2 m^2g^{-1} by N_2-BET analysis. However, the surface area of nanofer 25 (uncoated) was found to be 20 ± 1 m^2g^{-1} (Lenka et al. 2012). It is believed that the increase in surface area between the (uncoated) nanofer 25 and the new nanofer ZVI is caused by the coating of particle which prevents agglomeration (Figs. 4(a) and 4(b)). Unlike Fig. 4.4(b) which clearly displays individual particles, Fig. 4.4(a) does not show the existence of distinct particles. In Fig. 4.2, the TEM image shows that nanofer ZVI exhibits a chain-like structure due to the inherent magnetic interaction between particles. The enlarged image (insert, Fig. 4.2) also shows a dark area which is possibly the core of a single nanofer ZVI particle surrounded by a thin film of oxide shell. The thickness of the oxidizing shell (insert, Fig. 4.2) based on the TEM software output indicated that the layer surrounding the core varied from 2 to 4 nm

Li et al. (2006) investigated the characteristic of ion ZVI, coated by Pd. It was found that the average particle size is 70 nm and the surface area ranged from 30 to 35 m^2 g^{-1}. The oxide shell surrounding the core nanoparticle was less reactive due to metal coating.

Figs 4.1(c) and 1(d) show corresponding image of SEM-EDS elemental maps from agglomerate of the nanofer ZVI particles with both Cu II (Figure 4.1(c)) and TCE (Fig. 4.1(d)). The particle exhibits strong intensity in the bulk of the agglomerate, but depicts a clear increase in intensity at the edge region corresponding to the amorphous shell. The agglomerated image (Figs. 4.1(a) and 1 (b)) has much brighter light in the central of the amorphous region. Overlay of the elemental maps that are attached to the nanoparticle creating strong complex ligands. However, Weile (2011)

stated that the brighter colour in the SEM/EDS image represent amorphous oxide phase for both at the agglomerate surface and between the individual particles. In earlier studies less focus was given to the chemical composition and micro-structure of particle of the nanoparticle after use. The SEM/ EDS (Table 4.1) technique employed in this study is able to unambiguously map out elemental distribution at a nanometer-scale spatial solution and thereby provides direct evidence of a core layered structure existing in these nZVI materials.

The effect of particle suitability and mobility was studied using ζ potential and the impact of pH on nanofer ZVI. The iso-electic point (IEP) for the nanofer ZVI was found to be at pH of 4.3 (Fig. 4.5). However, increasing pH from 6.5 to 11, nZVI displayed a ζ-potential higher than ± 85 mV. It may be noted that this value of ζ-potential is considered to be suitable for groundwater remediation. The nZVI with pH lower than 8.3 and ζ-potential higher than ± 60 mV is hence an excellent reagent and is attractive for the removal of aqueous contaminants (Sun et al. 2006). Lenka et al. (2012) reported similar results for IEP for the nZVI with a different film coating. However, they found that the ζ potential for uncoated nZVI 25 is below ±30 mV for the pH range of 6 to10. The uncoated nZVI was considered to be slightly suitable for groundwater treatment. Weile (2011) detected that reduction-oxidation potential for Pd-ZVI was ±230 mV. Palladium in this case makes the ZVI more stable and mobile. However, the cost associated with the production of Pd-ZVI is considered be a hurdle as it is much more expensive than TEOS

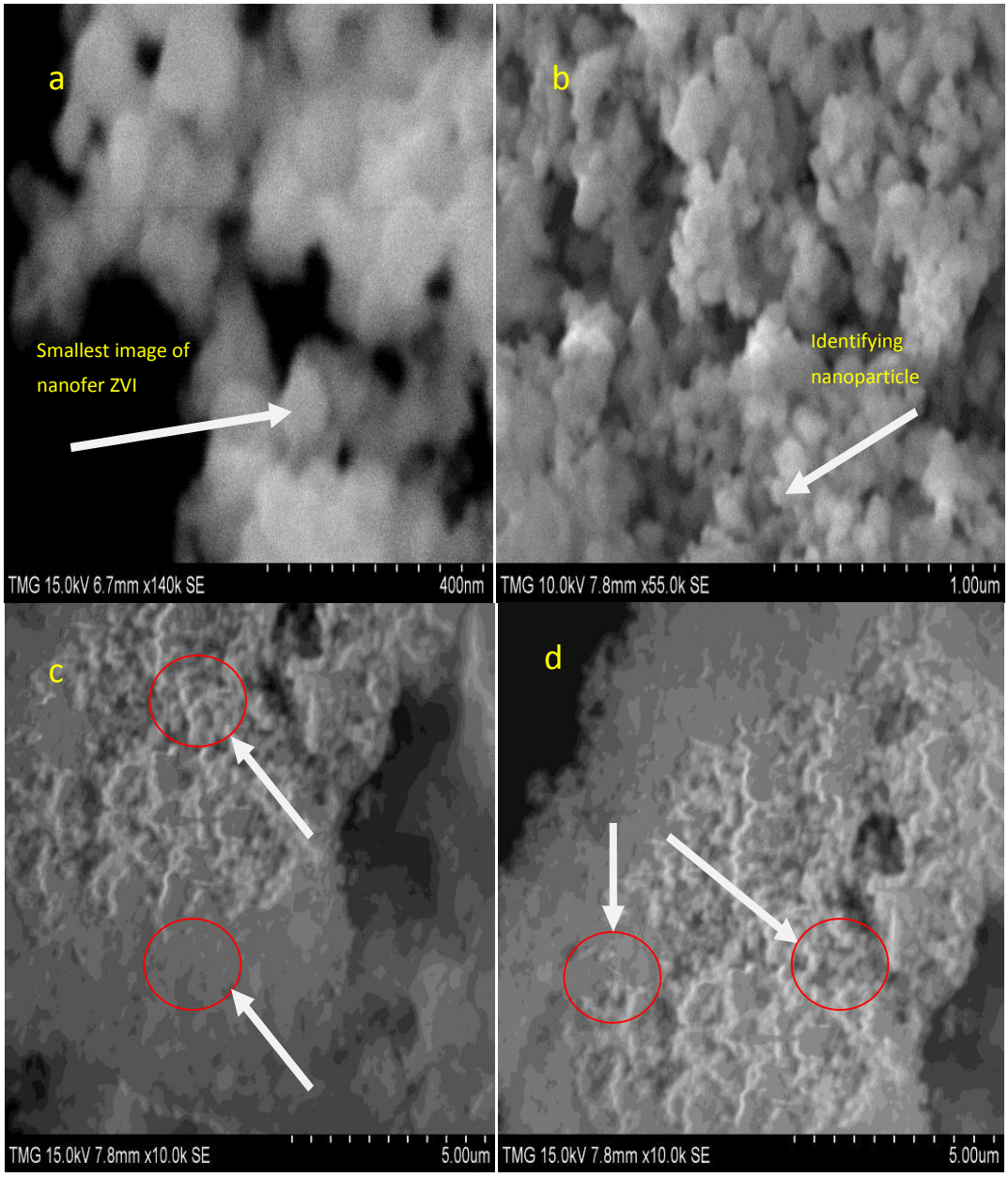

Fig 4.1: SEM images of nanofer ZVI (a) particle size in the range of 40 nm. (b) Particle size in the range of 100 nm. (c) Particle after oxidation of TCE. (d) Particle after Cu (II) adsorption: Arrow shows metal location

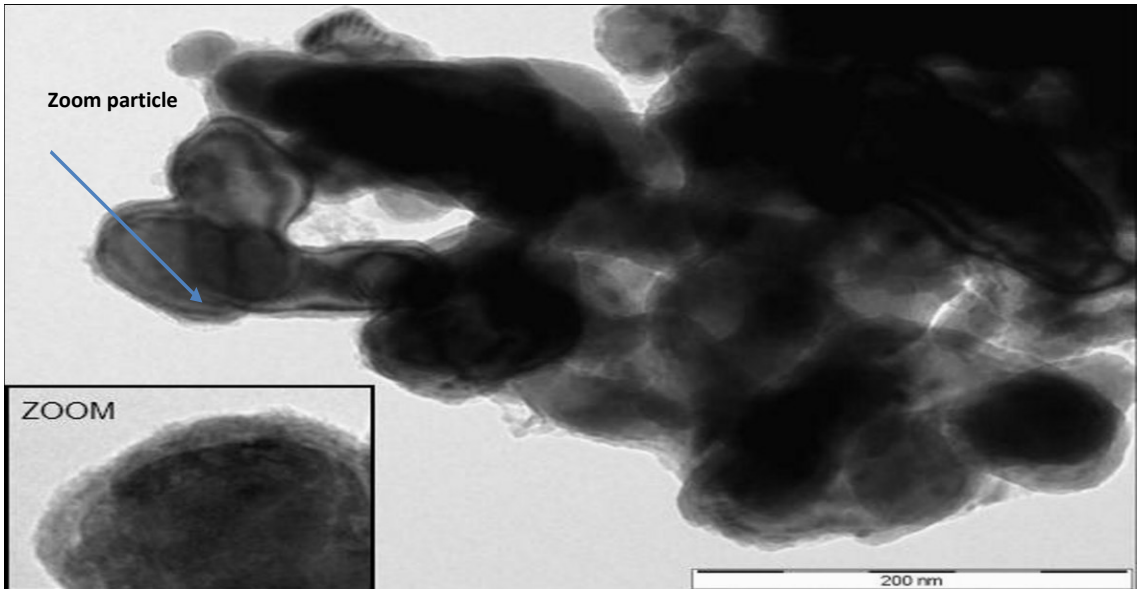

Fig. 4.2: TEM images of nanofer ZVI with the oxide shell. Tip of arrow indicates zoom location

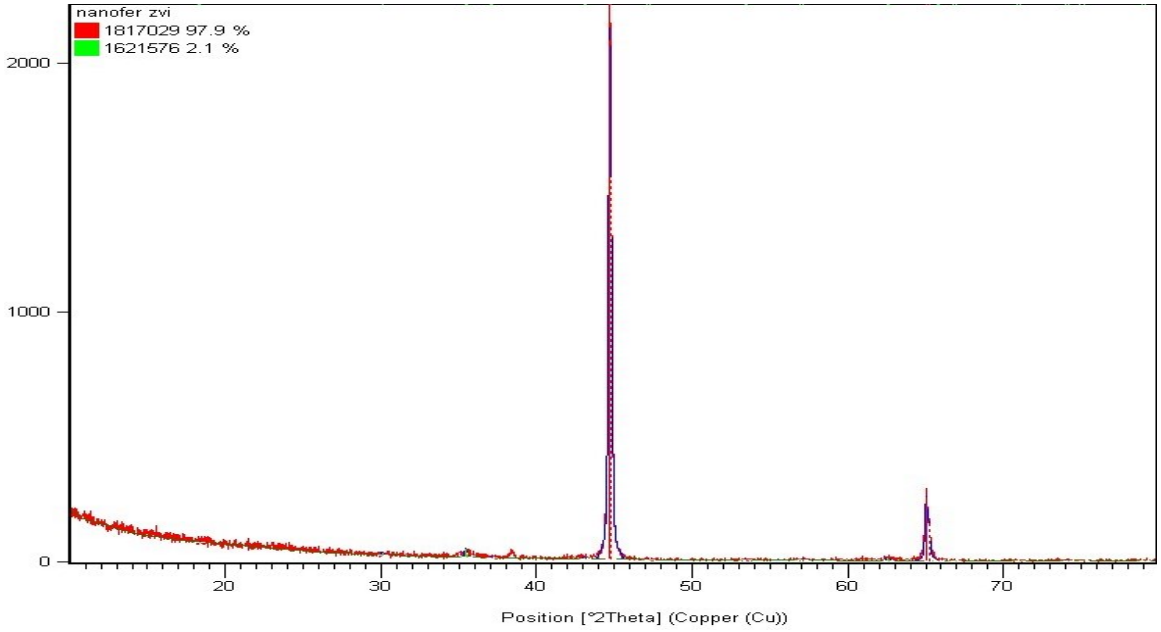

Fig. 4.3: XRD nanofer ZVI of α-Fe the particle size: 50-100 nm and high content of iron range of 70-90 wt. %, (λ=1.5418 Å, U=40 Kv, I 30= 30 mA); composition (green) 2.1%, FeO_3 and (red) α-Fe, 97.9%

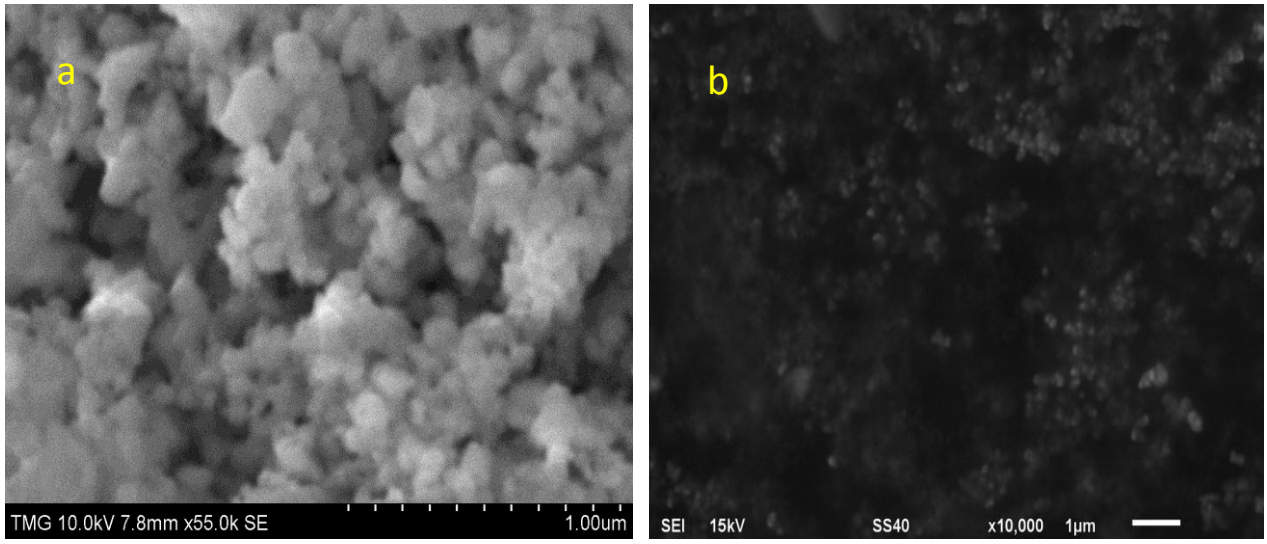

Fig. 4.4: SEM images: (a) non-coated nanofer 25 taken after [7]. (b) Coated with Silicon nanofer ZVI produce in TMG Lab Concordia University.

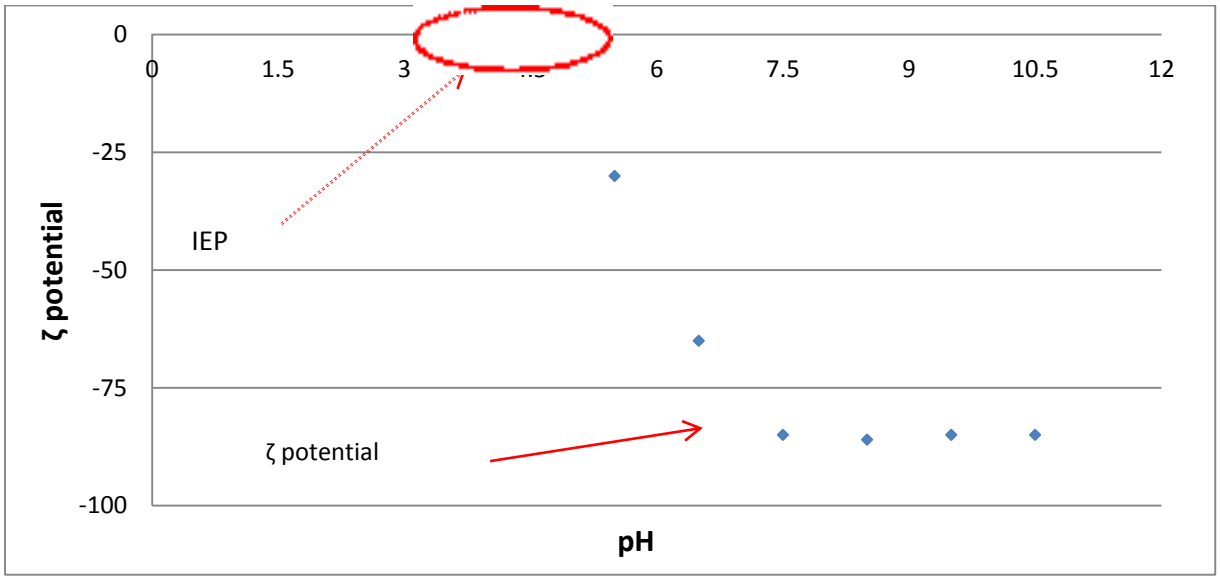

Fig. 4.5: ζ potential as function of pH for nanofer ZVI [Iso-electic point (IEP)]

4.7 Kinetics of Pb (II), Cu (II), Cd (II) and TCE adsorption.

To understand the metal affinities for nanofer ZVI as a function of time, adsorption edge experiments were performed (Figure 4.6). Preliminary studies indicated that the optimum nanofer ZVI dose was determined as 10 mg per 40 ml test solution. Further, these studies also indicated that the optimum pH values were 5.5 for Cu (II), 4.8 for Cd (II), 4.5 for Pb (II), and 5.6 for TCE. Kinetic experiments also, indicated that the adsorption of the metals and TCE is very rapid during the first 50 minutes of the initial step (Figure 4.6). This was followed by a much slower second step which was related to the solid state diffusion and the available surface area. Figure 4.6 (a) shows the rapid and the slow step for Cd removal rate. The equilibrium solid phase concentration at time interval (q_t) is calculated via the mass balance:

$$q_t = \frac{V * (C_0 - C_S)}{m} \qquad (4.1)$$

Where V is volume of contaminant (L), m is the mass of nZVI (mg), C_o is the initial or control concentration (mole) and C_e is the concentration after the sample is filtered at time interval (mole). The values of q_t will be use to determine the mass transfer coefficient K_f.

In these studies, removal rate of 99.2% for Cd (II), 99.7% for Pb (II), 99.9% for Cu (II), and 99.4 % for TCE were achieved in less than 180 min. Further, no significant changes were observed in the removal of both metal ions and TCE after 8 hrs of equilibration. During the first 10 min, the rate of adsorption Cu (II), Pb (II) and Cd (II) were 80%, 76% and 71% respectively. The adsorption of Cu (II) seems to be faster than the adsorptions of Pb (II) and Cd (II). This is probably related to their ionic hydrated radius and the electronegativity (TABLE 3.2). Chorstophi and Axe (2000) have stated that the degree of affinities to adsorption sites is a function of site capacity and the equilibrium constant, which often coincide with the electronegativity of the corresponding metal ions. Schwertman and Taylor (1989) reported that the affinities of metals ions for goethite in the crystal level also follow the order of Cu (II) > Pb (II) > Cd (II) as in the present case.

Although considerable studies have focused on the adsorption of TCE by ZVI, the mechanism of its degradation is not clearly understood and there is a general agreement that electron transfer at the absorbent is required for TCE degradation (Schwertman and Taylor 1989). In the presence of

oxygen, metallic iron gets oxidized and releases electrons which can be used in the reduction reaction of water. Depletion of oxygen can lead to an excess of positive charge in the solution causing the diffusion of chloride ions. Insoluble metal hydroxides can form and coat the external surface and thereby reduce the rate of TCE degradation. These specific results related to TCE degradation (Figure 6 (d)) are in agreement with results of many previous studies [Mohapatra et al. 2010, Nadeem et al. 2009, El-Ashtoukhy et al. 2008, Kang et al. 2008, Pehlivan and Altun, 2006, Saeed et al. 2005, Lowry and Johnson, 2004, Cheng and Wu, 2000, Gotpagar et al. 1999, Wang and W. X Zhang, 1997 and Benjamin and Leckie, 1980).

SEM/EDS images (Figure 4.1) show the nanofer ZVI samples obtained before and after metal adsorption and TCE degradation. The expected effect of localized corrosion of metals (iron) due to the presence of chloride ion is not very evident from the images (Figures 4.1(c) and 1(d)) since the effect of localized corrosion can be noticed, only after a much longer period of metal exposure to oxidation [Mueller et al. 2012, EPA, 2007, Schwertman and Taylor, 1989 and Strehblow 1984).

EDS techniques were used know the amount of metal adsorbed onto the nanoparticles. The results presented in Table 4.1 show that during step 1, the rapid adsorption (weight %) of Cu (II) was much more than that of Pb (II) and Cd (II). The result in agreement with the fact that Cu (II) has smaller ionic radius (Table 3.2) may allow it to be dipped into and attached to the outer surface of the nanofer ZVI.

4.8 Sorption kinetics

Adsorption kinetics depends on the adsorbate-adsorbent interaction and system conditions. Two fundamental attributes of an adsorption process unit are its mechanism and reaction rate. Several studies have described the kinetics of metal adsorption on solid surfaces. Lagergren, (1898) proposed the first order rate equation to describe the kinetic adsorption between the liquid–solid system based on solid capacity. Both the liquid film diffusion model and the homogenous solid diffusion model are generally used to describe the fundamental concept of kinetic adsorption controlled by liquid diffusion (Boyd et al. 1947) or Intraparticle diffusion (Cooney, 1999).

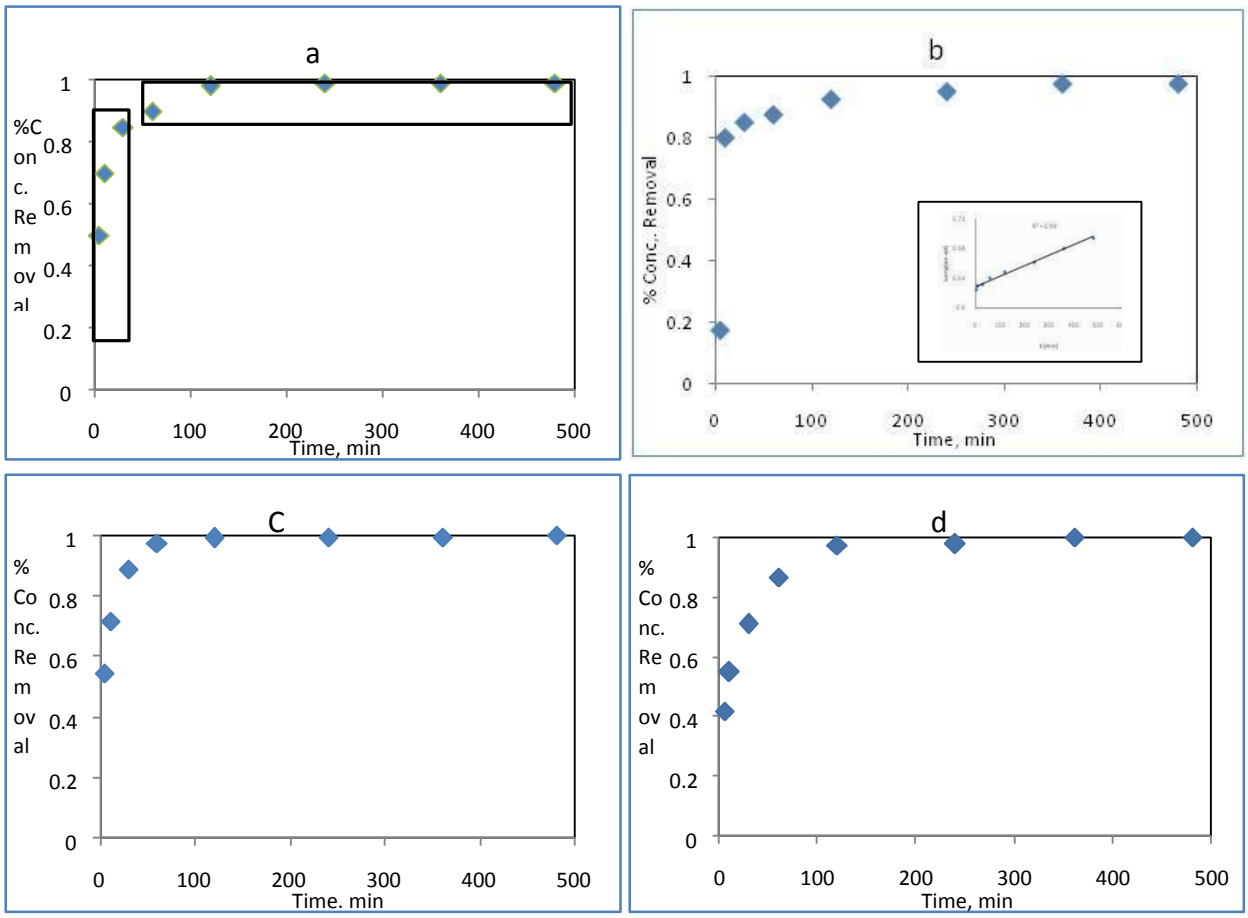

Fig. 4.6: Kinetic adsorption of organic and inorganic contaminants by nanofer star ZVI dose, 10 mg, Conc. 0.01 M, T: 20-22^{o} C, a: Cd (II), b: Cu (II), c: Pb (II) & d: TCE

Table 4.1: SEM/EDS analysis of kinetic experiments for single metal adsorption (Step 1; rapid rate)

	Cu (II)		Pb (II)		Cd (II)	
Element	Weight%	Atomic%	Weight%	Atomic%	Weight%	Atomic%
O	11.32	35.42	9.56	32.27	7.66	22.49
Fe	82.17	59.93	86.53	67.36	91.98	77.39
Cu	**6.51**	5.65				
Pb			**3.91**	0.37		
Cd					**0.39**	0.16

4.8.1 First order kinetic model

Equation (4.2) represents the Lagergren model (LM) which was used to determine the time interval required for ions [(Cu (II), Pb (II) and Cd (II)] and molecules (TCE) to migrate from the liquid phase (solute) to the solid phase (nanofer ZVI). The kinetics data presented in Figure 6 was fitted with the following expression:

$$\log(q_e - q_t) = log q_e - \left(\frac{k_1}{2.303}\right) t, \qquad (4.2)$$

Here q_e and q_t refer to the amount of metal ions adsorbed per unit weight of nanofer ZVI at equilibrium. The plots of log (q_e - q_t) versus t are straight lines. The correlation coefficients for metals removal were determined. The corresponding value of R^2 for Cu (II) ions (insert, Figure 6(b)) was 0.99. The R^2 values for Pb (II), Cd (II) were respectively 0.97 and 0.95. Further, for the initial concentration of 0.01 M of Pb (II), Cd(II) and Cu (II) ions, the corresponding pseudo-first-order rate constants (k_1) were determined to be 0.0137 $min^{-1,}$ 0.0165 min^{-1}, and 0.0187 min^{-1} respectively. These results show that compared to other metals, Cu (II) has the fastest reaction rate. The results are in agreement with the earlier SEM/EDS analysis which indicated that relatively a much larger percentage of Cu (II) was present on the surface of the nanofer ZVI (TABLE 3). For TCE, the R^2 value was 0.96 and k_1 value was 0.0142 min^{-1}.

4.8.2 Adsorption diffusion model

The adsorption diffusion models involve film diffusion, intraparticle diffusion and mass action (Qiu et al. 2009 and Meng, 2005). Liquid film diffusion model (LFDM) and Intraparticle diffusion model (IDM) are the rate limiting steps used to describe kinetic adsorption (Meng, 2005). However, these models are mainly developed to describe the process of film diffusion and Intraparticle diffusion once the contaminants move from the liquid phase (aqueous solution) to the solid phase. In our case, nanofer ZVI denotes the solid phase. The liquid film diffusion model is based on the linear driving force law and is given by Equation (4.2) (Conney, 1999). Consider

$$\frac{dq}{dt} = \mathrm{K_f}\frac{A_S}{V_P}(\mathrm{C} - \mathrm{Ci}) \qquad (4.3)$$

Where $V_P(dq/dt)$ demonstrates the rate of contaminant accumulation on the surface of nZVI. Here, q represents the average contaminant concentration in the solid phase (nZVI), and Vp is the volume of the particle. However, the rate of contaminant transfer across the liquid film is proportional to the surface area of the particle (A) and the driving force that is controlled by concentration gradient (C - C_i). Therefore, it is equal to K_f A_s (C- C_i), where K_f represents the film mass transfer coefficient.

The film diffusion mass transfer rate model ((4.3), (4.4)) was developed earlier by Boyd et al. [40] and later refined by Qiu et al. (2009). Consider

$$\ln\left[1 - \frac{q_t}{q_e}\right] = -Rt, \qquad (4.4)$$

$$R = \frac{3D_e}{r_0 \Delta r_0 K_f} \qquad (4.5)$$

The **R** (min^{-1}) is the liquid film diffusion constant; De (cm^2min^{-1}) is the effective liquid film diffusion coefficient. r_0

(cm) is the radius of particles (nanofer ZVI), Δr_0 (cm) is the thickness of liquid film (which is estimated to be from 2 to 4 nm) and K_f is the equilibrium constant of adsorption defined in (Eq4.3). By plotting (1-q_t/q_e) vs. t, (experimental data presented in Figure (4.6)), a straight line with slope of –**R** can be determined. Since film diffusion is the rate limiting step, the corrected film diffusion coefficient D_e can be evaluated using (Eq. 4.5). The values of liquid film diffusion constant (**R**) and the effective liquid diffusion coefficient (D_e) are presented in TABLE 4.2. Meng, (2005) successfully applied the liquid film diffusion model to predict breakthrough curve for the adsorption of phenol by a polymeric adsorption NDA-1000 under different condition.

The Intraparticle diffusion model (IDM) (Eq.4.6) is developed to describe the mass transfer in an amorphous and homogenous sphere (Cooney, 1999).

$$\frac{q_e}{q_t} = 6\left(\frac{D_s}{\pi R_S S^2}\right)^{0.5} t^{0.5} \qquad (4.6)$$

D_s is the intraparticle diffusion coefficient, R_s is the total particle radius. By plotting q_e/q_t against $t^{0.5}$ the value of D_s

(TABLE 4.2) were determined for adsorption of three metals n nanofer ZVI. It can be concluded that as the particle size increase the adsorption rate decreases. The values of D_e describe the movement of ions or particle in liquid film near the oxidizing layer which is consider the fast step. The values of D_s describe the motion or movement of ions through the core shell of nZVI. The process is much slow due to resistivity and limited free service area (Mohapatra et al. 2010 and Li et al. 2006). The LM and LFDM models are based on the first order kinetic model and the intraparticle diffusion models. Both these models are sequential steps (not independent entities). The two steps (two models) together yield factors such as D_s, K_f, and D_e.

Table 4.2: Calculated parameters of both liquid film diffusion model and Intraparticle diffusion model from kinetic data (C_0 =40 mg/l, T=21-25 ^{0}C),

	Parameters			
Metals	**R**	D_e	k_f	D_s
	min-1	cm^2min^{-1}	g/(mg·min)	cm^2min^{-1}
Cu (II)	0.0173	0.957	2.97	0.083
Pb (II)	0.0159	0.785	2.76	0.069
Cd (II)	0.0134	0.213	2.03	0.025

Table 4.2 includes all parameters of (Eq4. 3), (Eq. 4.4), (Eq 4.5) and (Eq. 4.6). The film diffusion coefficient D_e for the Cu (II) ion is seems to be higher than that for Pb (II) Cd (II). As mentioned earlier, the metal ions adsorption is often described as a two-step mechanism adsorption (Wilczak and Keinath, 1993). The first step represents the rapid metal adsorption occurring due to the diffusion of metal ions from the liquid phase to the external solid phase (nanofer ZVI). In the present study, the time interval for the initial fast step is estimated to be about 10 minutes. Subsequently, a slow step results in the Intraparticle diffusion which controls the adsorption rate and finally the metal adsorption reaches the equilibrium. Chiron et al. (2003) presented similar results for the adsorption of Cu (II) and Pb (II) from aqueous solutions by activated carbon and grafted silica.

The film mass transfer coefficients K_f (TABLE 4.2) represent the rapid step. It appears that the initial rate of Cu (II) diffusion is significantly higher than that for Pb (II) and Cd (II) ions. The

metal concentrations were measured by AA to the nearest 0.1 mg/L. The overall error of concentration measurement is estimated to vary typically from 1 to 3 %.

Admittedly, there is a slight ambiguity in interpreting results of Figure 4.6(b) and Figure 4.6(c). For instance, Cu II reaches 80% adsorption in less than 5 min compared to Pb II which attains 80% adsorption in 15 min, indicating that Cu II adsorption rate is faster in this range. However for 99% removal, Pb II is adsorbed faster. On the other hand, the data (TABLE 4.2) for effective liquid film diffusion coefficient (D_e, fast step) and intraparticle diffusion coefficient (D_s, slow step) predict that the Cu II has the highest adsorption rate while Cd II has the lowest adsorption rate in both the fast and slow steps and hence the results (TABLE 4.2) are unambiguous. The results of these models may contribute to understand the overall kinetics of adsorption mechanism, which was discussed earlier. The rapid step depends on external diffusion. In earlier studies, it is noted that the slow step (internal diffusion) is mainly controlled by intraparticle diffusion and probably this is independent of the particle agglomeration as well as individual metal characteristics (Chiron et al. 2003 and Wilczak and Keinath, 1993).

4.9 Conclusions

Batch studies indicated that the new and innovative adsorbent nanofer ZVI was capable of removing contaminant such as heavy metals [(Cu (II), Pb (II) and Cd (II)] as well as organic [TCE] from polluted water. The comprehensive physical and chemical characteristics of adsorbent (nanofer ZVI) before and after the experiment were determined using images captured by SEM, EDS, and TEM. Nanofer ZVI with 98% of α-Fe is very highly reactive and hence acts as an effective adsorbent that can remove contaminants from polluted water. The batch kinetic test data confirmed that almost all (99%) of the heavy metals such as ((Cu (II), Pb (II) and Cd (II)) can be adsorbed. In case of TCE, the nanofer ZVI got oxidized and releases electrons which reduce the reaction of water. Depletion of oxygen led to an excess of positive charge in the solution causing the diffusion of chloride ions to the surface of nanofer ZVI. The results also indicated that nanofer ZVI degrade TCE almost completely. Batch kinetic adsorption and EDS analysis indicated that the adsorption of Cu (II) was relatively higher compared to the adsorption of Pb (II) and Cd (II). Both the film diffusion model and the intraparticle diffusion model and confirmed that compared to the Pb (II) and Cd (II), the diffusion of Cu (II) was much faster. The models also implied that

the metals transfer to nanofer ZVI was achieved in two stages. In first stage involved the rapid step which was controlled by liquid diffusion. The second stage involved the slow step which was controlled by intraparticle diffusion.

4.10 References

1. Ayob, A., Norli, I., Tjoon, T., Ahmed, A., 2012 "Immobilization of Cu2+ using stabilized nano zero valent iron particles in contaminated aqueous solutions," *Environment Protection Engineering*, vol. 38, no. 3, pp. 119–131.
2. Benjamin, M. M., Leckie, J. O., 1980 "Multiple-site adsorption of Cd, Cu, Zn and Pb (II) on amorphous iron oxyhydroxide," *Journal of Colloid and interface Science*, vol. 79, no.1, pp. 209-221.
3. Boyd, G. E., Adamson, A. W., and Myers, L. S., 1947 "The exchange adsorption of ions from aqueous solutions by organic zeolites, II, Kinetics," *Journal of the American Chemical Society*, vol.69, no. 11, pp. 2836-2848.
4. Cheng, S. F., and Wu, S. C., 2000 "The Enhancement methods for the degradation of TCE by zero-valent metals," *Chemosphere,* vol. 41, no.8, pp. 1263-1270.
5. Chiron, N., Guilet, R., Deydier, E., 2003 "Adsorption of Cu (II) and Pb (II) onto a grafted silica: isotherms and kinetic models," *Water Research*, vol. 37, no.13, pp.3079-3086.
6. Christophi, C. A., and Axe L., 2000 "Competition of Cd, Pb (II), Cd adsorption on goethite," *Journal of Environmental Engineering*, vol.126, no.1, pp.66-74.
7. Cirtiu C. M, Raychoudhury T, Ghoshal S, and Moores A, 2011 "Systematic comparison of the size, surface characteristics and colloidal stabilityof zero valent iron nanoparticles pre- and post-grafted with common polymers," *Colloids and Surfaces A: Physicochemical Engineering Aspects*, vol. 390, pp. 95– 104.
8. Cornell, M., and Schwertmann, U., 2003 "The iron oxides: Structure, Properties, Reactions, Occurrences, and Uses, Wiley-VCH, Weinheim, 2nd edition, 2003.
9. Cooney O., 1999 "Adsorption design for wastewater treatment," Lewis Publishers, Boca Raton.
10. Cwiertny, D. M., Bransfield, S. J., and Roberts, A. L., 2007 "Influence of the oxidizing species on the reactivity of iron-based bimetallic reductants," *Environmental Science Technology*, vol. 41, no.10, pp. 3734−3740.

11. David L. D., 1998 “Handbook of Chemistry and Physics,” CRC, Frederikse H.P.R 78th edition, Boca Raton, 1998.
12. El-Ashtoukhy, E. S., Amina, N. K., Abdelwahab, O., 2008 “Removal of lead (II) and copper (II) from aqueous solution using pomegranate peel as a new adsorbent,” *Desalination*, vol. 223, no.1-3, pp.162–173.
13. Greenlee, F., Jessica, T., Amro, R., and Shaw, J., 2012 “Kinetics of Zero Valent Iron Nanoparticle Oxidation in Oxygenated Water,” *Environment Science Technology*, vol. 46, no.23, pp.12913−12920.
14. Gotpagar, J., Lyuksyutov, R., Cohn, E., and Bhattacharyya, D., 1999 “Reductive dehalogenation of trichloroethylene with zero-valent iron: surface profiling microscopy and rate enhancement studies,” *Langmuir*, vol. 15, no.24, pp. 8412-8420.
15. Kang, K. C., Kim, S. S., Choi, J. W., and Kwon, S. H., 2008 “Sorption of Cu^{2+} and Cd^{2+} onto acid and base pretreated granular activated carbon and activated carbon fiber samples,” *Journal of Industrial & Engineering Chemistry*, vol. 14, no., pp.131–135.
16. Karn, B., Kuiken, T., and Otto, M., 2009 “Nanotechnology and in situ remediation: a review of the benefits and potential risks,” *Environmental Health Perspectives*, vol. 117, no. 12, pp. 1823–1831.
17. Keenan C. R., and Sedlak, D. L., 2008 “Factors affecting the yield of oxidants from the reaction of nanoparticulate zero-valent iron and oxygen,” *Environmental Science and Technology,* vol. 42, no.4, pp.1262−1267.
18. Lenka, H., Petra, J., and Zdenek, S., 2012 “Nanoscal zero valent iron coating for subsurface application,” *in Proceeding of the 4th International Conference,* vol.10, pp. 23-25, Brno, Czech Republic, EU.
19. Li X-Q., Elliott D., and Zhang W., 2006 “Zero-valent iron nanoparticles for abatement of environmental pollutants: material and engineering aspects,” *Solid State and Materials Sciences,* vol. 31, pp. 111–122.
20. Li, X.-Q., and Zhang, W.-X., 2007 “Sequestration of metal cations with zerovalent iron nanoparticles: a study with high resolution X-ray photoelectron spectroscopy (HR-XPS),” *Journal of Physical Chemistry C*, vol. 111, no. 19, pp. 6939–6946.

21. Liu, Y., Majetich S. A., Tilton R. D., Sholl D. S., and Lowry G. V., 2005 "TCE dechlorination rates, pathways, and efficiency of nanoscale iron particles with different properties," *Environmental Science Technology*, vol. 39, no.5, pp. 1338−1345.
22. Lowry G. V., Johnson K. M., 2004 "Congener-specific dechlorination of dissolved PCBs by microscale and nanoscale zerovalent iron in a water/methanol solution," *Environmental Science Technology***,** vol. 38, no.19, pp. 5208-5216.
23. Mace, C., Desrocher, S., Gheorghiu, F., Kane, A., Pupeza, M., Cernik, M., Kvapil, P., Venkatakrishnan, R., Zhang, W., 2006 "Nanotechnology and groundwater remediation: step forward in technology understanding," *Remediation Journal*, vol. 16, no.2, pp. 23-33.
24. Meng, W., 2005 "Study on a mathematical model in predicting breakthrough curves of fixed-bed Adsorption onto resin adsorbent," [MS Thesis], Nanjing University, China, 2005.
25. Mohapatra, M., Mohapatra, I., Singh, P., Anand, S., Mishra, B., 2010 "A comparative study of Pb (II) II, Cu II, Co II, Cd (II) adsorption from single and binary aqueous solution on additive assisted nano-structed goethite," *International Journal of Engineering, Science and Technology*, vol. 2, no. 8, pp. 89-103.
26. Mueller, N., Braun, J., Bruns. J., Černík, M., Rissing, P., Rickerby, D., Nowack, B., 2012 "Application of nanoscale zero valent iron (NZVI) for groundwater remediation in Europe," *Environmental Science and Pollution Reseach*, vol. 19, pp. 550–558.
27. Mueller, N. C., and Nowack, B., 2010 "Nanoparticles for remediation solving big problems with little particles," *Elements,* vol. 6, no.6, pp.395-400.
28. Nadeem, M., Shabbir, M., Abdullah, A., Shah, S., McKay, G., 2009 "Sorption of cadmium from aqueous solution by surfactant modified carbon adsorbents," *Chemical Engineering Journals*, vol. 148, no.2-3, pp.365-370.
29. Nowack, B., 2008 "Pollution prevention and treatment using nanotechnology," in Nanotechnology, H. Krug, Ed., vol. 2 of Environmental Aspects, pp. 1–15, Wiley-VCH, Weinheim, Germany.
30. Nurmi, J.T., Tratnyek, P.G., Sarathym V., Baer, R., Amonettem E., Pecherm K., 2005 "Characterization and Properties of Metallic Iron Nanoparticles: Spectroscopy, Electrochemistry, and Kinetics," *Environmental Science Technolology*, vol. 39, no.5, pp. 1221-1230.

31. O'Carroll, D., Sleep, B., Krol, M., Boparai, H., Kocur, C., 2013 "Nanoscale zero valent iron and bimetallic particles for contaminated site remediation," *Advances in Water Resources,* vol. 51, pp. 104–122.

32. Pehlivan E., Altun, T., 2006 "The study of various parameters affecting the ion exchange of Cu2+, Zn 2+, Ni2+, Cd2+, and Pb (II)2+ from aqueous solution on Dowex 50 W synthetic resin," *Journal of Hazardous Material*, vol. 134, no.1-3, pp.149-156.

33. Qiu. H., Lv, L., Pan, B.-C., Zhang, Q.-J., Zhang, W.-M., Zhang Q.-X., 2009 "Critical review in adsorption kinetic models," *Journal of Zhejiang University* A, vol. 10, no. 5, pp. 716–724.

34. Rangsivek, R., and Jekel, M. R., 2005 "Removal of dissolved metals by zero-valent iron (ZVI): kinetics, equilibria, processes and implications for stormwater runoff treatment," *Water Research*, vol. 39, no. 17, pp. 4153–4163.

35. Raychoudhury, T., Naja, G., Ghoshal, S., 2010 "Assessment of transport of two polyelectrolytestabilized zero-valent iron nanoparticles in porous media," *Journal of Contaminant Hydrology*, vol. 118, pp. 143– 151.

36. Saberi. A., 2012 "Comparison of Pb removal efficiency by zero valent iron nanoparticles and Ni/Fe bimetallic nanoparticles'Iranica," *Journal of Energy and Environment*, vol. 3, no. 2, pp. 189–196.

37. Saeed, A., Akhter, W., Iqbal, M., 2005 "Removal and recovery of heavy metals from aqueous solution using papaya wood as a new biosorbent," *Separation and Purification Technology*, vol. 45, no.1, pp.25–31.

38. Schwertman, U., and Taylor, R. M., 1989 ''Iron oxides.'' Minerals in Soil Environments, SSSA Book Series No. 1, pp. 379–427, Soil Science of America, Madison, Wis. USA, 2nd Edition, 1989.

39. Strehblow, H. H., 1984 "Breakdown of passivity and localized corrosion: Theoretical concepts and fundamental experimental results," *Material and Corrosion*, vol. 35, no.10, pp. 437−448.

40. Stone, V., Nowack, B., Baun, A., 2010 "Nanomaterials for environmental studies: classification, reference material issues, and strategies for physico-chemical characterisation," *Science of the Total Environment*, vol. 408, no. 7, pp. 1745–1754.

41. Sun, Y., Li, X., Cao, X. J., Zhang, W., Wang, H. P., 2006 "Characterization of zero-valent iron nanoparticles," *Advance Colloid Interface Sciences*, vol. 120, pp. 47–56.
42. U.S. EPA, 2007 "Nanotechnology white paper," EPA 100/B-07/001, Environmental Protection Agency, Washington, DC, USA.
43. Wang, C. B., and Zhang, W. X., 1997 "Synthesizing nanoscale iron particles for rapid and complete dechlorination of TCE and PCBs," *Environmental Science Technology*, vol. 31, no.7, pp.2154-2156.
44. Wilczak, A., and Keinath, T. M., 1993 "Kinetics of sorption and desorption of copper (II) and lead (II) on activated carbon," *Water Environmental Research*, vol. 65, no.3pp.238–
45. Wiele, Y., 2011 "Iron-based nanoparticles: Investigating, the nanostructure, surface chemistry, and reaction with environmental contaminants," [Dissertation], Lehigh University.

CHAPTER FIVE

Removal of Pb (II), Cd (II), Cu (II) and TCE from Water by Nanofer ZVI: Modeling and Isotherm Studies

Abstract

Zero valent iron nanoparticle (nanofer ZVI) is a new reagent due to its unique structure and properties. Images of scanning electron microscopy/electron dispersive spectroscopy (SEM/EDS), transmission electron microscopy and X-ray diffraction revealed that nanofer ZVI is stable, reactive and possessed a unique structure. The particles exhibited a spherical shape, a chain-like structure with a particle size of 20 to100 nm and a surface area between 25-30 m^2g^{-1}. The time interval for particles to agglomerate and settle was between 4-6 hrs. SEM/EDS Images showed that the particle size increased to 2 μm due to agglomeration. Investigation of the adsorption and the oxidation behavior of nanofer ZVI used for the removal of Cu(II), Pb(II), Cd(II) ions and TCE from aqueous solutions showed that the optimal pH for Pb(II), Cu(II), Cd(II) and TCE removal were 4.5 and 4.8, 5.0 and 6.5 respectively. Test data were used to form Langmuir and Freundlich isotherms. The maximum loading capacity was estimated as 270, 170, 110, 130 mg per gram of nanofer ZVI for Cu (II), Pb (II), Cd (II) and TCE respectively. The adsorption of metal ions was interpreted in terms of their hydrated ionic radii and their electronegativity. TCE oxidation followed the dichlorination pathway resulting in nonhazardous byproducts.

5.1 Introduction

Nano-zero valent iron (nZVI) is a new and innovative nanomaterial that is used for water and groundwater treatment. The application of engineered nanomaterials for environmental clean-up emerged when small amount of nZVI was used to oxidize trichloroethylene (TCE) and polychlorinated biphenyls (PCB) (Zhu and Lim, 2007 and Wang and Zhang, 1997). Since then, intensive studies have focused on the degradation of water and groundwater contaminants by nZVI. Weile et al. (2011) studied more than more three hundred publications dealing with the use of nZVI for removal of contaminants from environmental media and classified them. The classification included studies linked to removal of halogenated organic compounds, Cr (VI), arsenic, radionuclides and some heavy metals. However, with increasing attention for field

application in both in situ groundwater and soil treatment, research focus on enhancing the removal efficiency, stability, mobility, particle separation, and long term eco-impact (Tratnyek, Johnson, 2006)

Although there is an intense research focus resulting in a huge number of publications on the nZVI application to remove contaminants, some aspects of the fundamental knowledge of nanoparticles, surface morphology, physiochmistry, interaction with of contaminants and the change of nZVI properties based on environmental media warrants further investigation [Mueller et al. 2012, Stone et al. 2010 and Lenka et al. 2012). Mueller et al. (2012) reviewed the practical application of nZVI and found that the application of bimetallic nZVI to remove chlorinated compounds such as TCE and PCB was challenging due to the dynamic change of reactivity of nZVI with co-existence of other contaminants. As a result, many uncertainties concerning the fundamental aspect of the use of nZVI on the PRB technology remain to be probed.

Recent studies of Li & Zhang (2006) dealing with the core shell of ZVI nanoparticle suggested that the passivation of the oxide layer surrounding the nanoparticle surface is an important factor for particle stability and reactivity. It is capable of absorbing contaminants, forming coordinative bonds and also remains permeable to electron and mass transports. Nanofer ZVI is the new generation of nZVI produced by NANOIRON ltd in 2012. The material developed to overcome the problems faced by the coated and non-coated nZVI (Lenka et al 2012, Li and Zhang 2006 and Lowry and Johnson, 2004). The nanofer ZVI was first covered by polyvinylpyrrolidone (PVP) which served as the anchor polymer for silica deposition using tetraethyl orthosilicate (TEOS). Various tests related to ζ potential and particle settling revealed that dipping nanofer ZVI in TEOS increases the stability for subsurface applications and reduces agglomeration. Further detailed studies are needed to investigate the reactivity of this new coated material with different organic and inorganic water contaminants such as class A metals and TCE.

Earlier studies on different forms of nZVI and impregnated ZVI with other metals have focused on the reductive dehalogonation of organic compounds such as TCE, BCP and reductive precipitation of hexavalent chromium, and arsenic (Lowry and Jonson 2004). The number of studies examining the specific functions of nZVI specially the metal-core and the oxide-shell on metals adsorption are limited. The effect of solution chemistry dealing pH, contaminant

concentration and other related aspects have received less attention and are not widely discussed in literature. The objective of the present study is to determine the effect of solution chemistry dealing with pH, contaminant concentration, dose responses and other related aspects on the stability and reactivity of the new coated nanofer ZVI towards different contaminants [Pb (II), Cd (II), Cu (II) and TCE] on the basis of its nanostructure using SEM/EDS, TEM, XRD, AAs, and GC. These contaminants are specifically different from each other in terms of electrochemical properties and are used to probe various reactive pathways permissible with nZVI applications. For each contaminant selected, the isotherms, pH factor, concentration effects, dose responses and the contaminant concentration at the outer surface of nZVI based on spectroscopic and solution phase evidence will be discussed. Further, the reactivity and stability of the new coated nanofer ZVI to reduce adsorb and transform contaminants and its potential in treating diverse group of water contaminants will be examined.

5.2 **Materials and Methods**

The chemical solutions used in the study are presented in the previous chapter [Tables (3.1) and (3.2)]. Nanofer zero valent iron particles were prepared as previously discussed earlier (Chapter3).

5.2.1 Batch equilibrium experiments

Stock solutions were prepared using the indicated chemicals (Table 3.1). Equilibrium tests were performed in closed, 1000-ml glass serum bottles in which the solution volume was 1000 ml. An appropriate volume of the stock solution was diluted with de-ionized water to 1000 ml. The solutions were mixed using a magnetic mixer and left over night. After the mixing, the amount of nZVI and stock solution were added to a 40 ml bottle. Following this, the bottles were closed and the cap was sealed with a Teflon liner to prevent air leakage. The bottles were agitated on a mechanical shaker at 250 rpm. After 24 hours, the reaction was stopped by separating the solution and the particles with a vacuum filtration, using 0.2 μm filter paper (42 Whatman). The particles were dried and stored in a N_2-filled glove box ahead of solid phase analysis, and the solution was acidified with HNO_3 to pH less than two and stored at 4^0 C before solution analysis. A control was performed under identical conditions in parallel, except for the case where no iron nanoparticles were added. For experiments involving volatile compounds (e.g.TCE), 250-ml serum bottles containing 40 ml aqueous solutions were used. After charging a small amount of nZVI, the bottles

were capped with Teflon Mininert valves and placed on a mechanical shaker at 250 rpm at 25 ºC. Both pH and temperature were measuring before and after adding the nZVI to each bottle. All bottles were cleaned using 0.1 mole HCl and washed to insure that no residual contaminants were present. More detail are presented in (Chapter 3).

5.3 Results and discussions

5.3.1 Effect of pH

Batch experiments were carried out to analysis the sorption of Pb (II), Cu (II), Cd (II) and TCE, by nanofer iron as a function of pH. For sorption of heavy metals, pH is an important parameter. The result of experiments for the Pb (II), Cu (II) II, Cd (II) and TCE, are presented in Fig. 5.1. In the present investigation, the rate of removal of Pb (II), Cu (II) and Cd (II) ions in nanofer ZVI is mainly controlled by pH of the solution. The experiments showed that the bulk of adsorption generally occurs over a relatively narrow pH range of two units. This pH range (or adsorption edge) moves to a higher pH as the initial adsorbate concentration increases. These features have also been noted as the characteristics of metal ion adsorption in several previous adsorption studies (Li et al. 2006 and Ho, 2005). In present studies, the optimal pH for Pb (II), Cu (II) and Cd (II) removal were 4.5 and 4.8, and 5.0 respectively. At higher pH, metals were precipitated due to the formation of metal hydroxides and consequently the removal due to sorption was very low. At a low pH, the concentration of protons was high and metal binding sites became positively charged repelling the metal cations. With an increase in pH, the negative charge density on the nanofer ZVI increases due to deprotonation of the metal binding sites, thus permitting increased metal sorption. These results are in agreement with previous studies (Ho, 2005, Brooks et al. 2008, Basu et al 2009, Hui-Qiu et al. 2009, El-Ashtoukhy et al. 2008, Li et al. 2009, Kocaoba and Akcin, 2005 and Jeon et al. 2003). Their results also showed that pH for metals adsorption was in the range of 4.0 to 7.0 for different adsorbents. Various reasons might be attributed to the metal adsorption behavior of the adsorbent relative to solution pH. Since the nanofer ZVI contains large number of active sites, the pH dependence of metals adsorption can largely be related to these active sites and also to the chemistry of the solution. The solution chemistry of transition metal is complicated due to the hydrolysis phenomenon as the pH increases from an acid to neutral, various hydrolyzed species exist and the affinities of these species to the adsorbent surface can vary (Juang and Chung, 2004).

Fig. 5.1, C demonstrated the Cd (II) removal using nanofer ZVI at pH ranging from 2 to 9 units. It is apparent that the adsorption is quite low at pH from 2-4. However, with the increase in pH from 5 to 7, significant enhancement in metal adsorption is reached. The optimum pH for Cd (II) adsorption was 5.5 with a removal efficiency of 99.9 %. After pH 6, Cd (II) adsorption capacity leveled off at the maximum value and beyond this pH, Cd (II) ions get precipitated. It is also interesting to note that at any pH, removal of all metals is very much greater through adsorption than through hydroxide precipitation. At pH $\geq$ 8.0, the dominant species is $Cd(OH)_2$. However, at pH$\leq$ 8.0, Cd (II) will form $Cd(OH)^+$. Therefore, at lower pH there is a competition between the hydronium (H_3O^+) ions and Cd (II) ions to be adsorbed. Cd (II) in this case and other metals has to compete with H_3O^+ for the available sites of nanofer ZVI. However, as pH increases, the competing effect of H_3O^+ ions decreases and the positively charged Cd (II) and $Cd(OH)^+$ ions hook up to the free binding sites. Hence, in the pH range from to 2 to 6, the metal adsorption increases. Agrawal et al. (2006) studied the Cd (II) adsorption on manganese nodule residue (NMR) and obtained similar results.

The adsorption of Pb (II) and Cd (II) is essentially similar. One notes that, optimum pH range for Pb (II) is 4 to 6, while it is 5 to 7 for Cd (II) (Figs.5.1b and 5.1c). The adsorption of Pb (II) by nanofer ZVI is showing in Fig 5.1b. The optimum pH to achieve 99.9% removal efficiency ranged from 4 to 6. The adsorption of metal ions in the acidic range with ZVI adsorbent is commonly traced to both ion exchange and complex formation (Christophi and Axe, 2000).

The maximum percent removal of Cu (II) ions was observed at pH 4 to 5 (Fig. 5.1a). At low pH, H^+ competes for the sorption sites along with the metal ions. Hence, as stated earlier, at higher H^+ concentration, the nZVI surface becomes more positively charged, thus reducing the attraction between adsorbent and metal ions (Chang et al. 1997). However, as pH increases, more negatively charged surface become available, thus facilitating greater metal adsorption. Similar results were observed by Chang et al. (1997) for adsorption of Cu (II) on biomass of Pseudomonas aeruginosa. At a higher pH, the metal ions precipitated as the hydroxide forming a greenish color layer which decreased the rate of adsorption. Based on XPS and XRD analysis, Ponder et al. (2001) suggested that metal ions are reduced to their metallic form and possibly other insoluble phases.

In case of TCE adsorption by nZVI, the proton availability may influence the rate of reaction. It is observed that rate of hydrogenolysis of carbon tetrachloride too increases linearly with decreasing pH (Chen et al. 2001). However, the relationship between bulk pH and availability of protons at the metal surface of nZVI is unknown (Li et al. 2006 and Rao and Jawitz, 2003). Matheson and Tratnyek et al. (1994) showed that the order of reaction with respect to protons is approximately 0.15 indicating that protons are not involved in the rate-determining step but are an indirect effect such as enhancing iron corrosion in aqueous solution. The optimum pH for TCE degradation ranged of 6 to 8 (Fig. 5.1d). This is in agreement Chen et al. (2001). They observed that there is a trade-off between the increased degradation rate constant of TCE at lower pH and the consumption of ZVI by corrosion thus effectively decreasing the surface area.

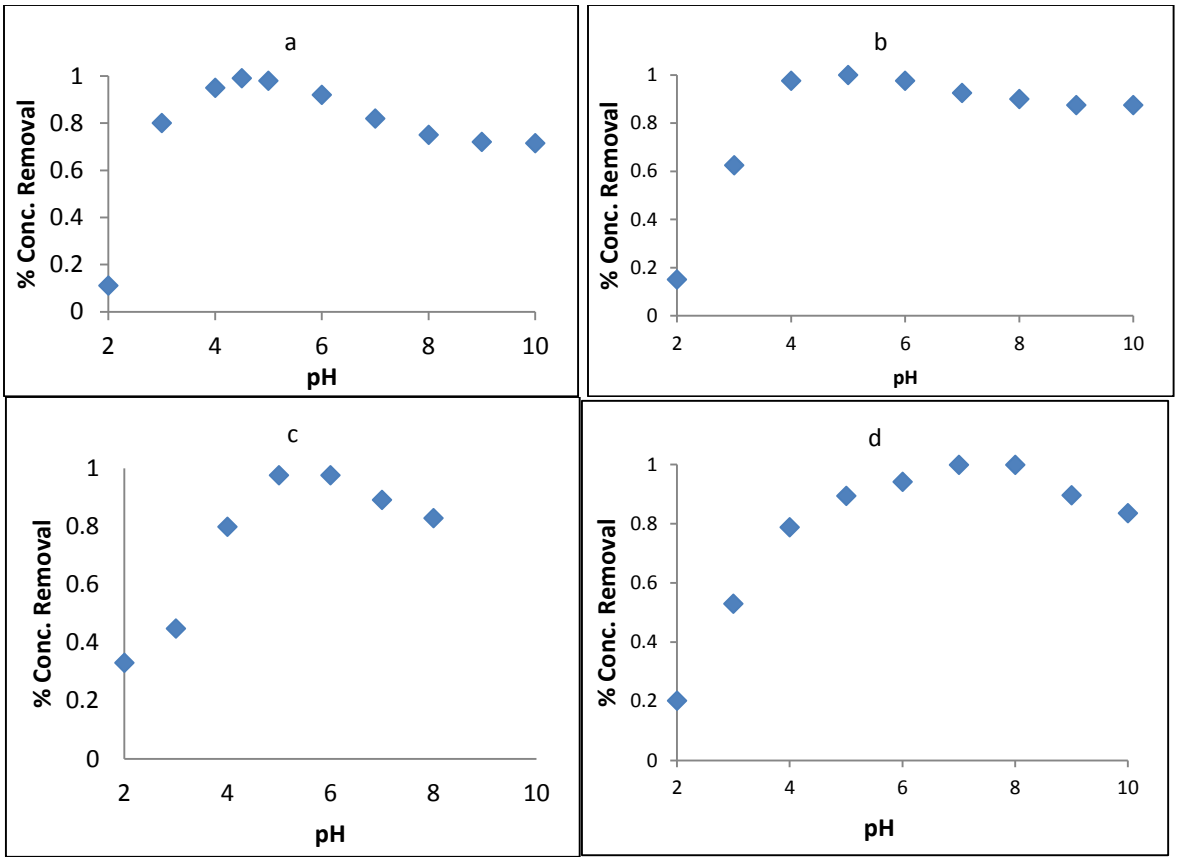

Fig. 5.1: Effect of pH on the removal of metal ions & TCE using nanofer ZVI star, Dose: 10 mg, Conc: 0.01 mM, T: 20-22 0C, a: Cu II, b: Pb II, c: Cd II and d: TCE

5.3.2 Effect of nanofer ZVI dose

It is important to fix the amount of sorbent (nanofer ZVI dose) to design the optimum treatment systems. A series of batch experiments were conducted with 40 ml solutions using adsorbent dose that ranged between 2 to 80 mg. When the addition of the adsorbent dose increased, the percentage removal of metal ions also increased. To keep particles in suspension, all samples were placed in a shaker during the experimental period to insure maximum contact time. A maximum removal efficiency for 99.9 % for Cu (II), 99.2 % for Pb (II), 98.7% for Cd (II) and 99.6% for TCE respectively was achieved (Fig. 5.2). The adsorbent dose of 10 mg appears to be sufficient for optimal removal of metals ions as well as TCE. However, for Cu (II) the optimum dose was 30 mg. The ability of the adsorbent to be effective for metal ions as well as TCE at low dosages (10 mg) can be traced to the greater availability of the exchangeable sites or surface area at higher concentrations. Pehlivan et al. (2006) reported similar findings for metal ions (Pb (II), Cu (II), and Cd (II) removals from aqueous solutions by using Dowex 50 W which is a synthetic resin.

It can easily be inferred that the percent removal of metal ions [Cu (II), Pb (II), and Cd (II)] increases with increasing weight of the adsorbents as shown from the maximum adsorption capacity is achieved in 10 mg. As it stated earlier that Dechlorination follows pseudo first-order kinetics, the important factor that influences is the surface area of the nZVI. Increased surface area nZVI particles would have high surface energies (adsorption capacity) and thus are even more reactive sites. Also, the nanofer ZVI will form surface hydroxyl groups can be coordinated to one, two, or three iron atoms, giving sites with very different reactivates. Thus, nanofer particles are easier to stay suspend in solution for certain time and which help transport and diffusion processes (Lien et al. 2001). Together, these factors will generate a surface with a wide range of adsorption capacity. However, Chen et al. (2001) found that the cleanness of surface material is more important the surface area.

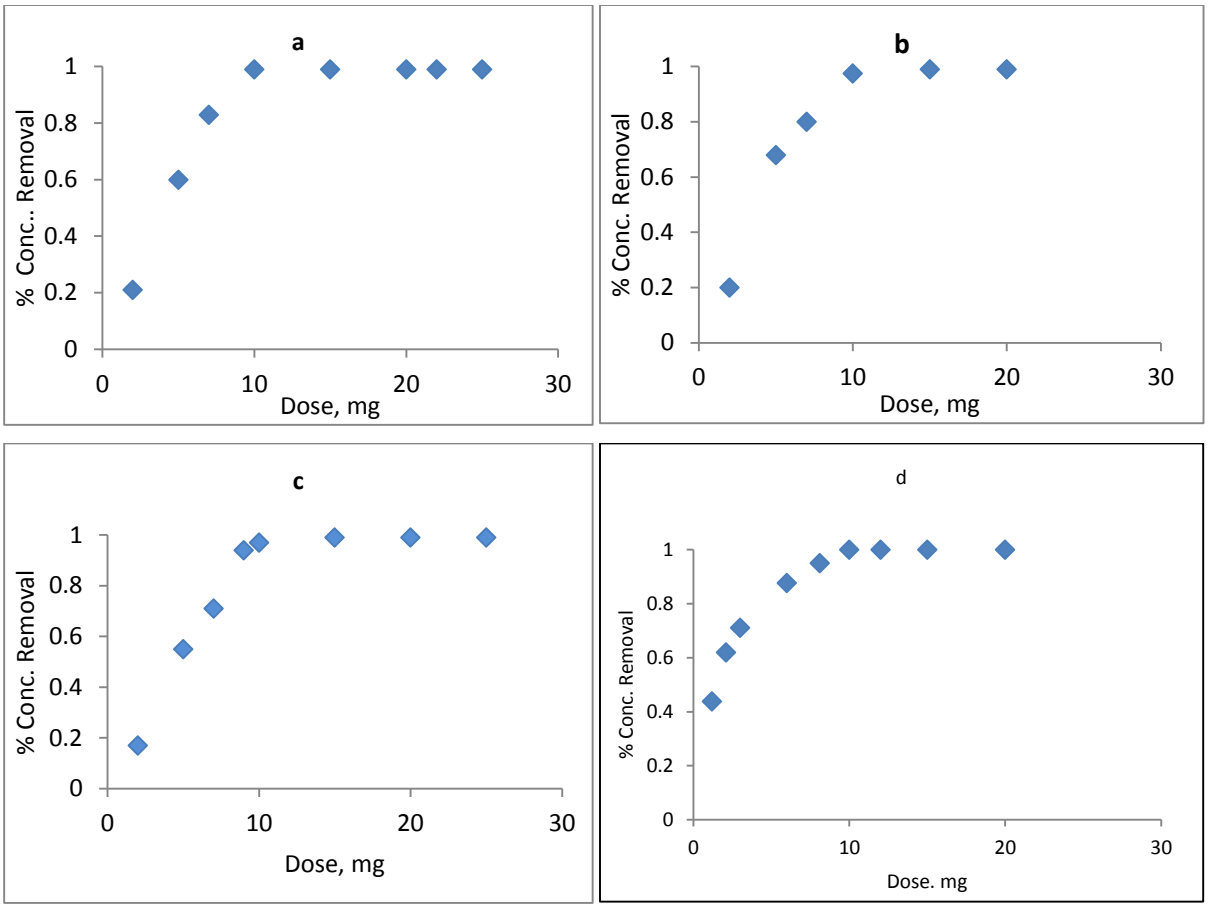

Fig: 5.2: Effect of adsorbent on the removal of metal ions & TCE using nanofer ZVI star, Dose: 10 mg, Conc: 0.01 mM, T: 20-22 0C, a: Cu II, B: Pb II, C: Cd II and D: TCE

5.3.3 Effect of metal ion concentration

The metal adsorption by nanofer ZVI particle's mechanism is particularly dependent on concentration of metals and TCE. Initial concentrations of 0.01 and 0.25 mM of metals and TCE were selected for the comparative study in 0.0 1 M of nanofer ZVI filled in 40 ml tubes. Fig. 5.3a, b and c show the effect of metal ion concentration on the removal of Pb (II), Cu (II), and Cd (II) by nanofer ZVI. At the metal ion concentration of 0.01 mM and the optimum dose of 10 mg and optimum pH, the maximum removal of Pb (II) and Cd (II) was achieved within 60 min. The heavy metals are absorbed by specific sites provided by the acidic functional groups on the nZVI, while with increasing metal concentrations the specific sites are saturated (El-Ashtoukhy et al. 2008 and Kang et al. 2008). However, as the metal concentration increases, the maximum removal efficiency decreases. This indicates that the removal of metal ions is highly dependent on the concentration of the adsorbent.

TCE concentration ranged from 10 ml to 100 ml per liter of di-ionized water and the optimum pH ranged from 6 to 8 (Fig. 5.3d). The maximum removal of TCE was achieved at the concentration of 10 to 40 ml/L within 180 min. This is consistent with the fact that lag time was due to the hydrogen-terminated surface of the nanofer ZVI.

5.4 Sorption isotherms models

The adsorption isotherms are very important in describing the adsorption behavior of solutes on the specific adsorbents. Two isotherm models such as Langmuir and Freundlich were selected and studied. The Langmuir isotherm (Langmuir, 1917) takes an assumption that the sorption occurs at specific homogeneous sites within the ZVI. The linear form of isotherm equation can be written as:

$$\frac{1}{q_c} = \left(\frac{1}{bq_{max}}\right)\left(\frac{1}{C_e}\right) + \left(\frac{1}{q_{max}}\right) \qquad (5.1)$$

Here, q_{max} is the maximum uptake of metals and TCE corresponding to the saturation capacity of the nanofer ZVI and b is the energy of adsorption. The variables q_e and C_e are the amounts adsorbed on the nanofer ZVI and the equilibrium concentration in the solution respectively. The q_{max} constants and b are the characteristics of the Langmuir isotherm and can be determined using equation (5.1). The data fit the Langmuir isotherms model well for single component ions and TCE (Fig. 5.3).

The Freundlich expression is an empirical equation based on a heterogeneous surface [equation (5.2)].

$$\log q_e = \log k_f + \frac{1}{n}\log C_e \qquad (5.2)$$

Here, the intercept log K_f is a measure of sorption capacity, and the slope 1/n is the intensity of sorption. The average strength of nZVI bonds with metal ions varies with adsorption densities. The variables q_e and C_e are the amounts adsorbed and the equilibrium concentration in solution.

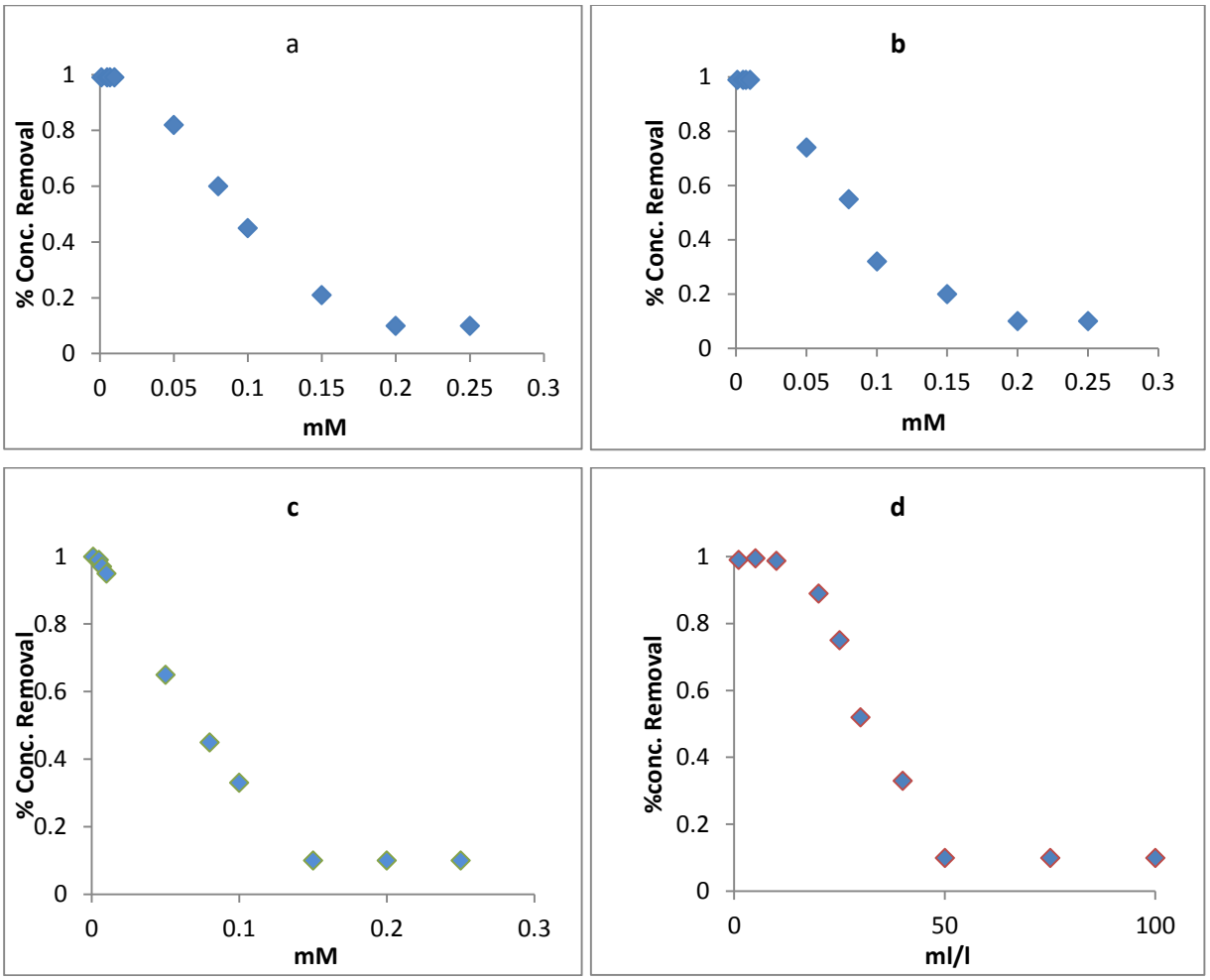

Fig. 5.3: Effect of ion and TCE concentration on the removal efficiency of nanofer ZVI star, Dose: 10 mg, a: Cu II pH- 4.5, b: Pb II pH-4.8, c: Cd II, pH-4.9 and D: TCE, pH-6.5, T: 20-22 ^{0}C

The values of Langmuir and Freundlich parameters for the removal of both metal ions and TCE are presented in Table 5.1. The correlation coefficient (R^2) for the sorption of Pb (II), Cd (II), Cu (II) and TCE are between 0.94 and 0.98. The linearity of the plots in Fig. 5.2-5.3 supports the application of the Langmuir equation, and confirms the monolayer formation of the sorption for metals and TCE on the surface. The values of b and q_{max} indicate that sorption is dependent on concentration and pH.

The expression of separation factor (R_L) in the dimensionless form of the Langmuir isotherm is $R_L = 1/ (1 + bC_0)$, where C_0 is the initial concentration of metal ion and b is the Langmuir constant. R_L can be used to predict affinity between nanofer ZVI and metal ions in the sorption system. The

characteristics of R_L value indicate the nature of sorption as unfavorable (R_L >1), linear (R_L = 1), favorable (0 < R_L < 1), and irreversible (R_L = 0) (Jakcok and Parfitt, 1981). It is observed that, for the selected concentration (0.01 mM) of metal ions, the separation factor (R_L) is less than 1.0 (Table 4) which indicates that the sorption conditions are favorable for all metals and TCE.

Both isotherm models show a better fit with the data. The R2 values for both models are quite high. Generally, it has been found that the Langmuir model is more physically consistent with adsorption isotherm than the Freundlich model (Christophi and Axe, 2000). The Metal capacities (Table 5.1) are consistent with the electronegativity (Table 3.2). The b values indicate that the equilibrium constant for Langmuir model follows the order Pb >Cu > Cd. This trend is in consistent with corresponding hydrated ion radii (Table 3.2). This is in agreement with earlier studies (Christophi and Axe, 2000, Benjamin, M.M., and Leckie, 1981a, Benjamin, M.M., and Leckie, 1981b and Mohapatra et al. 2010, Nurmi et al. 2005, Sun et al. 2006 and Cornell and Schwertmann, 2003).

Table 5.1: Sorption isotherm models parameters

Components	Langmuir parameters				Freundlich parameters		
Inorganics	**q_{max} mg/mg**	**b ml/mg**	**R^2**	**R_L**	**K_f (mg/g)(0.01 mM)^n**	**n**	**R^2**
Cu(II)	0.27	45.25	0.94	0.69	0.53	0.32	0.97
Pb (II)	0.17	15.34	0.98	0.87	0.32	0.06	0.99
Cd (II)	0.11	8.18	0.98	0.92	0.24	0.16	0.97
Organic		**ml/mg**					
TCE	0.12	13.88	0.96	0.88	0.65	0.76	0.96

5.5 Effect of particle aging and agglomeration

The major problem facing application of nZVI in the subsurface is its tendency to agglomerate and rapidly precipitate in aqueous media. However, several studies have focused on developing methods of coating the surface of nZVI particles which protects the particle agglomeration. In the present study, the nanofer ZVI particles were covered by TEOS. Both the agglomeration and sedimentation behavior of the particles was assessed to determine the time during which they stay in suspension. However, after two hours, it was noticed that nZVI particles started to agglomerate

and precipitate (Fig 5.4). This is due to the fact that in the presence of the hydroxyl group, metals share more than one particle creating a ligand which increases the particle size (Weile, 2011). Fig. 5.6b shows the precipitated nanofer ZVI near the bottom of the tube. It took more than 24 hrs to settle most of the agglomerated particles. However, Fig 5.4b indicates that some particles still stay in suspension even after 24hrs. Figs. 5.5a and 5.5b show the SEM/EDS images of particles before and after the experiments. They indicate that the particles lose their structure and morphology creating a sort of cloth like bigger particle. The EDS analysis (Table 5.2) showed that there was a large increase of oxygen level. Lenka et al. (2012) studied the effect of agglomeration between uncoated and coated nanofer ZVI for a period of 60 min. They too found that the coated nanoparticle suspension remained unchanged during the 60 min while the uncoated nanoparticles (nanofer ZVI 25) began to agglomerate as soon as it was introduced to water and sank as precipitate in about 20 min.

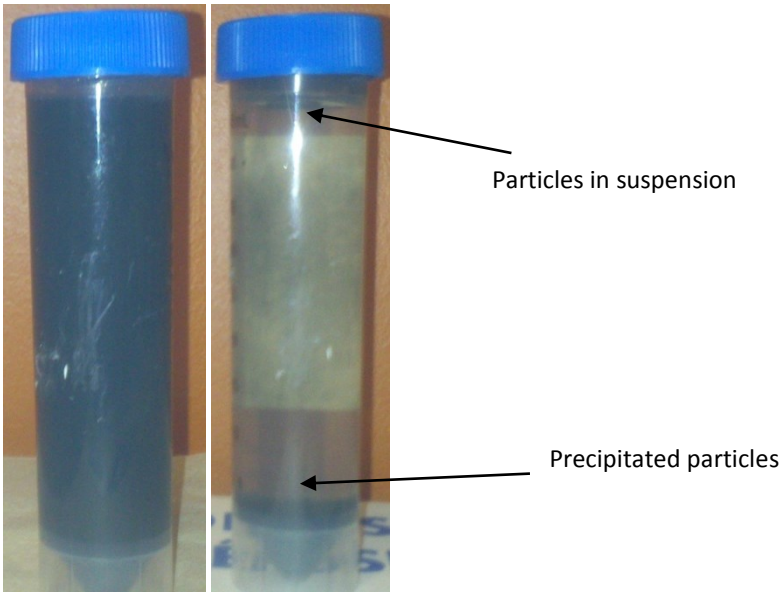

Fig. 5.4: Settling of nanofer ZVI in de-ionized water;
a: Sample after adding the nanofer ZVI and placed in 250 rmp shaker, (at 0.02 hrs)
b: Sample after adding the nanofer ZVI and placed in 250 rmp shaker, (at 24 hrs)

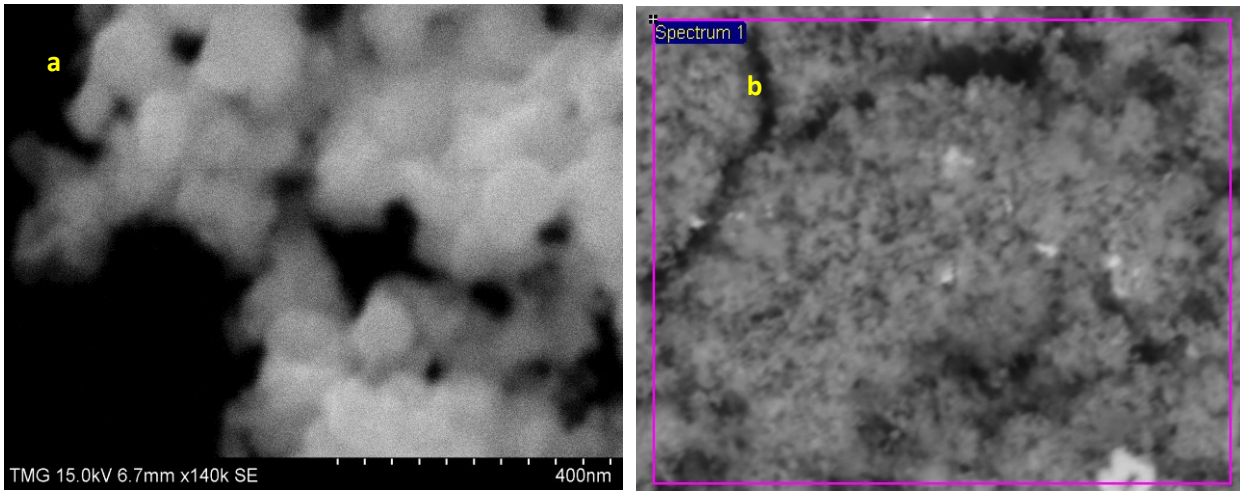

Fig. 5.5: SEM/EDS images for nanofer ZVI before and after the hydroxyl experiment; a: image before the experiments, b: image after 24 hr of settling

Table 5.2: SEM/EDS analysis of before and after the particle settling experiments with di-ionized water

Element	Before		After	
	Wight %	Atomic %	Wight %	Atomic %
Oxygen	4.89	15.29	14.68	38.23
Iron	94.27	84.48	84.52	61.16
Silicon	0.84	0.23	0.80	0.21

5.6 Conclusions

Nanofer ZVI successfully removes inorganic contaminants [Cu II, Cd II, and Pb II] as well as organic [TCE] contaminants from water. The new nanomaterial coated with TEOS is environmentally friendly, inexpensive and can be used replace the ZVI which is commonly used for direct subsurface injection to remediate groundwater. Further, it shows good potential to overcome the setback of the old nanofer ZVI 25 related to fast agglomeration as well as instability in the aqueous media.

Results indicate that the metal adsorption follow the order Cu II > Pb II > Cd II. The test data show that there is threshold concentration that has to be reached for TCE degradation. The TCE reduction by nanoZVI forms a new nonhazardous substance possibly ethanol and other byproducts.

Due to the large surface area and hence the vast availability of active sites as little as 10 mg of nanofer ZVI were adequate to remove the metals and TCE.

For the chosen concentration of the contaminants, the optimum nanofer ZVI dose was found to be 10 mg. and the optimal pH for Pb (II), Cu (II), Cd (II) and TCE removal were 4.5 and 4.8, 5.0 and 7.2 respectively. The isotherm data fitted to Langmuir and Freundlich models showed that the maximum loading capacity is close to 270, 170, 110, 130 mg per gram of nanofer ZVI for Cu (II), Pb (II), Cd (II) and TCE respectively.

The agglomeration test demonstrated that the particle can stays in suspension for a period of 2 to 4 hrs. The test revealed that the time for total agglomeration (sedimentation) is almost 24 hrs. SEM/EDS images of particles before and after the experiments indicate that the particles lose their structure and morphology creating a sort of cloth like bigger particle. The EDS analysis showed that there was a large increase of oxygen level.

5.7 References

1. Agrawal, A., Sahu K.K., 2006 "Kinetic and isotherm studies of cadmium adsorption on manganese nodule residue," *Journal of Hazardous Material*, vol. 137, no.2, pp. 915-924.
2. Basu, NB., Rao, C., Poyer., C., Nandy, S., Mallavarupu, M., Naidu, R., Davis, B., Patterson, B., 2009 "Integration of traditional and innovative characterization techniques for flux-based assessment of dense non-aqueous phase liquid (DNAPL) sites," *Journal of Contaminant Hydrology*. vol. 105 no. 3-4, pp. 161-172.
3. Benjamin M.M., Leckie J.O., 1981a "Multiple-site adsorption of Cd, Cu, Zn and Pb on amorphous iron oxide," *Journal of Colloid Interface Sciences,* vol.79, pp. 209–221.
4. Benjamin, M.M., Leckie, J.O., 1981b "Competitive adsorption of Cd, Cu, Zn, and Pb on amorphous iron oxyhydroxide," *Journal of Colloid Interface. Science*, vol. 83, no. 2, pp.410–419.
5. Brooks, C., Wood, L., Annable, D., Hatfield, K., Cho, J., Holbert, C., Rao, C., Enfield, C., Lynch, K., Smith, R., 2008 "Changes in contaminant mass discharge from DNAPL source mass depletion: Evaluation at two field sites," *Journal of Contaminant Hydrology*, vol.102, no. 1-2, pp. 140-153.
6. Chang, J., Law, R., Chang, C., 1997 "Biosorption of lead, copper and cadmium by biomass of Pseudomonas aeruginosa," *Water Research*, vol. 31, no.7, pp. 1651–1658.

7. Chen, J.L., Al-Abed, S.R., Ryan, J.A., and Li, Z, 2001 "Effects of Ph on Dechlorination ofTrichloroethylene by Zero-Valent Iron," *Journal of Hazardous Materials*, vol. 83, no. 3, pp. 243-254.
8. Christophi A., Axe L, 2000 "Competition of Cd, Cu, and Pb adsorption on goethite," *Journal of Environmental Engineering*, vol, 126, no. 1, pp.66–74.
9. Cornell M, Schwertmann U, 2003 "The iron oxides: structure, properties, reactions, occurrences, and uses," 2nd ed. Weinheim: Wiley-VCH, 2003.
10. El-Ashtoukhy Z, Amina, K., Abdelwahab O., 2008 "Removal of lead (II) and copper (II) from aqueous solution using pomegranate peel as a new adsorbent," *Desalination,* vol. 223, no. 1-3, pp. 162–173.
11. Ho, S., 2005 "Effect of Ph on lead removal from water using tree fern as the sorbent," *Bioresource Techology,* vol. 96, no.11, 1292–1296.
12. Qiu, H., Lu, L.V., Bing-Cai, P., Zhang, Q., Zhang, W.M., Zhang, Q.X., 2009 "Critical review in adsorption kinetic models," *Journal of Zhejiang University Science A,* vol. 10 no. 5, pp.716-724.
13. Jeon B-H., Dempsey B.A., Burgos W.D.., Royer R.A, 2003 "Sorption kinetics of Fe(II), Zn(II), Co(II), Ni(II), Cd(II), and Fe(II)/Me(II) onto hematite," *Water Research* , vol. 37, no. 17, pp. 4135–4142.
14. Juang R-S., Chung J-Y, 2004 "Equilibrium sorption of heavy metals and phosphate from single and binary-sorbate solutions on goethite," *Journal of Colloid Interface Science*, vol. 275, no.1, pp. 53–60.
15. Kang K. C., Kim S.S., Choi J.W., Kwon. S.H., 2008 "Sorption of Cu2+ and Cd2+ onto acid and base pretreated granular activated carbon and activated carbon fiber samples," *Journal of Industrial Engineering and Chemical*, vol, 14, no. 1, pp. 131–135.
16. Kocaoba, S., Akcin, G., 2005 "Removal of chromium (III) and cadmium (II) from aqueous solutions," *Desalination,* vol.180, no. 1-3, pp. 151-156.
17. Kumar, V., Kumar, M., Jha M.K., Jeong, J., Chun, J., Lee J.C., 2009 "Solvent extraction of cadmium from sulfate solution with di- (2-ethylhexyl)phosphoric acid diluted in kerosene," *Hydrometallurgy*. vol. 96, no. 3, pp.230-234.
18. Langmuir I., 1917 "The constitution and fundamental properties of solids and liquids. Part I: Solids," *Journal of American Chemical Society*, vol. 38, no. 9, pp 1848-1906.

19. Lenka. H., Petra. J., and Zdenek. S., 2012"Nanoscal zero valent iron coating for subsurface application," *Brno , Czech Republic, EU* vol. 10, pp 23-25.
20. Li X-Q., Elliott, D., and Zhang, W., 2006 " Zero-valent iron nanoparticles for abatement of environmental pollutants: material and engineering aspects," *Critical Reviews in Solid State and Materials Sciences,* vol. 31, pp. 111–122.
21. Li, S. L., Yan, W. L., Zhang, W. X., 2009 "Solvent-free production of nanoscale zerovalent iron (Nzvi) with precision milling," *Green Chemistry*, vol. 11, pp.1618- 1626.
22. Li, X. Q., Zhang, W. X., 2006 "Iron nanoparticles: the core-shell structure and unique properties for Ni(II) sequestration," *Langmuir, v*ol. 22, no. 10, pp. 4638-4642.
23. Lien, H.-L., Zhang, W., 2001 "Nanoscale iron particles for complete reduction of chlorinated ethenes," *Colloids and Surfaces A: Physicochemical and Engineering Aspects,* vol. 191, no.1-3, pp. 97–105.
24. Lowry, G. V., Johnson, K. M., 2004 "Congener-specific dechlorination of dissolved PCBs by microscale and nanoscale zerovalent iron in a water/methanol solution," *Environmental. Sciences Technology*, vol. 38 no.19, pp 5208-5216.
25. Jakcok, M.J., Parfitt, G.D., 1981 "Chemistry of interfaces," Ellis Horwood, New York, 1981.
26. Matheson, L. J., Tratnyek, P. G., 1994 "Reductive dehalogenation of chlorinated methanes by iron metal*," Environmental Science Technology* , vol. *28, no.*12, pp 2045-2053.
27. Mohapatra, M. L., Mohapatra, P., Singh, S., Anand B., and. Mishra K.,, 2010 "A comparative study on Pb(II), Cd(II), Cu(II), Co(II) adsorption from single and binary aqueous solutions on additive assisted nano-structured goethite," *International Journal of Engineering Science and Technology*, vol. 2, no. 8, pp. 89-103.
28. Mueller. N., Braun. J., Bruns. J., Černík. M., Rissing. P., Rickerby. D., Nowack. B., 2012 "Application of nanoscale zero valent iron (NZVI) for groundwater remediation in Europe," *Environmental Science Pollution Research*, vol. 19, pp. 550–558.
29. Nurmi, T., Tratnyek, G., Sarathy. V., Baer, R., Amonette, E., Pecher. K., 2005 "Characterization and properties of metallic Iron nanoparticles: spectroscopy, electrochemistry, and kinetics," *Environmental Science and Technology*, vol. 39, no. 5, pp. 1221-1230.

30. Pehlivan, E., Altun, T, 2006 "The study of various parameters affecting the ion exchange of Cu2+, Zn 2+, Ni2+, Cd2+, and Pb2+ from aqueous solution on Dowex 50 W synthetic resin," *Journal of Hazardous Material*, vol. 134, no.1-3, pp. 149-156.
31. Ponder, S. M., Darab, J. G., Bucher, J., Caulder, D., Craig, I., Davis, L., Edelstein, N., Lukens, W., Nitsche, H., Rao, L. F., Shuh, D. K., Mallouk, T. E., 2001 **"**Surface chemistry and electrochemistry of supported zerovalent iron nanoparticles in the remediation of aqueous metal contaminants," *Chemistry of Material,* vol, 13. No, 2, pp. 479-486.
32. Rao P.S.C., Jawitz, J.W., 2003 "Comment on 'Steady state mass transfer from single component dense nonaqueous phase liquids in uniform flow fields' by T.C. Sale and D.B. McWhorter," *Water Resource. Research*, Vol. 39, no.3, pp 23-35.
33. Stone, V., Nowack, B., Baun, A., Brink, N., Kammer, F., Dusinska, M., Handy, R., Hankin, S., Hassellov, M., Joner, E., Fernandes, T., 2012 "Nanomaterials for environmental studies :Classification, reference material issues, and stra tegies for physicchemical characterization," *Science of Total Envirnment*, vol. 408 no.7, pp 1745-1754.
34. Sun, Y., Li, X., Cao, X. J., Zhang, W., Wang, H. P., 2006 "Characterization of zero-valent iron nanoparticles," *Advance Colloid Interface Science*, vol, 120. No. 1-3, pp. 47–56.
35. Tratnyek, P. G., Johnson, R. L., 2006 "Nanotechnologies for environmental cleanup," *Nano Today*, vol. 1, no 2, pp. 44-48.
36. Wang, C. B., Zhang, W. X., 1997 "Synthesizing nanoscale iron particles for rapid and complete dechlorination of TCE and PCBs," *Environental Science Technology*, vol. 31, no 7, pp. 2154-2156.
37. Weile Yan., 2011"Iron-Based nanoparticles: investigating the nanostructure, surface chemistry and reactions with environmental," [Dissertation], Lehigh University.
38. Zhu, B. W., Lim, T. T., 2007 "Catalytic reduction of chlorobenzenes with Pd/Fe nanoparticles: reactive sites, catalyst stability, particle aging, and regeneration," *Environmental Science Technology*, vol. 41. No.21, pp. 7523-7529.

CHAPTER SIX

Competitive adsorption and oxidation behavior of Heavy metals on new coated zero valent iron nanoparticle with tetraethyl orthosilicate

Abstract

Zero valent iron nanoparticle (nanofer ZVI) is a new powerful adsorbent due to its coating with Tetraethyl orthosilicate (TEOS). TEOS imparts higher reactivity and decreases particle agglomeration. The competitive adsorption and displacement of multi-metals are influenced by time, pH and initial concentration, the presence and properties of competing metals ion in the solution. For both the isotherm and kinetic studies performed for multi-metals adsorption experiments, compared to Pb II and Cd II, Cu II achieved the higher adsorption capacity during the initial 5 min. After 120 min, all metals achieved removal efficiency in the range of 95 to 99%. Comparing the results of single and competitive adsorption kinetic tests for all three metals during the initial 5 min, the presence of other metals generally reduce metal removal efficiency. Both kinetic adsorption and electron dispersive spectroscope (EDS) analysis found that Cu II gets adsorbed faster than the other metals. The Langmuir model for multi metal adsorption was employed to understand the mechanism of isotherm studies. Both pseudo first and second order models were employed using experimental data. R^2 values for the corresponding experimental data indicated that multi metal adsorption systems follow pseudo second order behavior.

6.1 Introduction

In the past, some studies have dealt with the removal of individual heavy metals from aqueous solution using nanoparticles. Only limited studies have discussed competitive adsorption of heavy metal in polluted water. In particular, none these studies have dealt with the competition of metal ions on nZVI. Multiple competing ions are more frequently encountered than single ions (Christophi and Axe, 2000). Benjamin and Leckie (1981) studied the competitive adsorption of heavy metals on amorphous iron oxyhydroxide. They stated that the competition between metals occur when the total of number of adsorbed sites are limited. In the competition for adsorption between Cu and Cd on amorphous iron oxyhydroxide, it was found that adsorption of Cd was slightly decreased when copper introduced to the aqueous solution (Cowan et al. 1991). They concluded that the competitive interactions between metals in this case were minimal, because

each metal got adsorbed to different sites on the oxide surface. However when metals exceed their saturation, both precipitation and adsorption may have occurred. This leads to difficultly in distinguishing adsorption from surface precipitation. However, Swallow et al. (1980) did not observe the competition between Cu and Pb using the same adsorbent. In fact, they found a reduction in Cu adsorption in the presence of Fe, in an oxygen-free environment.

Cowan et al (1991) studied Cd adsorption on iron oxide, in the presence of Ca, Mg, Ba and Sr. Competition was observed primarily between Cd and all alkaline earth metals. The adsorption of Cd was reduced more than 25%, whenever Ca was added to the aqueous solution. The reduction in Cd adsorption was less than 8% in presences of Mg, Br and Sr. They concluded that other factors such as surface characteristics, density, net surface charge, metal speciation and pH could play a role in the competition between metals on any adsorbent. The effect of site density on the competition of metals was examined by Zasoki and Burau. (1988) in isotherm studies related to Cd and Zn adsorption on hydrous manganese oxide (δ-MnO_2). The site density consists of both high energy sites which get filled first, followed by low energy sites. During the first step linked to the high energy sites, Cd adsorption was faster than Zn, whereas Zn adsorption was faster at the lower energy sites. The overall results indicated that adsorption of Cd decreased by 25% in presence of Zn and the adsorption of Zn decreased by more than 50% in presence of Cd.
Christophi and Axe, (2000) studied the competitive adsorption of Cu, Cd and Pb on goethite. The competition between Cu-Cd and Cu-Pb indicated that Cu displaces Cd and Pb on more than 60% of the available sites. Thus, the metal competitive adsorption experiments showed a slight decrease of Cu adsorption (4.6%). It was explained by the fact that Cu species exist as electrochemically inactive $Cu(OH)_{2\,aq}$ in the presence of Cd and Pb. However, no variation in the adsorption of Pb and Cd were observed. They concluded that if site density is limited, both electronegativity and hydrated ion are the key curial factors that will dominate metal adsorption. Srivastava et al. (2005) studied the effect of pH (adsorption edge) in the competition of Cu, Cd, Pb and Zn by kaolinite. It was found that competition is greatly affected by pH. At lower pH, the adsorption of these metals decrease rapidly. Once pH increases, adsorption and competition of metals increase. However, Cd uptake was slower until pH reached 7.5 when the hydroxyl group was forming and enhanced the mobility and reactivity of Cd. Also, they found that the presence of Cd and Zn decreased the uptake of Cu and Pb on the exchange sites.

Recent studies done by Chen et al. (2010) investigated the adsorption isotherms of Cu, Cd and Pb on nano-hydroxyapatite (nano-HAP). The experiments were done using metal nitrate salt species at different mole ratios. Further, equilibrium metal adsorption capacity significantly decreases in the multi-metal ions adsorption systems than in single-metal sorption system. The highest adsorption capacity was detected for Pb and this was followed by Cu than Cd. These results are in contradiction with some of the early studies [Christophi and Axe, 2000, Benjamin and Leckie 1981a, Benjamin and Leckie 1981b, Cown et al 1991, Swallow et al. 1980, and Zasoski and Burau, 1988). Most of these investigations discussed the competition of heavy metals on different adsorbents using only isotherm studies (adsorption edge and concentration). However, no study has investigated the effect of kinetic adsorption (time) on heavy metal adsorption competition.
Nanofer zero valent iron (nanofer ZVI) is a relatively new and innovative material capable of removing organic as well as inorganic contaminants in water. This new adsorbent also displays a decrease in agglomeration when it is coated with Tetraethyl orthosilicate (TEOS). TEOS imparts an increase in reactivity to nanofer ZVI. The mechanisms of heavy metal removal using nZVI depend on the standard redox potential (E^o) of the metal contaminant. For instance, Cd which is more electronegative than Fe^0 gets removed by adsorption to the iron hydroxide shell. On the other hand, metals with E^0 which is much more positive than Fe^0 (e.g. Cu) are more readily removed by reduction and precipitation. Pb which is slightly more electropositive than Fe^0 gets removed by reduction and adsorption (Li and Zhang 2007). In general, metal removal is also linked to oxidation and co-precipitation which in turn depend on prevailing chemical conditions (pH, initial concentration and speciation of contaminant metals).

The main objective of this study is to investigate the potential of using ZVI nanoparticle coated with TEOS (nanoferZVI) to evaluate the competitive sorption of Cu, Pb and Cd in binary and multi-metal reaction systems. To this end, the effects of different factors, such as adsorption edge (pH), adsorption capacity, metal speciation and kinetic adsorption (time) will be examined. Also, the pseudo first and pseudo second order models along with Langmuir model are selected to fit and describe the experimental data.

6.2 Materials and methods

The chemical solutions used in the study are presented in the previous chapter [Tables (3.1) and (3.2)]. Nanofer zero valent iron particles were prepared as previously discussed earlier (Chapter3).

6.3 Experimental procedures

6.3.1 Batch equilibrium experiments

The competition adsorption experiments as function of pH (adsorption edge) and concentration (isotherm adsorption) were prepared using the indicated chemicals fisher grade (Table 3.1). The stock solutions were performed in closed, 1000-ml glass serum bottles in which the solution volume was 1000 ml. An appropriate volume of the stock solution was diluted with de-ionized water to 1000 ml. The solutions were mixed using a magnetic mixer and left over night. After the mixing, the amount of nZVI and stock solution were added to a 40 ml bottle. Following this, the bottles closed and the cap was sealed with a Teflon liner to prevent air leakage. The bottles were agitated on a mechanical shaker at 250 rpm at 21^0 C. After a suitable time interval (typically 24 hours for reactions with metal species), the reaction was stopped by separating the solution and the particles with a vacuum filtration using 0.2 μm filter supplied by (grad 42 Whatman). The particles were dried and stored in a N_2-filled glove box ahead off solid phase analysis, and the solution was acidified with 0.1 mole HCl before the analysis. After charging a small amount of nZVI (10 mg), the bottles were capped with Teflon Mininert valves and placed on a mechanical shaker at 250 rpm at 25 ^{o}C. Both pH and temperature were measuring before and after adding the nZVI to each bottle. All bottles were cleaned using 0.1 mole HCl and washed to insure that no residual contaminants could occur. After the liquid phase analyses done the samples acidified and drop to pH less than two and stored at 4^0 C. For each set of experiments, a control was performed under identical conditions in parallel except for the case where no iron nanoparticles were added. The adsorption edge experiments were conducted at 0.01 M for binary and multi- concentration of metals. The equilibrium pH of the suspension was varies from 4.5 to 7.5 with a 1 increments unit using radiometer standard buffers (4, 7, 10). The suspension was equilibrated for the metal adsorption for 2 hrs. More detail are presented in (Chapter 3).

6.3.2 Batch kinetic experiments

Kinetic experiments of reactions with selected organic and inorganic species were performed. The amount of chemical added was diluted with de-ionized water to 1000 ml, sealed and were left in the mixer overnight. After mixing, nZVI and stock solution were added to 40 ml bottle. Following this, the bottles were closed and the caps with a Teflon liner sealed the bottles to prevent leakage. The head room in the bottle was kept to the minimum. The bottles were agitated on a mechanical shaker at 250 rpm at 21^0 C. Time was recorded for each bottle at the moment of adding the nZVI. Each bottle was given suitable time and code. After a suitable time interval, the bottles the nZVI were separated using with vacuum filtration with 0.2 μm filter supplied by (grad 42 Whatman). The pH and temperature were measured before and after adding the nZVI. The filtered solutions was immediately, acidified, and stored at 4^0 C prior to analysis. The Atomic absorption spectroscopies (AAS Perkin Elmer) were used to analysis of metals. However, the TCE was analyzed by the gas chromatography (GC Varian 3800).

Before starting multi metal adsorption tests, a few single metal (Cu II, Pb II and Cd II) adsorption experiments under identical conditions were also conducted for further evaluation. More detail are presented in (Chapter 3).

6.4 Results and discussions

6.4.1 Isotherm studies

The material set-up for the metal competitive displacement experiments was similar to the batch isotherm and kinetic studies. The isotherm studies of metal competition were conducted at pH = 4.5. The nanofer ZVI dosage was 10 mg which was derived from the earlier results of batch tests of single metal adsorption (inserts, Figs. 5.2). The total volume for each binary and mixed solution was 1000 mL, and 10 mg of nanofer ZVI. Reducing the nanofer ZVI below 0.05 mole limits the total available sites which are less than those needed for either one of two metals to be completely absorbed. The metal concentrations were below saturation and were selected on the basis of site densities to promote metal competition (Table 3.2). The results of the metal experiments are shown in Figs. 6.1 to 6.4 and they are related to Cu II-Cd II (Fig.6.1), Cu II-Pb II (Fig.6.2), Cd II-Pb II (Fig.6.3) and Cu II-Cd II- Pb II (Fig.6.4).

The isotherm adsorption of the metals in multi-element system (Figs. 6.1-6.4) differed from their corresponding behavior in single element systems (inserts-Figs.6.1-6.4). Most notable was the reduction of Cd II sorption in both binary (Fig 6.1, 6.2) and multi element systems (Fig 6.4). The surface speciation curve for the metals adsorption reveals that the adsorption in single-element system predominantly occurred on permanent negatively charge sites in the first stage up to pH~4.5 to 5 (Chrestophi and Axe, 2000, Chen et al 2010 and Benjamin and Leckie , 1981b). The predominance of the uptake for Cu II adsorption in both binary metal and multiple metal system adsorptions in Figs. 6.1, 6.3 can be explained by considering the behavior of both Cd II (Fig 6.1) and Pb II (Fig. 6.3). For instance, when Cu II gets adsorbed on nanofer ZVI, the variable charged hydroxyl edge began at pH ~ 3 in single element system; however, the Cu II adsorption took place predominantly on the permanent charge surface up to pH ~4.5. However, in case of Pb II and Cd II shown in Fig 6.2, no significant competition is seen. Only less than 10 % reduction of the adsorption capacity was noticed between the single-element adsorption (insert Figs.6.1-6.4) and the binary-element adsorption (Figs. 6.1, 6.2, 6.3).

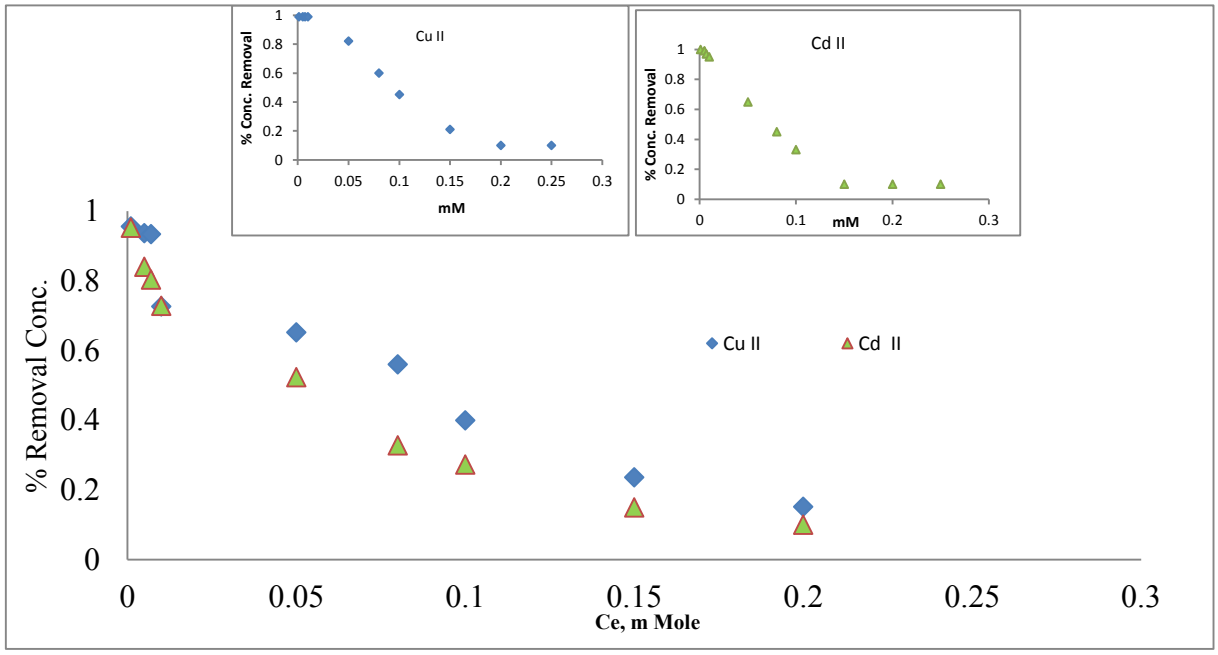

Fig. 6. 1: Isotherm studies of metal competition, Cu II - Cd II, insert: Single isotherm studies of metals pH: 4.5, T: 22 ^{O}C

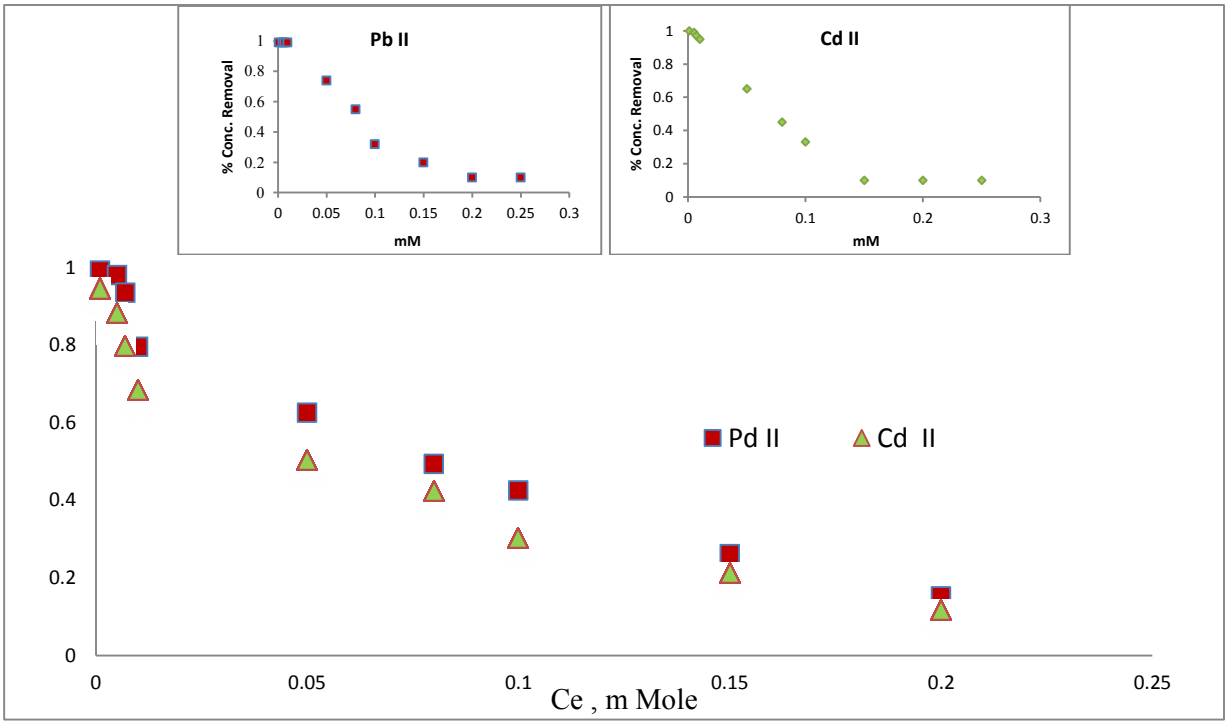

Fig.6.2: Isotherm studies of metal competition, Pb II - Cd II, insert: Single isotherm studies of metals, pH: 4.5, T: 22 ^{O}C

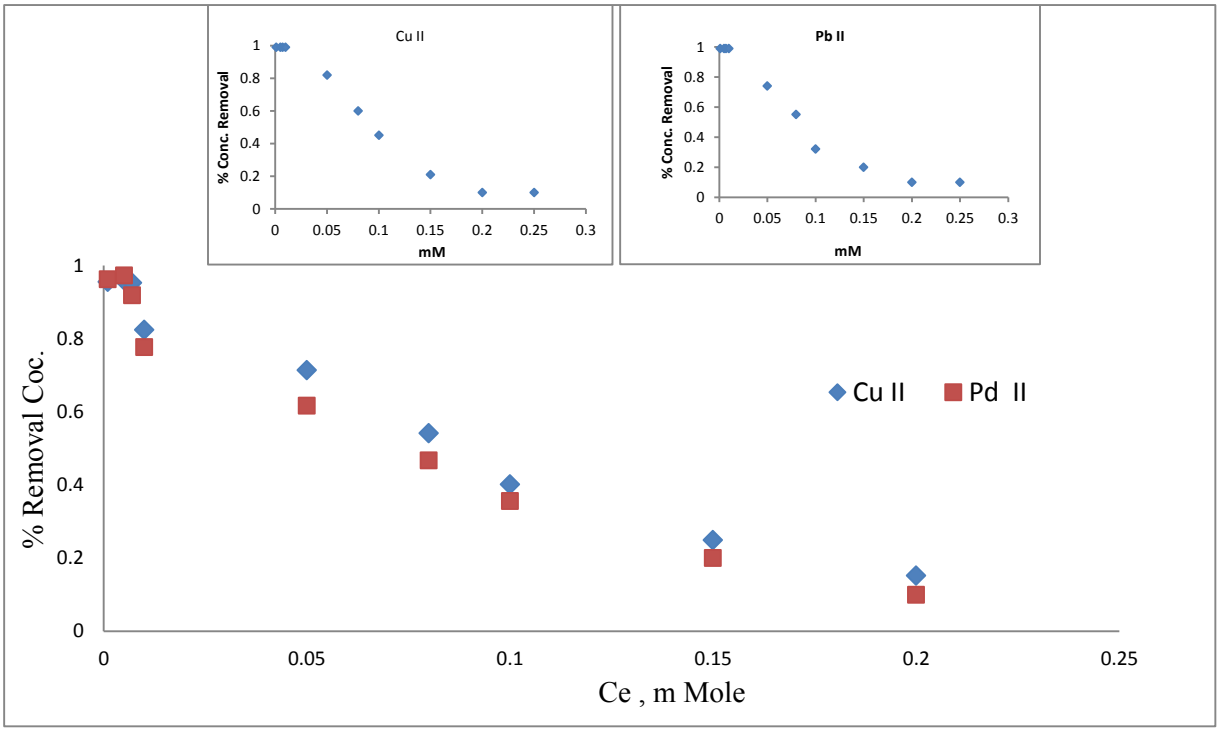

Fig. 6.3: Isotherm studies of metal competition, Cu II - Pb II, insert: Single isotherm studies of metals, pH: 4.5, T: 22 ^{O}C

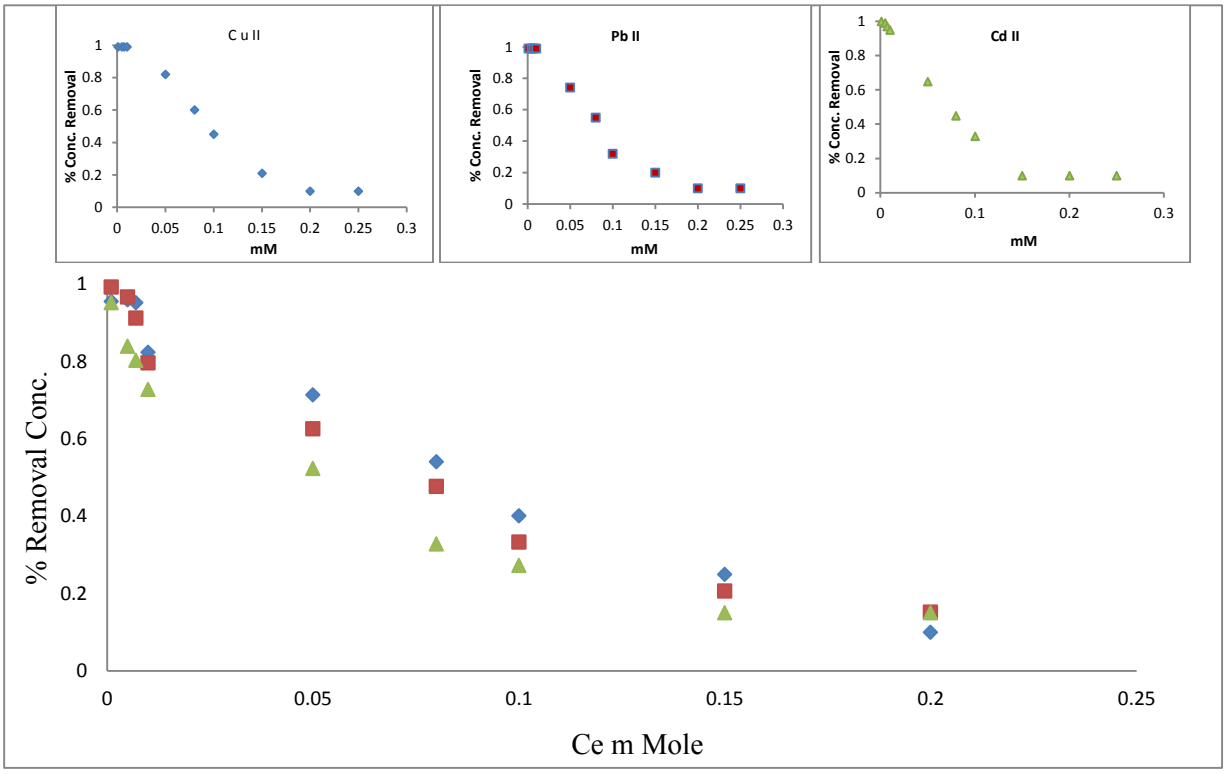

Fig. 6.4: Isotherm studies of metal competition, Cu II - Pb II- Cd II, insert: Single isotherm studies of metals pH: 4.5, T: 22 ^{O}C.

Fig. 6.4 presents the multi-element adsorption of Cu II, Pb II and Cd II. The data reveals that metals that form hydrolysis products get more readily (Cu II and Pb II) adsorbed to variable charge surface when pH is close to 4.5. However, because of its low tendency to form hydrolysis products, Cd II does not compete effectively to get adsorbed on variable charge surfaces, and so its adsorption is more restricted to permanent charge sites. Similar results have been reported by Srivastava et al, (2005). Atanassova and Okazaki, (1997) reported that in a multi-component system, an increase in Cu adsorption resulted in a reduction in the uptake of other heavy metals such as Ni, Cd, and Zn. Since Cu II is specifically adsorbed (inner-sphere complexation), it can be expected that increasing the amount of more strongly adsorbed Cu reduces the number of sites available for Cd II and Pb II adsorptions. Although there is a slight reduction of the adsorption in multi-element systems, nanofer ZVI provides a large number sites available for the metals to compete. Just as the presence of Cu II and Pb II suppresses the uptake of Cd II by the variable charge surface, the presence of Cd II and Pb II slightly decreases the uptake of Cu II in multi-element systems.

Values of Langmuir parameters q_{max} and b are shown in Table 6.1 for multi-metal systems. The results for q_{max} at pH ~ 4.5 were slightly different from the single metal adsorption data. An average

of 5 to10 % reduction between both single and multi-metal systems adsorption is detected. However, it is expected that a small reduction of the adsorption capacity for metal at multi system occurs due to metal ion competition to get adsorbed on the same sites. Ikhsan et al. (1999) studied the adsorption of transition metals on kaolinite at pH 5.5 and 7.5. Compared to Co II, Mg II and Zn II, they found that the adsorption of Pb II and Cu II is significantly greater at all solution concentrations. The values of the isotherm constant b determined from the two-site Langmuir model are in the order Cu II >Pb II > Cd II. The experimental results and the Langmuir parameters agreed with the fact that both ionic radii and electronegativity (Table 3.2) play a significant role on the adsorption capacity of metals by nanofer ZVI. The high R^2 (Table 6.1) values are indicative of the strong influence by competing metals on the release of metals for adsorption on nanofer ZVI in the multi systems. Conversely, low values for R^2 mean that other factors besides those that were stated earlier may be involved. The results are in agreement with those of Christophi and Axe, 2000 and Srivastava et al, (2001).

Table 6.1: Langmuir Parameters for adsorption of metal at binary and multi system at pH 4.5

Metal	q_{max} m Mole ± 0.1	b ml/mMole ±0.1	R^2
Binary-metal system			
Cu II + Cd II			
Cu II	0.25	42.20	0.81
Cd II	0.09	7.21	0.79
Cu II +Pb II			
Cu II	0.22	39.7	0.85
Pb II	0.15	14.2	0.88
Pb II + Cd II			
Pb II	0.16	15.1	0.91
Cd II	0.1	7.9	0.87
Multi-metal system			
Cu II +Pb II+ Cd II			
Cu II	0.21	38.40	0.82
Pb II	0.12	10.53	0.78
Cd II	0.07	6.51	0.74

6.4.2 Kinetic studies

The kinetic adsorption of the metals in the multi-element systems are presented in Fig 6.5. The time profile for the displacement and competition in multi systems is set as 120 min. Although equilibrium conditions were not clearly obvious from the data obtained, the information was useful in the derivation of the equilibrium time that was used in the subsequent competitive displacement experiments. The time profile for binary metal experiments (Cu II-Cd II, Cu II-Pb II, and Cd II-Pb II) are presented in Figs. 6.5a, 6.5b and 6.5c respectively. The results of competitive adsorption of multi- systems involving three metals are shown in Fig.6.5d. The inserts in Figs.6.5 represent the adsorption of single contaminant (Cu II, Cd II or Pb II) for the same experimental conditions. After 5 minutes of contact time between the metals and nanofer ZVI in multi metal systems, the samples were analyzed. The data revealed that in case of Cu II-Cd II (Fig. 6.5a), Cu II achieved almost 55% removal efficiency, while Cd II attained less than 30% removal efficiency. However, in the case of competition between Cu II-Pb II (Fig. 6.5b), after 5 minutes Cu II achieved only 40% removal and Pb II achieved 35% removal. This may suggest that Cu II and Pb II compete for the same type of sites. 42% and 29% removal efficiency was achieved for Pb II and Cd II respectively (Fig 6.5c). In both Cu II-Cd II (Fig 6.5a) and Cu II- Pb II (Fig. 6.5b) systems, the maximum Cu II adsorption achieved was between 35-40 mg II per gram of nanofer ZVI. Compared to Pb II and Cd II, Cu II has a smaller hydrated ionic radii (Table 3.2) and a higher electronegativity. Hence, it displaces both Pb II and Cd II in the multiple metal systems. The total sites occupied per gram of nanofer ZVI are less than the one observed in the single isotherm studies, suggesting that Cu II, Pb II and Cd II compete for the same sites available**.**

The results of electron dispersive spectroscope (EDS) analysis for the multi metal adsorption are presented in Table (6.2). EDS is an analytical technique used for elemental analysis of the sample. In this study, the method is used to investigate the chemical composition of elements absorbed by nanofer ZVI. The Cu concentration at surface of nanofer ZVI is much higher than both Pb and Cd (Table 6.2). The result is in agreement with the fact that Cu has smaller ionic radius (Table 3.2). Data of Table 6. 2 supports the results of comparative study of multi metal adsorption tests.

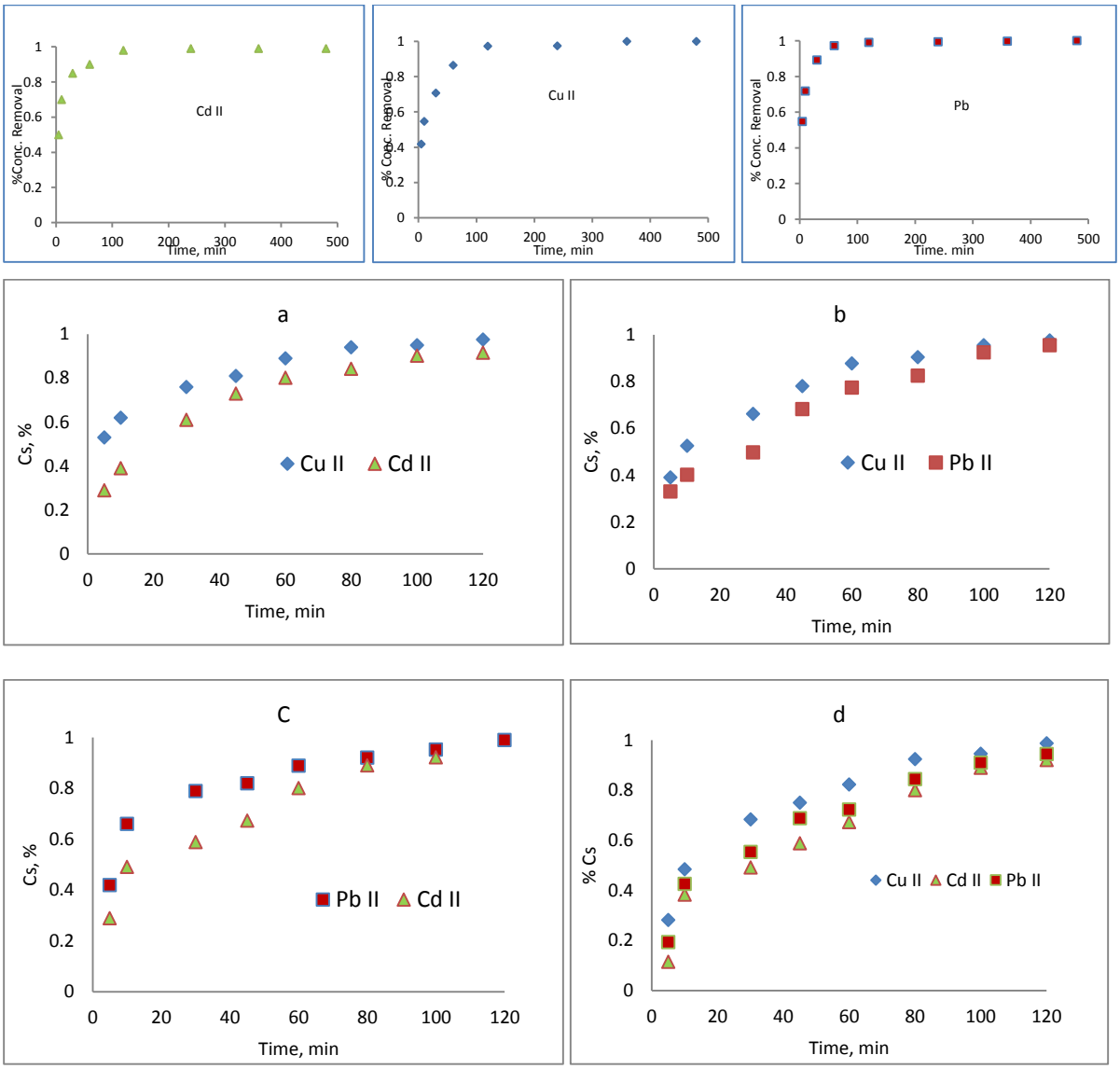

Fig. 6.5: Kinetic studies of metal competition, a. Cu II vs. Cd II, b. Pb II vs. Cd II. C. Cu II vs. Pb II and d. Cu II, Cd II , Pb II. Error bar: ± 0.1, pH: 5.5, T: 20 ^{O}C, insert: Single adsorption experiment for each metal.

6.4.3 Kinetic adsorption models

In order to elucidate the adsorption mechanism, the pseudo- first and second order kinetic models were tested to fit the experimental data obtained from batch kinetic experiments. Hence, the determination of a good fitting model could allow for a sound water treatment process design. The simple kinetic model that describes the process of adsorption is the pseudo first order equation (Ho and McKay, 1999).

$$\frac{dq_t}{dt} = k_1(q_c - q_t), \qquad (6.1)$$

Here, k_1 (min^{-1}) is the rate constant of adsorption. Here q_c is calculated from the Langmuir adsorption isotherm. The following expression is a result of integrating Eq.6.1 with the condition q_c =0 at t=0,

$$\ln(\frac{q_c - q_t}{q_c}) = -k_t t, \qquad (6.2)$$

Another simple kinetic model, cited by Hamadi et al. (2004) is the pseudo second order adsorption.

$$\frac{dq_t}{dt} = k_2(q_c - q_t)^2, \qquad (6.3)$$

Here k_1 ($gmmol^{-1}$ min^{-1}) is the rate constant of the pseudo second order adsorption. Integration leads to:

$$(\frac{1}{q_c - q_t} - \frac{1}{q_c}) = -k_2 t, \qquad (6.4)$$

Knowingq_e, the rate constant k_1 and k_2 can be obtained from the plot of experimental data. Thus, metal competitive adsorption can be expressed as function of time, for pseudo-first and second-order model using the following expression:

$$q_t = q_c(1 - e^{-k_1 t}), \qquad (6.5)$$

$$q_t = q_c \frac{q_c k_2 t}{1 + q_c k_2 t} \qquad (6.6)$$

The pseudo-first (Eq.6.5) and pseudo-second (Eq.6.6) order models are applied using the multi metal adsorption experiments data. Using Eq. (6.5) and (6.6) and linear regression, the kinetic parameters were calculated (Table 6.3). The correlation coefficient R^2 estimated showed that the (kinetic) experimental data follow the pseudo-second order reaction.

Table 6.2: SEM/EDS analysis of kinetic experiments for mixed metal adsorption

ELEMENT	WEIGHT %	ATOMIC %
O	9.60	33.42
Fe	83.07	58.40
Cu	5.09	6.65
Pb	2.11	1.37
CD	0.13	0.16

Table 6.3: Pseudo-first and pseudo-second model parameters and correlation coefficients calculated using the multi metal adsorption experimental data.

Metal	**Pseudo-first model**		**Pseudo-second model parameter**	
	K_1 (min^{-1})	R^2	K_2 ($gmmol^{-1}min^{-1}$)	**R^2**
Cu II-Cd II				
Cu II	0.066	0.89	2.75	**0.98**
Cd II	0.036	0.82	2.06	**0.95**
Cu II- Pb II				
Cu II	0.058	0.87	2.54	**0.97**
Pb II	0.051	0.82	2.31	**0.93**
Pb II-Cd II				
Pb II	0.044	0.84	2.37	**0.98**
Cd II	0.043	0.80	2.31	**0.97**
Cu II-Pb II-Cd II				
Cu II	0.058	0.81	2.54	**0.97**
Pb II	0.043	0.76	2.12	**0.94**
Cd II	0.022	0.77	1.79	**0.95**

6.5 Conclusions

The competitive adsorption and displacement of metals are complicated processes that are influenced by a multitude of factors. The occurrence of more than one possible adsorption mechanism, on nanofer ZVI contributes to the multi-faceted nature of these interactions. The binding of metal ions is thought to occur through a combination of both the hydrated ionic radii and electronegativity of metals. The mechanisms for multi adsorption involved are influenced by time, pH and initial metal concentration, the presence and properties of competing metal ion in the solution. Metal speciation effectively determines metal adsorption and further controls the possibility of getting displaced by a more preferred competing metal.

For both the isotherm and kinetic studies performed for multi adsorption experiments, during the initial 5 min, Cu II achieved the higher adsorption capacity, compared to Pb II and Cd II. However,

after 120 min, all metals achieved a removal efficiency in the range of 95% to 99%. Comparing the results of single and competitive adsorption kinetic tests for all three metals during the initial 5 min, the presence of other metals slightly reduces removal efficiency. This is traced to the fact that several metals are competing to get adsorbed on the limited available specific sites of nanofer ZVI. Both kinetic adsorption and EDS analysis found that Cu II gets adsorbed faster than the other metals. The Langmuir model for multi metal adsorption was employed to understand the mechanism of isotherm studies. Based on the above analysis, these models complement the experimental results and EDS analysis that Cu II adsorption was slightly higher than other metals. Both pseudo first and second order models were employed using the kinetic experimental data. R^2 values for the corresponding experimental data indicated that multi metal adsorption systems follow pseudo second order behavior. For direct injection into groundwater for the removal of individual contaminants or mixed contaminants formed by metals and organics, nanofer ZVI is a viable adsorbent in place of commonly use nanofer ZVI 25.

6.6 References

1. Atanassova. I., Okazaki, M., 1997 "Adsorption -desorption characteristics of high levels of copper in soilclay fractions," *Water, Air and Soil Pollution*, vol. 98, pp.213-228.
2. Benjamin, M., and Leckie. J., 1980a "Multiple-site adsorption of Cd, Cu, Zn and Pb (II) on amorphous iron oxyhydroxide," *Journal of Colloid and interface Science*, vol. 79, no.1, pp. 209-221.
3. Benjamin, M., and Leckie. J., 1981b''Competitive adsorption of Cd, Cu, Zn, and Pb on amorphous iron oxyhydroxide,'' *Journal Colloid and Interface Science*, vol.83,pp. 410–419.
4. Chen, S., Ma, Y., Chen, L., and Xian, K., 2010 "Adsorption of aqueous Cd2+, Pb2+, Cu2+ ions by nano-hydroxyapatite: Single- and multi-metal competitive adsorption study," *Geochemical Journal*, Vol. 44, pp. 233 - 239.
5. Christophi, C., and Axe, L., 2000 "Competition of Cd, Pb (II), Cd adsorption on goethite," *Journal of Environmental Engineering*, vol.126, no.1, pp.66-74.
6. Cowan, C., Zachara, M., and Resch, T., 1991 ''Cadmium adsorption on iron oxides in the presence of alkaline-earth elements,'' *Environmental Science and Technology*, vol.25, pp. 437–446.

7. Hamadi, K., Swaminathan, S., Chen, D., 2004 "Adsorption of Paraquat dichloride from aqueous solution by activated carbon derived from used tires," *Journal of Hazardous Materials*, vol. 112, no. 1-2, pp.133-141.
8. Ho, S., McKay, G., 1999 " The sorption of lead(II) ions on peat," *Water Resource*, vol. 33, no.2, pp.578–584.
9. Ikhsan, J., Johnson, B., and Wells, D., 1999 "A comparative study of the adsorption of transition metals on kaolinite," *Journal of Colloid and Interface Science*, vol. 217, no. 2, pp. 403-410.
10. Li, X-Q., Zhang, W., 2007 "Sequestration of metal cations with zerovalent iron nanoparticles – a study with high resolution X-ray photoelectron spectroscopy (HR-XPS)," *Journal Physical Chemistry C*, vol. 46, no.111, pp.6939-6949.
11. Srivastava, P., Singh, B., Angove, M., 2005 "Competitive adsorption behavior of heavy metals on kaolinite," *Journal of Colloid and Interface Science*, vol. 290, pp. 28–38.
12. Swallow, K., Hume, N., and Morel, M., 1980 ''Sorption of copper and lead by hydrous ferric oxide,'' *Environmental Sciences and Technology*, vol.11,pp. 1326–1336.
13. Zasoski, J., and Burau, G., 1988 ''Sorption and sorptive interactions of cadmium and zinc on hydrous manganese oxide,'' *Soil Sciences. Society American Journal*, vol.52, pp.81–87.

CHAPTER SEVEN

Degradation of TCE by TEOS Coated nZVI in The Presence of Cu II for Groundwater Remediation

Abstract

The removal of TCE by nZVI coated with TEOS (nanofer ZVI) in the presences of Cu II at different environmental conditions was examined. Rapid degradation kinetics of TCE by the nanofer ZVI was observed. Increasing the pH was found to reduce degradation performance due to the formation of the hydroxyl group which can create passive film surrounding the nanoparticle. At dosage of 25 mg of nanofer ZVI almost 45% TCE was removed, when 0.01M $CuCl_2$ and 0.15 TCE were present, compared to 80 % degradation of TCE in the absence of Cu II. This indicates that although Cu gets adsorbed faster to nanoferZVI, it works as intermediate catalysis to enhance TCE degradation. The images of SEM/EDS (Fig. 7) indicate that Cu II is reduced to Cu^0 and Cu_2O. These formations on the surface of nanoferZVI are considered to be responsible for the enhancing the dechlorination of TCE. TCE degradation by nanofer ZVI involved both direct and indirect reduction of both. Direct reduction such as hydrogenolysis and β-elimination in the transformation of TCE can form an organic chemisorptions complex at the metal surface where metal itself serves as a direct electron donor. The indirect reduction involves atomic hydrogen and no direct electron transfer from metals to reactants. The nanofer ZVI containing almost 98% pure iron (α-Fe) which could get dissolved faster causing the generation of localized positive charge regions and form metal chlorides to maintain electroneutrality in the system, after hydrolysis of the chlorides to form metal hydroxides and hydrochloric acid. Local accumulation of hydrochloric acid inside the pits regenerates new reactive surfaces to serves as sources of continuous electron generation. However, no significant effect was noticed for either increasing or decreasing the Cu II sequestering to the surface of the nanofer ZVI. Cu II found to be move faster due to its small hydrate radii and high electronegativity.

7.1 Introduction

During the last few years, a great deal of effort has been directed to develop and improve the zero valent iron nanoparticle (nZVI) to clean groundwater contaminants. The direct injection of nZVI has been known as effective processes to treat organic as well as inorganic groundwater contaminants. The treatment of mixed contaminants formed by a combination of organics and inorganics poses a challenge to groundwater remediation technologies due to the vast difference in the physicochemical properties of the treated contaminants. This is particularly true when we are dealing with aliphatic chemicals, such as polychlorinated biphenyls (PCBs), hydrocarbons, and polar contaminants, such as heavy metals and radionuclides. Consequently, mixed pollutants can be removed only in small quantities and this is not efficient. Elektorowicz, (2009) stated that the mixture of organic and inorganic contaminants especially from petroleum source can pose a difficult challenge for remediation technologies. Whenever, organic and inorganic contaminants are present, their behavior and properties can get altered. This could make it difficult to achieve the removal of the target contaminants. Using an integrated treatment such as applying an electric field can enhance ionic migration and hence metal removal. However, it was also noted that it can be difficult if several contaminants are simultaneously present. As such, it was observed that further studies are needed in the area of mixed contaminant removal.

The mechanism of degradation of contaminants in the presence of iron is not fully understood. There are many studies related to the degradation mechanism comprising heterogeneous reactions (Nowack, 2008). The reactions occur when the reactant molecules reach the iron solid surface. They then associate with the surface at sites that may be either reactive or nonreactive. According to him, competition for the available sites can occur between the reactant solute of interest and other solutes. The reactive sites refer to those where the breaking of bonds in the reactant solute molecule occur (i.e. chemical reaction) whilst non-reactive sites are those where only sorption interactions occur and the solute molecule remains intact.

The degradation hypothesis for halogenated compounds by iron is better accepted as there is a reductive dehalogenation of the contaminant coupled with the corrosion of iron. With a standard reduction potential ($E_h\pm$) of - 0.44 V, ZVI primarily acts as a reducing agent. Iron is oxidized

while alkylhalides (RX) are reduced. At pH 7, the estimated standard reduction potentials of degradation of various alkyl halides range from + 0.50 V to + 1.25 V (Ghauch, et al. 2001). Hence, the net reaction is thermodynamically very favorable under most conditions. For example, groundwater contaminated with chlorinated solvents such as trichloromethane (TCM), trichloroethylene (TCE) and perchloroethylene (PCE) are treated using iron barriers. The preferred electron acceptor is typically dissolved oxygen under aerobic conditions (E_h +1.23 V). This acceptor can compete with chlorinated hydrocarbons that have oxidizing potentials similar to oxygen. Aerobic groundwater enters the iron fillings wall and causes the oxidation of metallic iron (Fe^0) to ferrous iron (Fe^{2+}), with the subsequent release of two electrons. Chlorinated solvents also react as electron acceptors, resulting in dechlorination and the release of a chloride ion. The reaction takes place in several steps resulting in reducing halogenated organic compounds through intermediates to non-toxic compounds such as ethylene, ethane, and acetylene (Farrell et al 2000). Intermediate compounds like vinyl chloride which has a higher toxicity than the original compounds are not formed in high concentrations (Janda et al. 2004). nZVI also reacts with water producing hydrogen and hydroxide ions resulting in an increase in the pH of water. The resulting hydrogen can also react with alkyl halides. According to Deng, et al. (1999) the bulk dehalogenation reaction is usually described by first-order kinetics. They found that the lower the degree of chlorination, the slower is the rate of dechlorination. Batch and column tests have also indicated highly variable degradation rates due to operating conditions and experimental factors such as pH, metal surface area, concentration of pollutants, and mixing rate. Wang, et al. (1997) suggested that since the reaction is heterogeneous, the rate of reaction is proportional to a specific surface area of the iron used. Therefore the adsorption, desorption or diffusion of reactants and chemical reaction itself can limit the processes. Several limitations of this technique, including the accumulation of chlorinated by-products and the decrease in the activity of iron over time have been reported (Doong et al. 2003). Wang, et al. (1997) used improved methods that involved physical and chemical processes which increased the surface area of iron by reducing its particle size to enhance reactivity.

Only few studies in the past have investigated the effect of organics and inorganics (mixed contaminants) on TCE degradation by nZVI. Liu et al. (2007) stated that dehalogenation of TCE was not significantly affected by the presence of other organics. As stated earlier Nowack, (2008)

observed that the reaction between metal and nZVI depends on the nonreactive surface. This implies that if mixed contaminants are present, the organics react only with the reactive sites and the metal (inorganics) gets adsorbed to nonreactive surface. Lien et al (2007) stated that the presence of other metals specially the ones that have standard reduction potential higher than iron may increase the reactivity and efficiency of the degradation of organic contaminants. However, intermediate reaction between metal and the organic can result in a chemical compound that is more hazardous than the original one.

In the present study, the effect of Cu II on the removal of TCE by nZVI coated with Tetraethylorthosilicate (TEOS) is investigated. Cu II was chosen since this cation is generally found in groundwater as a common pollutant. Further, Cu II can enhance the degradation of halogenated organics. Compared to other cations (metals) present as groundwater pollutants, Cu II has a higher reactivity, a smaller ionic radii and a higher electronegativity. In order to assess the applicability of coated nZVI for the degradation of TCE, batch isotherm and kinetic tests will be conducted. These studies will also consider the effects of environmental factors (concentration, pH, dosage and time) on both the degradation of TCE, the adsorption of Cu II and identify the reaction mechanisms.

7.2 Materials and methods

The chemical solutions used in the study are presented in the previous chapter [Tables (3.1) and (3.2)]. Nanofer zero valent iron particles were prepared as previously discussed earlier (Chapter3).

7.3 Experimental procedures

7.3.1 Batch equilibrium experiments

The competition adsorption experiments as function of pH (adsorption edge) and concentration (isotherm adsorption) were prepared using the indicated chemicals fisher grade (Table 3.1). The stock solutions were performed in closed, 1000-ml glass serum bottles in which the solution volume was 1000 ml. An appropriate volume of the stock solution was diluted with de-ionized water to 1000 ml. The solutions were mixed using a magnetic mixer and left over night. After the mixing, the amount of nZVI and stock solution were added to a 40 ml bottle. Following this, the bottles closed and the cap was sealed with a Teflon liner to prevent air leakage. The bottles were

agitated on a mechanical shaker at 250 rpm at 21^0 C. After a suitable time interval (typically 24 hours for reactions with metal species), the reaction was stopped by separating the solution and the particles with a vacuum filtration using 0.2 μm filter supplied by (grad 42 Whatman). The particles were dried and stored in a N_2-filled glove box ahead off solid phase analysis, and the solution was acidified with 0.1 mole HCl before the analysis. After charging a small amount of nZVI (10 mg), the bottles were capped with Teflon Mininert valves and placed on a mechanical shaker at 250 rpm at 25 ^{o}C. Both pH and temperature were measuring before and after adding the nZVI to each bottle. All bottles were cleaned using 0.1 mole HCl and washed to insure that no residual contaminants could occur. After the liquid phase analyses done the samples acidified and drop to pH less than two and stored at 4^0 C. For each set of experiments, a control was performed under identical conditions in parallel except for the case where no iron nanoparticles were added. The adsorption edge experiments were conducted at 0.01 M for binary and multi- concentration of metals. The equilibrium pH of the suspension was varies from 4.5 to 7.5 with a 1 increments unit using radiometer standard buffers (4, 7, 10). The suspension was equilibrated for the metal adsorption for 2 hrs. More detail of the experimental work are presented in (Chapter 3)

7.3.2 Batch kinetic experiments

Kinetic experiments of reactions with selected organic and inorganic species were performed. The amount of chemical added was diluted with de-ionized water to 1000 ml, sealed and were left in the mixer overnight. After mixing, nZVI and stock solution were added to 40 ml bottle. Following this, the bottles were closed and the caps with a Teflon liner sealed the bottles to prevent leakage. The head room in the bottle was kept to the minimum. The bottles were agitated on a mechanical shaker at 250 rpm at 21^0 C. Time was recorded for each bottle at the moment of adding the nZVI. Each bottle was given suitable time and code. After a suitable time interval, the bottles the nZVI were separated using with vacuum filtration with 0.2 μm filter supplied by (grad 42 Whatman). The pH and temperature were measured before and after adding the nZVI. The filtered solutions was immediately, acidified, and stored at 4^0 C prior to analysis. The Atomic absorption spectroscopies (AAS Perkin Elmer) were used to analysis of metals. However, the TCE was analyzed by the gas chromatography (GC Varian 3800). Before starting multi metal adsorption tests, a few single metal (Cu II, Pb II and Cd II) adsorption experiments under identical conditions were also conducted for further evaluation. More details are presented in (Chapter 3).

7.4 Results and discussions

7.4.1 Oxidative degradation of TCE by nanofer ZVI suspension in the presence of Cu (II)

From the practical point of view, it is important to studies or investigate the presence of co-existing contaminants, especially metals. In the preliminary studies, compared to other metals (Pb and Cd), Cu was removed from the aqueous solution at a faster rate due to its greater electronegativity and small ionic radii (Eglal and Ramamurthy, 2014). Fig. 7.1a shows the degradation of TCE by nanofer ZVI in the presence of Cu II (pH = 6) at different concentrations. After Cu II addition, the reaction rate was improved and the removal efficiency was increased. It is hypothesized that there may be three reasons for this. First reason relates to the electrocatalysis of copper chloride. For instance, $CuCl_2$ and nanofer ZVI have a replacement reaction and copper ions adhere to the surface of nanofer ZVI, and further the numerous tiny batteries that are formed augment iron corrosion. The electrode potential of copper intensifies the electrolysis. The standard electrode potential for Fe^0/Fe^{2+} is - 0.44, and the electrode potential for Cu/Cu^{2+} is + 0.34. The value of Cu/Fe is about + 0.78 V (Doong and Lai, 2006). This results in intensified iron corrosion. Secondly, the reaction of TCE and nanofer ZVI is a solid – liquid contact reaction. Both should have effective contact during the experiments. Generally, passivation layer easily forms on the nanofer ZVI surface. However, copper ions adhering to the nanofer ZVI can prevent formation of the passive layer. This increases the contact between TCE and nanofer ZVI. Finally, hydrogen production is important to TCE dechlorination because the free radicals can provide a great deal of electrons.

7.4.2 Effect of Cu II on the degradation isotherm of TCE by nanofer ZVI

Fig. 7.2a represent the degradation of TCE at different concentration for different nanofer ZVI dosages in the presence of 0.01 M Cu II. Three different TCE concentrations (0.05, 0.1, 0.15 M) were selected around the edge of the optimum concentration determined from the degradation of the TCE alone. At dosage of 25 mg of nanofer ZVI almost 45% TCE was removed, when 0.01M $CuCl_2$ and 0.15 TCE were present, compared to 80 % degradation of TCE in the absence of Cu II. This indicates that although Cu gets adsorbed faster to nanoferZVI, it still enhances TCE degradation. Zhang et al. 2012 studied the effect of adding Cu ion and carbon (C) on TCE degradation over the surface of micro ZVI. They found that Cu ion increases the TCE degradation by 72%, when the molar ratios of Cu ion to TCE was 10:1. In the case of C, they observed that

addition of an appropriate C mass may maximize the TCE removal due to adsorption as well as the synergetic role Fe/C. Their results are in agreement with Zhou and Yang (2008).

It is well accepted that metal mediated dechlorination is mainly a surface reaction. The surface reaction usually involve steps in the overall reaction including diffusion of a reactant to the surface, a chemical reaction on the surface and the diffusion of the product back into the solution. The rate limiting step (i.e., the slow step reaction requiring great activation energy) determines the overall kinetics of a reaction. In general, a typical minimum value of the activation energy for chemical controlled reaction is ~29 kJ/mole (Lien and Zhang 2007). The activation energy for the nanoferZVI is estimated to be in the range of 35 to 45 kJ/mole (Lenka et al. 2012). The decrease of the activation energy indicated that the dechlorination by nanoferZVI is a catalytic reaction. The Cu II in this case served as a catalyst. Furthermore, the value of the activation energy also indicates that the rate limiting step for the TCE degradation in presence of Cu II is the surface chemical reaction rather than diffusion.

In general, the TCE degradation by metal surface involved either direct or indirect reduction of both. Direct reduction such as hydrogenolysis and β-elimination in the transformation of TCE by nanoferZVI may occur via formation of an organic chemisorption complex at the metal surface where metal itself serves as a direct electron donor (Liu et al. 2005). However, indirect reduction involves atomic hydrogen and no direct electron transfer from metals to reactants. Atomic hydrogen is a very powerful reducing agent that reductively dechlorinates contaminants effectively. It is probable that TCE degradation follows both direct and indirect pathways. First the nanofer ZVI donates electrons. However, the results of dechlorination by iron may result in many intermediate compound that could be hazardous (Liu et al 2007). Lien and Zhang, (2007) investigated the effect of palladium on the dechlorination of TCE. They found that the use of catalytic metal may lead to lesser amount of chlorinated intermediates. The molecular structures may be responsible for the different surface intermediate products.

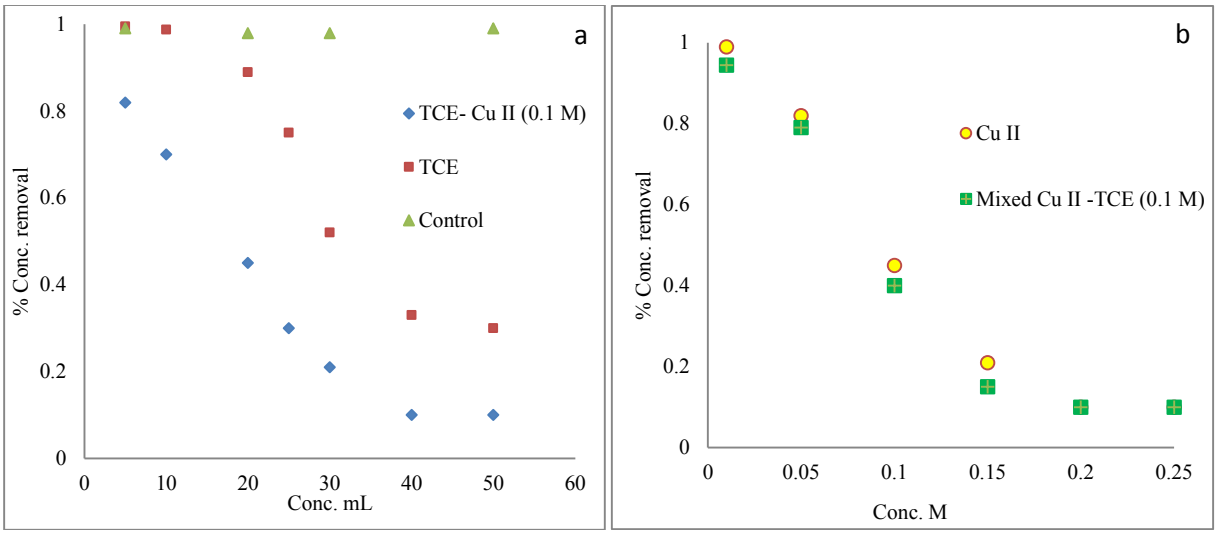

Fig. 7.1: Effect of Concentration on the TCE removal by nanofer ZVI in presence of Cu II. NanoferZVI dose =10mg, initial pH=6, T: 21^0 C, standard error 1%, TCE standard solution in de-ionized water. a: Cu II (0.1 M), Control = TCE (40 mL) in de-ionized water. b: TCE (40 mL),

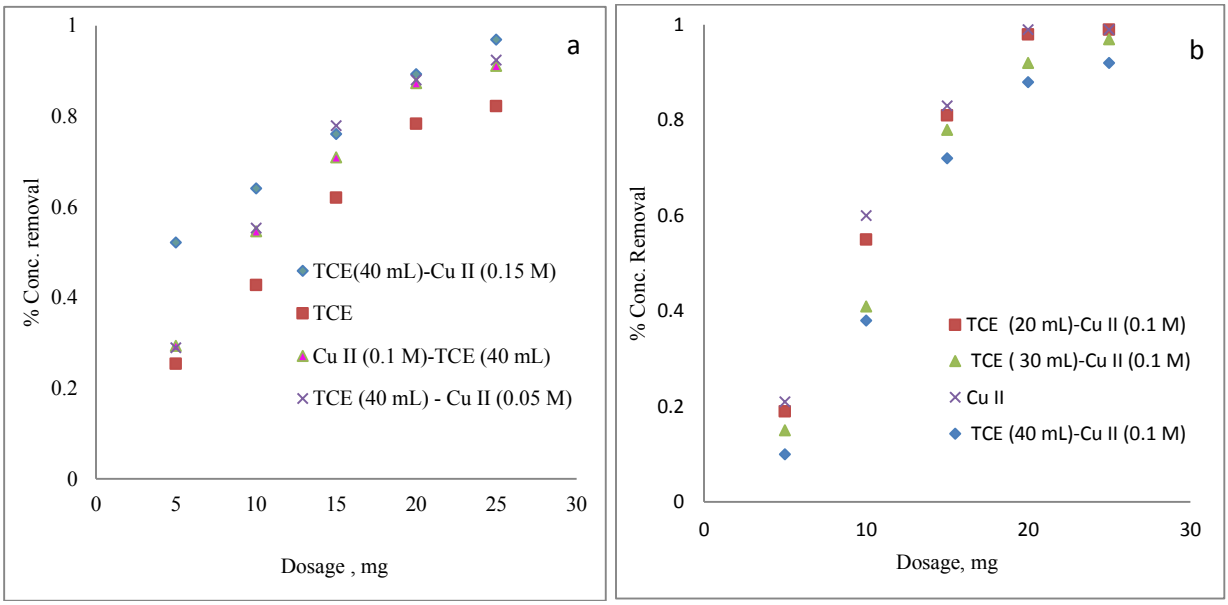

Fig. 7.2: Effect of dosage response on the adsorption of TCE by nanofer ZVI in presence of Cu II), initial pH=6, T: 21^0 C, standard error 1%. a: Conc. Cu II (0.05, 0.1 and 0.15 M), TCE constant (40 mL), b: TCE (20,30 and 40 mL), Cu II (0.1 M)

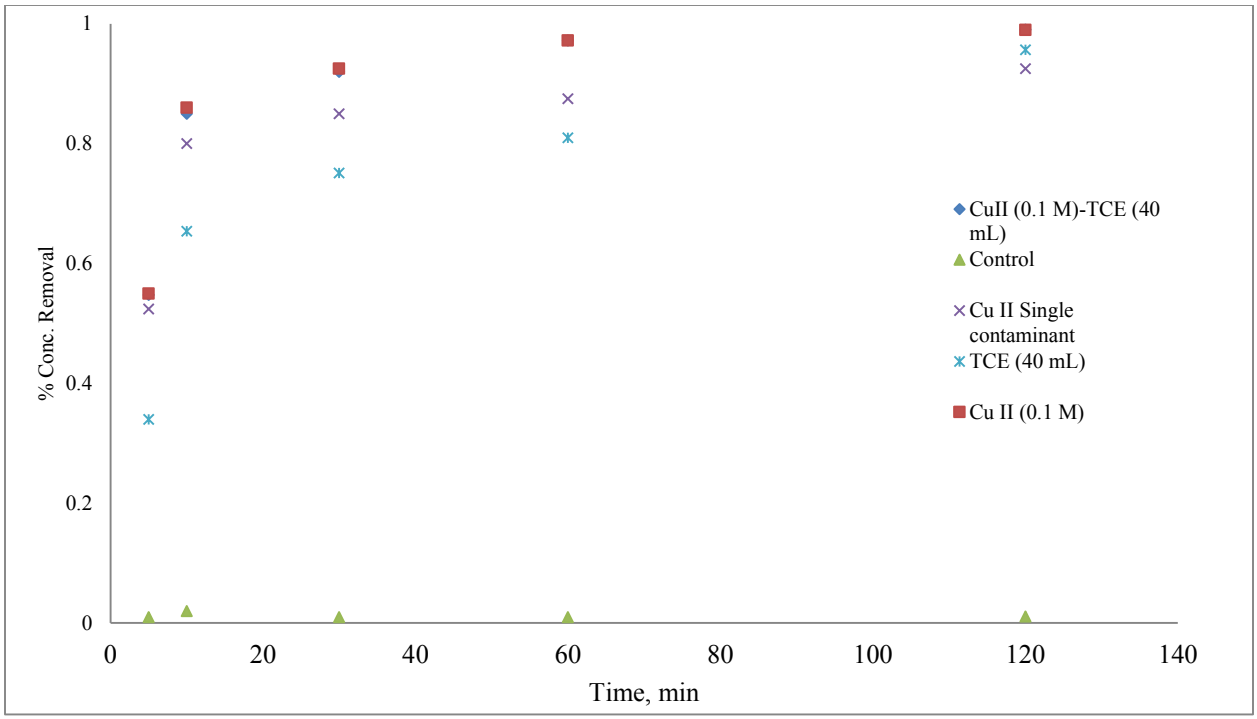

Fig. 7.3: Effect of time on the adsorption of Cu II by nanofer ZVI in presence of TCE (40 Ml), Conc. 0.1mM, 0.05 mM and 0.15 mM, initial pH=6, T: 21^0 C, standard error 1%.

7.4.3 Effect of Cu II on degradation kinetic of TCE by nanofer ZVI

The combined effect of nanofer ZVI and Cu II on TCE degradation is presented in Fig. 7.3. It shows the effect of time on the degradation efficiency of TCE as well as the adsorption of sequestrating of Cu II ion. As stated earlier, Cu II and TCE were added to the de-ionized water at the same time and at a fixed concentration (1 mM). The value of pH was 6. Addition of 10 mg of nanoferZVI was followed after the solution was mixed for 2 hrs. In the initial period (0-5 minutes), the presence of Cu II increased the dechlorination of TCE considerably. At 120 minutes, the increase in degradation of TCE was only marginal. The images of SEM/EDS (Fig. 7.4) indicate that Cu II is reduced to Cu^0 and Cu_2O. These formations on the surface of nanoferZVI are considered to be responsible for the enhancing the dechlorination of TCE. Henderson and Demind, (2007) studied the effect of Pb^{2+}, As^{5+} and Cr^{6+}on the dechlorination of carbon tetrachloride by zero valent iron power. They found that the addition of Pb^{2+} favored of toxic products such as dichloromethane. The influence of As^{5+} was insignificant and that Cr^{+6} was even negative. Fig. 7.3 also presents the adsorption and reduction of Cu II and TCE in single adsorption test. On the other hand, TCE had no effect on Cu II removal. This may be due to the fact that Cu II moves faster to

the surface of nanofer ZVI and acts as an intermediary between nanofer ZVI and TCE. The result is in agreement with Shih et al. (2011) who found that the deposition of Cu on iron particles resulted in a significant increase in dechlorination of pentachlorophenol by Pd/Fe in presence of Cu II ions. They noted through images of XANES (X-ray Absorption Near Edge Structure). However, they noted that $CuSO_4$ was found to lower the pH to 5.21 as compared to the case where no salt was present. In the present case, pH in both the individual and combined tests were set around 6. It is based on the preliminary tests were completed earlier to determine the optimum pH for both Cu II sequestering and TCE degradation using nanoferZVI ranged from 5.5 to 6.5.

When TCE particles dissociate, chloride ions are produced (Fig. 7.5b). Chloride serves as a corrosion promoter and whenever present, it accelerates electron generation from metallic species and creates new reactive sites on the surface of metals Jonson et al. (1998). Chloride also destabilizes the passive films present on the nanoferZVI surface. This can also induce corrosion pit formation (Fig. 7.5b). The nanofer ZVI containing almost 98% pure iron (α-Fe) as shown in Fig. 7.5 which could get dissolved faster causing the generation of localized positive charge regions and form metal chlorides to maintain electro neutrality in the system. After hydrolysis of the chlorides to form metal hydroxides and hydrochloric acid. Local accumulation of hydrochloric acid inside the pits regenerates new reactive surfaces to serves as sources of continuous electron generation (Fig. 7.5b). Such effects have been hypothesized by Jonson et al. (1998) and Gotpagar et al. (1999) earlier to elucidate the rate enhancements observed for the reduction of TCE and carbon tetrachloride by iron metal. The structures of the fresh and the aged (after experiments) nanofer ZVI were also examined using XRD (Fig. 7.6). The % of pure iron α-Fe (blue pattern) decreases to about 59.9 % when TCE (40 ml) was introduced, compared to % α-Fe present in fresh nanofer ZVI (98%, red patterns). However, in the case of Cu II (0.1 ml) and TCE (40ml) experiments (blue pattern), the % of α-Fe decreases to about 35.5%. This clearly indicates that when Cu II is introduced to the solution containing TCE, it helps to increase TCE degradation. Several of the expected XRD peaks for Fe, Cu and iron oxide phases are within close proximity and therefore have overlaps (Fig. 7.6).

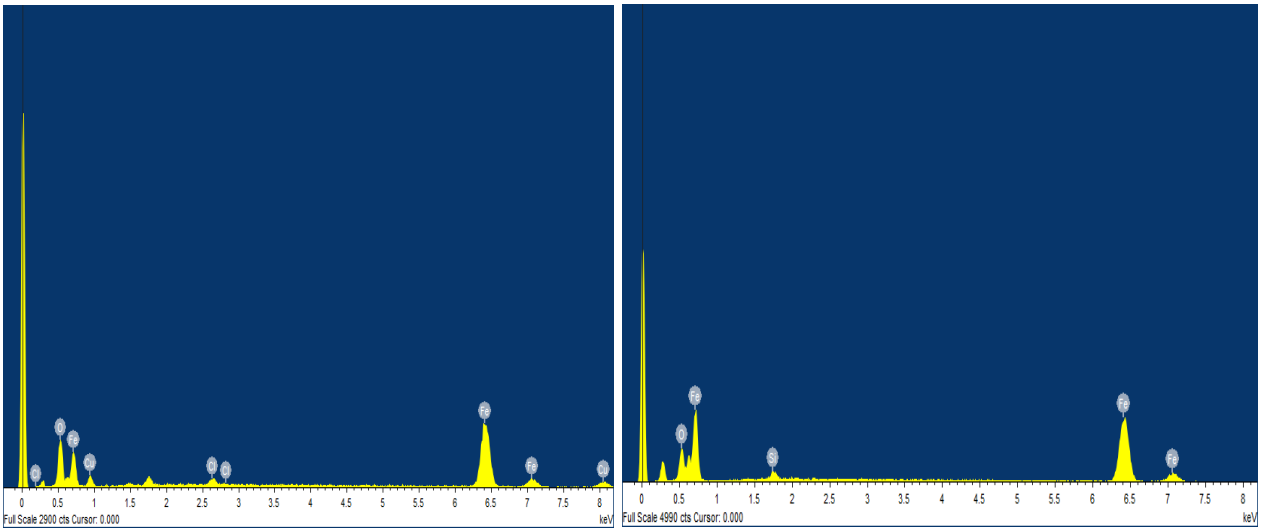

Fig. 7.4: EDS analysis of nanofer ZVI after the experimental test, pH =6 T= 21^0 C, a: TCE concentration (1 mM) and Cu II concentration (1 mM), b: nanofer ZVI in de-ionized water

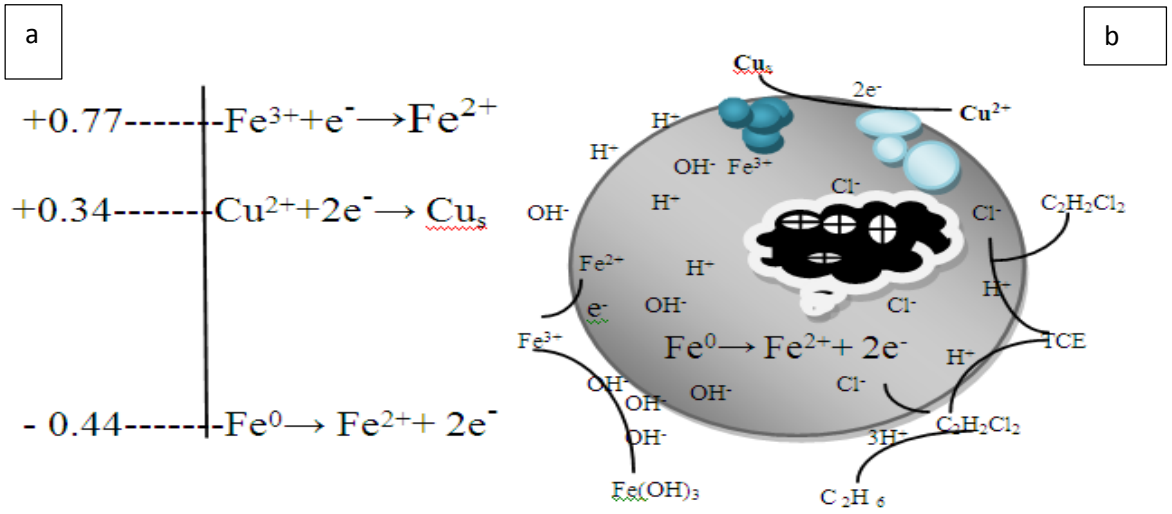

Fig 7.5: Schematic diagram illustrating the effect of cations on degradation of TCE by nanofer ZVI in presences of Cu II and the formation of corrosion pit. nanofer ZVI, Cu^{2+}, Cu & Cl

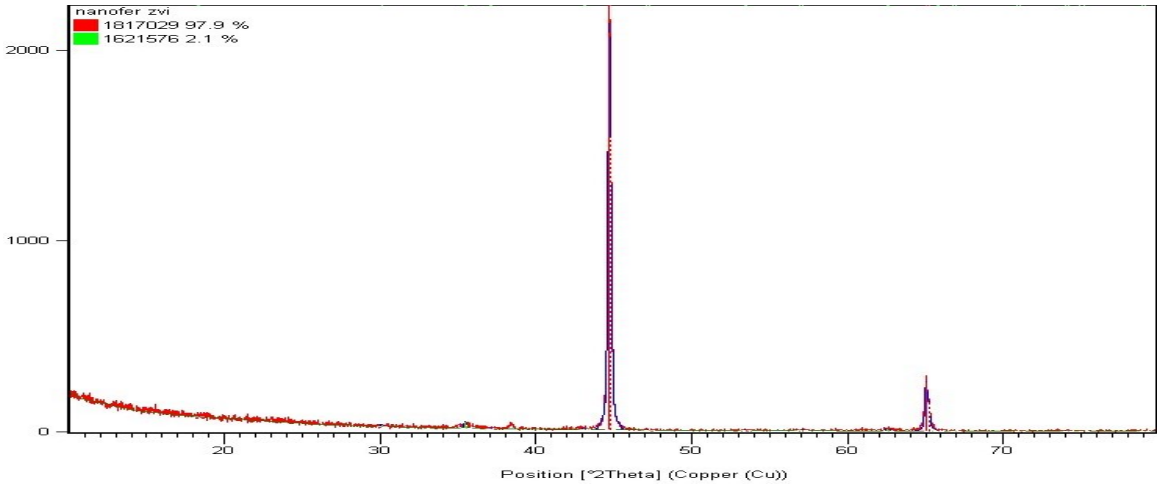

Fig 4.3**:** XRD nanofer ZVI of α-Fe; the particle size: 50–100nm and high content of iron in range of 70–90 wt. % (λ = 1.5418 ˚ A, = 40 Kv, and *I*30 = 30 mA); composition: (green) 2.1%, FeO3 and (red) α Fe, 97.9%,

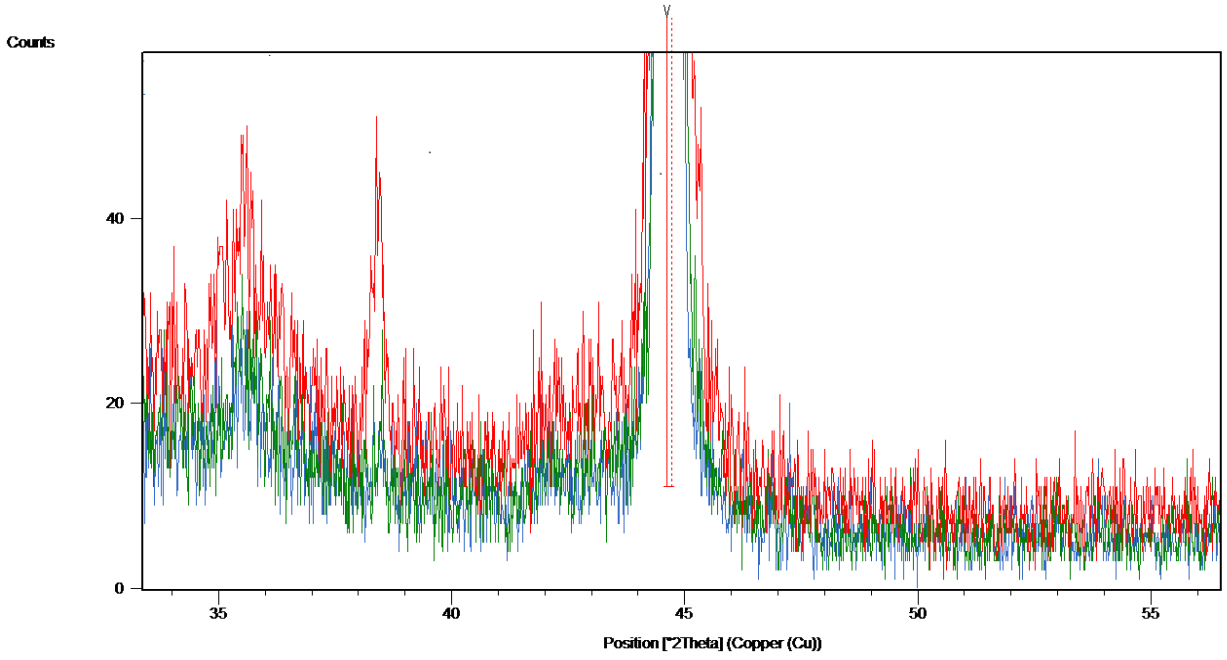

Fig. 7.6**:** XRD image of nanofer ZVI before and after the experiments; (λ = 1.5418 ˚ A, = 60 Kv, and *I*30 = 30 mA); Green line represent the TCE experiment; TCE Conc.40 ml; Blue line represent Cu II Conc. 0.1 M and TCE Conc. 40 ml; Red line represent the nZVI before the experiment. Time: 2 hrs. T; 22 ^{0} C.

7.4.4 Sequestration of Cu II by nanofer ZVI in the presence of TCE

Figs 7.1b and 7.2b show the results for the removal of Cu II by nanofer ZVI in presence of TCE. Fig 7.1b outlines the effect of TCE (0.01M) on the removal of Cu II at different concentrations (0.01 to 0.1 M). However, other factors such as pH (6), Temperature (21^0 C) and the nanofer ZVI dosage (10 mg) were kept constant in all tests. The results indicated that TCE had no significant effect on the removal of Cu II at all concentration tested. The removal of Cu II ions was attributed to the deposition on the nanofer ZVI surface. This was confirmed by SEM-EDS analysis (Fig. 7.4). The Two copper species (CuO and Cu^0), identified at the surface of the nanoparticle indicated that the reduction of Cu II by iron nanoparticle is involved as noticed in Fig. (7.5a). The standard reduction ($E^{0)}$ potential for Cu^{2+}/Cu^0 and Fe^{2+}/Fe^0 couple is +0.34 and -0.44 V, respectively (Fig. 7.5a) and hence the overall E^0 for the reaction is +78 V at 25^0 C, which indicates thermodynamically favorable reaction. The formation of Cu_2O could be attributed to the reaction between the Fe II and Cu II in the aqueous solution. These are in agreement with the results of Maithreepala and Doog, (2004). Li and Zhang, (2007) suggested that any metal with a standard reduction potential higher than iron can be immobilized at the surface of iron nanoparticle by adsorption and chemical reduction. This suggested mechanism supports the results shown in Figs 7.1b and 7.2b. Whenever organics and a metal with a higher standard reduction potential than iron are present, the process of metal adsorption to the surface of nanofer ZVI will be much faster than the degradation rate of the organic (TCE).

Fig. 7.3 shows the effect of time on Cu II reduction and TCE degradation by nanofer ZVI. Although, a moderate increase in the TCE degradation was noticed due to the presence of Cu II, the presence of TCE had insignificant effect on Cu II removal. This is due to the effect of copper getting adsorbed to the surface and acting as an intermediate (catalyst). Similar conclusions were draw by Lien and Zhang (2007) who studied the catalytic effects of palladium on hydrodechlorination and by Lien et al (2007) who studied the effect of heavy metals on dechlorination of carbon tetrachloride by iron nanoparticles.

7.5 Conclusions

In the study related to the removal of TCE by nZVI coated with TEOS (nanofer ZVI) in the presences of Cu II at different environmental conditions indicated that the rapid degradation kinetics of TCE by nanofer ZVI was observed. Increasing the pH was found to reduce degradation due to the formation of the hydroxyl group which can create a passive film around the nanoparticle. At a dosage of 25 mg of nanofer ZVI, almost 45% TCE was removed, when 0.01M Cu II and 0.15 TCE were present, compared to 80 % degradation of TCE in the absence of Cu II. This indicates that although copper gets adsorbed faster to nanofer ZVI, its role in the intermediate catalysis enhances TCE degradation. The images of SEM/EDS showed that reduction of Cu II leads to formation of Cu0 and Cu_2O. These formations on the surface of nanofer ZVI are considered to be responsible for enhancing the degradation of TCE. TCE degradation by nanofer ZVI involved both direct and indirect reduction. Direct reduction such as hydrogenolysis and β-elimination in the transformation of TCE can form an organic chemisorption complex at the metal surface where the metal itself serves as a direct electron donor. The indirect reduction involves atomic hydrogen and no direct electron transfer from the metal to reactants. Almost 98% iron (α-Fe) present in nanofer ZVI could get dissolved faster causing the generation of localized positive charge regions and form metal chlorides to maintain electro neutrality in the system, after hydrolysis of chlorides to form metal hydroxides and hydrochloric acid. Local accumulation of hydrochloric acid inside the pit regenerates new reactive surfaces to serve as source of continuous electron generation. However, no significant effect of TCE was noticed for either increasing or decreasing Cu II sequestering to the surface of nanofer ZVI.

7.6 References

1. Deng, B., Burris, R., and Campbell, J., 1999 "Reduction of Vinyl chloride in Metallic Iron-Water System," *Environmental Science and Technology*, vol. 33, pp 2651-2656.
2. Doong, R. A., Chen, K.T., and Tasi, H.C,, 2003 "Reductive Dechlorination of Carbon Tetrachloride and Tetrachloroethylene by Zero-valent Silicon-Iron Reductants," *Environmental Science and Technology,* vol. 37, pp. 2575-2581.
3. Doong, R. A., & Lai, Y. L., 2006 "Effect of metal ions and humic acid on the dechlorination of tetrachloroethylene by zero valent iron," *Chemosphere*, vol.64, pp. 371–378.

4. Eglal, M., and Ramamurthy, A., 2014"Nanofer ZVI: Morphology, Particle characteristics, kinetics and applications," *Journal of Nanomaterials,* vol, 11 pp,11-22.

5. Elektorowicz, M., 2009 "Electrokientic remediation of mixed metals and organic contaminants," in (Electorchemical rmediation technologies for polluted soils, sediments and groundwater)., Wiley & Son, Inc. Chapter 15, 2009.

6. Farrell, J., Kason, M., Melitas, N., and Li, T., 2000 "Investigation of the Long-term Performance of Zero-valent Iron for Reductive Dechlorination of Trichloroethylene," *Environmental Science and Technology*, vol. 34, pp 514-521.

7. Ghauch, A., Gallet, C., Charef, A., Rima, J., and Martin-Bouyer, M., 2001 "Reductive Degradation of Carbaryl in Water by Zero-valent Iron," *Chemosphere,* vol. 42, pp. 419-424.

8. Gotpagar, J., Lyuksyutov, S., Cohn, R., Grulke, E., Bhattacharyya, D., 1999 "Reductive dehalogenation of trichloroethylene with zero-valent iron: surface profiling microscopy and rate enhancement studies," *Langmuir*, vol.15, pp. 8412–8420.

9. Henderson. D., and Demind, A. H., 2007 "Longterm performance of zerovalent iron permeable reactive barriers: a critical review," *Environmental Engineering and Sciences,* vol. 24, pp. 401–423.

10. Janda, V., Vasek, P., Bizova, J., and Belohlav, Z., 2004 "Kinetic Models for Volatile Chlorinated Hydrocarbons Removal by Zero-valent Iron," *Chemosphere*, vol. 54, pp. 917-925.

11. Johnson, T.L., Fish, W., Gorby, Y.A., Tratnyek, P.G., 1998 "Degradation of carbon tetrachloride by iron metal: complexation effects on the oxide surface," *Journal of Contaminants Hydrology*, vol. 29, pp.379–398.

12. Lenka, H., Petra, J., and Zdenek, S., 2012 "Nanoscal zero valent iron coating for subsurface application," Brno, Czech Republic, EU, vol.10, pp. 23-25.

13. Li, X-Q., Elliott, D., and Zhang, W., 2006 " Zero-valent iron nanoparticles for abatement of environmental pollutants: material and engineering aspects," *Critical Reviews in Solid State and Materials Sciences*, vol. 31, pp. 111–122.

14. Lien, H. L., and Zhang, W. X., 2007 "Nanoscale Pd/Fe bimetallic particles: Catalytic effects of palladium on hydrodechlorination," *Apply catalysis B Environmental*, vol. 77, pp. 110-116.

15. Liu, Y., Phenrat, T., and Lowery, G. V., 2007 " Effect of TCE concentration and dissolved groundwater solutes on NZVI promoted TCE dechlorination and H2 evolution," *Journal of Environmental Science and Technology*., vol.41, no.22, pp.7881-7887.

16. Liu Y., Majetich, S. A., Tilton, R. D., Sholl, D. S., and Lowery, G. V., 2005 " The dechlorination rates, pathways and efficiency of nanoscale iron particles with different properties," *Journal of Environmental Science and Technology*, vol.39, no:5, pp:1338-1345.

17. Maithreepala, R. A., and Doog, R., 2004 "Synergistic effect of copper ion on the reductive dechlorination of carbon tetrachloride by surface-bound Fe (II) associated with goethite," *Environmental Sciences and Technology,* vol.38, pp260-268.

18. Nowack B., 2008 "Pollution Prevention and Treatment Using Nanotechnology. In Nanotechnology", Vol. 2 (ed. H. Krug). WILEY-VCS Verlag GmbH&Co.

19. Shih, Y.H., Chen, M.Y., Su, Y.F., 2011b. Pentachlorophenol reduction by Pd/Fe bimetallic nanoparticles: effects of copper, nickel, and ferric cations," *Apply catalysis B Environmental,* vol.105, pp. 24–29.

20. Wang, C.B., and Zhang, W.X., 1997 "Synthesizing Nanoscale Iron Particles for Rapid and Complete Dechlorination of TEC and PCBs," *Environmental Science and Technology,* vol. 31, pp. 2154-2156.

21. Zhang W., Li, L., Lin, K., Xiong, B., Li, B., Lu, S., Guo, M., Cui, X., 2012 "Synergetic degradation of Fe/Cu/C for groundwater polluted by trichloroethylene," *Water Science and Technology,* vol. 65, no. 12, pp. 2254-2264.

22. Zhou, X. M., and Yang, Y. Y., 2008 "Study on treatment of pnitrochlorobenzene wastewater by Fe/C micro electrolysis," *Anhui Chemical Industry*, vol.34, pp.54–56.

CHAPTER EIGHT
Conclusions and Future Studies

8.1 Conclusions

8.1.1 Morphology and charaterization of the nanofer ZVI

The new nanomaterial selected was coated with TEOS to render it environmentally friendly, inexpensive and can replace the ZVI which is commonly used to remediate groundwater. Further, it showed a good potential to overcome the setback of the old nanofer ZVI 25 which is prone to fast agglomeration as well as instability in the aqueous media. Nanofer ZVI was found to contain 98% of α-Fe which is very highly reactive and hence can act as an effective adsorbent that could remove contaminants from polluted water. The increase of pure iron (ferrite) is caused by the coating of nanofer ZVI with TEOS. The thickness of the oxidizing shell varied from 2 to 4 nm. The average nano-particle size was 50 nm (20-100 nm) and the corresponding surface area of the nanofer ZVI was determined to be quite high (27.5±2 m^2g^{-1}). This also contribute to its high reactivity. The iso-electic point for the nanofer ZVI was found to be at pH of 4.3. Increasing pH from 6.5 to 11, nZVI displayed a ζ-potential higher than ± 85 mV. It may be noted that this value of ζ-potential is considered to be suitable for groundwater remediation.

8.1.2 Reactivity of nanofer ZVI with single contaminant

Batch studies indicated that the new and innovative adsorbent nanofer ZVI was capable of removing contaminants such as heavy metals [(Cu (II), Pb (II) and Cd (II)] as well as organic contaminant [TCE] from polluted water. The batch kinetic test data confirmed that almost all (99%) of the heavy metals such as ((Cu (II), Pb (II) and Cd (II)) can be adsorbed. In the case of TCE, nanofer ZVI got oxidized and releases electrons which reduce the reaction with water. Depletion of oxygen led to an excess of positive charge in the solution causing diffusion of chloride ions to the surface of nanofer ZVI. The results also indicated that nanofer ZVI degrade TCE almost completely. Batch kinetic adsorption and EDS analysis indicated that the adsorption of Cu (II) was relatively higher compared to the adsorption of Pb (II) and Cd (II). Both the film diffusion model and the intraparticle diffusion confirmed that compared to Pb (II) and Cd (II), the diffusion of Cu (II) was much faster. The models also implied that metals transfer to nanofer ZVI was achieved in two stages. In first stage involved the rapid step which was controlled by liquid

diffusion. The second stage involved the slow step which was controlled by intraparticle diffusion. For the chosen concentration of the contaminants, the optimum nanofer ZVI dose was found to be 10 mg. and the optimal pH for Pb (II), Cu (II), Cd (II) and TCE removal were 4.5 and 4.8, 5.0 and 7.2 respectively. The isotherm data fitted to Langmuir and Freundlich models showed that the maximum loading capacity was close to 270, 170, 110, 130 mg per gram of nanofer ZVI for Cu (II), Pb (II), Cd (II) and TCE respectively.

The test data show that there is threshold concentration that has to be reached for TCE degradation. The TCE reduction by nanoZVI forms a new nonhazardous substance possibly ethanol and other byproducts. Due to the large surface area and hence the vast availability of active sites in small amounts (10 mg) of nanofer ZVI, it was effective in removing metals as well as TCE.

8.1.3 Competitive adsorption and displacement of metal on nanofer ZVI

The competitive adsorption and displacement of metals are complicated processes that are influenced by a multitude of factors. The occurrence of more than one possible adsorption mechanism, on the nanofer ZVI contributes to the multi-faceted nature of these interactions. The binding of metal ions is thought to occur through a combination of both the hydrated ionic radii and electronegativity of metals. The mechanisms for binary and multi adsorption involved are influenced by time, pH and initial concentration, the presence and properties of competing metals ion in the solution. Metal speciation is effectively determines metal adsorption and further it controls the possibility of get displaced by a more preferred competitor.

For both the isotherm and kinetic studies performed for binary and multi adsorption experiments, compared to Pb II and Cd II, Cu II achieved the higher adsorption capacity during the initial 5 min. However, after 120 min, all metals achieved removal efficiency in the range of 95 to 99%. Comparing the results of single and competitive adsorption kinetic tests for all three metals, during the initial 5 min, the presence of other metals slightly reduce the removal efficiency. This is traced to the fact that several metals are competing to get adsorbed on the available specific sites of nanofer ZVI. For direct injection into groundwater for the removal of individual contaminants or mixed contaminants formed by metals and organics, nanofer ZVI is a viable adsorbent.

8.1.4 Competitive adsorption of Cu II and TCE degradation

The removal of TCE by nZVI coated with TEOS (nanofer ZVI) in the presences of Cu II at different environmental conditions was examined. Rapid degradation kinetics of TCE by the nanofer ZVI was observed. Increasing the pH was found to reduce degradation performance due to the formation of the hydroxyl group which can create passive film surrounding the nanoparticle. At dosage of 25 mg of nanofer ZVI almost 45% TCE was removed, when 0.01M $CuCl_2$ and 0.15 TCE were present, compared to 80 % degradation of TCE in the absence of Cu II. This indicates that although Cu gets adsorbed faster to nanoferZVI, it works as intermediate catalysis to enhance TCE degradation. The images of SEM/EDS (Fig. 7) indicate that Cu II is reduced to Cu^0 and Cu_2O. These formations on the surface of nanoferZVI are considered to be responsible for the enhancing the dechlorination of TCE. TCE degradation by nanofer ZVI involved both direct and indirect reduction of both. Direct reduction such as hydrogenolysis and β-elimination in the transformation of TCE can form an organic chemisorption complex at the metal surface where metal itself serves as a direct electron donor. The indirect reduction involves atomic hydrogen and no direct electron transfer from metals to reactants. The nanofer ZVI containing almost 98% pure iron (α-Fe) which could get dissolved faster causing the generation of localized positive charge regions and form metal chlorides to maintain electroneutrality in the system, after hydrolysis of the chlorides to form metal hydroxides and hydrochloric acid. Local accumulation of hydrochloric acid inside the pits regenerates new reactive surfaces to serves as sources of continuous electron generation. However, no significant effect was noticed for either increasing or decreasing the Cu II sequestering to the surface of the nanofer ZVI. Cu II found to be move faster due to its small hydrate radii and high electronegativity.

8.2 Future studies

This study has investigated the fundamental properties of nanofer ZVI, the mechanisms and the effect of coating the particles to enhance their remediation capability. In a broader sense, direct characterization of nanofer ZVI using chemical and physical analysis is a relatively new field. The methodology developed in this study, i.e., combining solution analysis with surface and microscopic analyses, is applicable not only to iron nanoparticles and water contaminants, but also to many other aqueous/solid heterogeneous systems. Of particular interest is the interactions of nanoparticles with geochemical and biological surfaces in the natural environment, since these processes are expected to influence the aggregation state, surface reactive properties, and the long

term fate and transport of nanoparticles. It is felt necessary to investigate the following aspects in the context of groundwater remediation using nanofer ZVI:

1- The effects of NOM (natural organic matter) and common groundwater solutes on nanofer ZVI surface chemistry.
2- Application of nanofer ZVI in the in-situ groundwater remediation.
3- Defining methods of removing nanofer ZVI after completing remediation.